Functional constraints of *wtf* killer meiotic drivers

Authors:
Ananya Nidamangala Srinivasa[1,2], Samuel Campbell[1], Shriram Venkatesan[1], Nicole L. Nuckolls[1], Jeffrey J. Lange[1], Randal Halfmann[1,3], Sarah E. Zanders*[1,2]

[1]Stowers Institute for Medical Research, Kansas City, Missouri, United States of America
[2]Department of Cell Biology and Physiology, University of Kansas Medical Center, Kansas City, Kansas, United States of America
[3]Department of Biochemistry and Molecular Biology, University of Kansas Medical Center, Kansas City, Kansas, United States of America

*Corresponding Author
Email: sez@stowers.org

Abstract

Killer meiotic drivers are selfish DNA loci that sabotage the gametes that do not inherit them from a driver+/driver- heterozygote. These drivers often employ toxic proteins that target essential cellular functions to cause the destruction of driver- gametes. Identifying the mechanisms of drivers can expand our understanding of infertility and reveal novel insights about the cellular functions targeted by drivers. In this work, we explore the molecular mechanisms underlying the *wtf* family of killer meiotic drivers found in fission yeasts. Each *wtf* killer acts using a toxic Wtf^{poison} protein that can be neutralized by a corresponding $Wtf^{antidote}$ protein. The *wtf* genes are rapidly evolving and extremely diverse. Here we found that self-assembly of Wtf^{poison} proteins is broadly conserved and associated with toxicity across the gene family, despite minimal amino acid conservation. In addition, we found the toxicity of Wtf^{poison} assemblies can be modulated by protein tags designed to increase or decrease the extent of the Wtf^{poison} assembly, implicating assembly size in toxicity. We also identified a conserved, critical role for the specific co-assembly of the Wtf^{poison} and $Wtf^{antidote}$ proteins in promoting effective neutralization of Wtf^{poison} toxicity. Finally, we engineered *wtf* alleles that encode toxic Wtf^{poison} proteins that are not effectively neutralized by their corresponding $Wtf^{antidote}$ proteins. The possibility of such self-destructive alleles reveals functional constraints on *wtf* evolution and suggests similar alleles could be cryptic contributors to infertility in fission yeast populations. As rapidly evolving killer meiotic drivers are widespread in eukaryotes, analogous self-killing drive alleles could contribute to sporadic infertility in many lineages.

Author Summary

Diploid organisms, such as humans, have two copies of most genes. Only one copy, however, is transmitted through gametes (e.g., sperm and egg) to any given offspring. Alternate copies of the same gene are expected to be equally represented in the gametes, resulting in random transmission to the next generation. However, some genes can "cheat" to be transmitted to more than half of the gametes, often at a cost to the host organism. Killer meiotic drivers are one such class of cheater genes that act by eliminating gametes lacking the driver. In this work, we studied the *wtf* family of killer meiotic drivers found in fission yeasts. Each *wtf* driver encodes a poison and an antidote protein to specifically kill gametes that do not inherit the driver. Through analyzing a large suite of diverse natural and engineered mutant *wtf* genes, we identified multiple properties—such as poison self-assembly and poison-antidote co-assembly—

that can constrain poison toxicity and antidote rescue. These constraints could influence the evolution of *wtf* genes. Additionally, we discovered several incompatible *wtf* poison-antidote pairs, demonstrating expanded potential for self-killing *wtf* alleles. Such alleles could potentially arise spontaneously in populations cause infertility.

Introduction

Genomes often contain selfish DNA sequences that persist by promoting their own propagation into the next generation without providing an overall fitness benefit to the organism [1,2]. Killer meiotic drivers are one class of selfish sequences that act by preferentially destroying gametes that do not inherit the driver from a heterozygote [3]. This gamete destruction leads to biased, or sometimes, complete transmission of the driver+ genotype from driver+/driver- heterozygotes. Killer meiotic drive systems generally decrease the fitness of the organism carrying the driver, both through their killing activities and through indirect mechanisms [4].

Distinct killer meiotic drive systems have repeatedly evolved in eukaryotes and drivers found in distinct species are generally not homologous [3,5–12]. Despite this, killer meiotic drivers fall into a limited number of mechanistic classes with shared themes [3,13,14]. Additionally, unrelated killer meiotic drivers have recurrently exploited conserved facets of cell physiology. This has enabled study of the killing and/or rescue activities of drive proteins outside of their endogenous species [5,11,15,16]. Overall, drivers represent unique tools that can be used to discover novel, unexpected insights into the exploited biological processes.

The *wtf* genes are a family of extremely diverse, rapidly evolving killer meiotic drivers found in multiple copies in most *Schizosaccharomyces* (fission yeast) species [17–22]. The *wtf* driver genes each produce a Wtf^{poison} and a $Wtf^{antidote}$ protein using distinct transcripts with overlapping coding sequences (Fig 1A) [17,22,23]. The amino acid sequences of the two proteins are largely identical, except the $Wtf^{antidote}$ proteins have an additional N-terminal domain of about 45 amino acids not found in the Wtf^{poison} (Fig 1A). All four developing spores (products of meiosis) are exposed to the Wtf^{poison}, but only spores that inherit a compatible $Wtf^{antidote}$ can neutralize the poison and survive [22].

Little is known about the mechanism of toxicity of the Wtf^{poison} proteins. The general mechanism used by $Wtf^{antidote}$ proteins is better understood. The antidote-specific N-terminal domain is the

most conserved region and includes targeting motifs (PY motifs) that are recognized by Rsp5/NEDD4 ubiquitin ligases which route the protein through the trans Golgi network to endosomes and, ultimately, to the vacuole (fungal lysosome; Fig 1B) [15,24]. When both proteins are present, the Wtf^{antidote} co-assembles with the Wtf^{poison}, and the Wtf^{antidote} thereby traffics the Wtf^{poison} to the vacuole [15,24]. This mechanism is similar to a non-homologous drive system recently described in rice, where an antidote protein rescues the gametes that inherit the drive locus from a toxic poison protein by co-trafficking the poison to the autophagosome [5].

In general, the poison protein encoded by one *wtf* gene is not compatible with (i.e., neutralized by) the antidotes of widely diverged *wtf* genes [17,19,25]. However, Wtf^{poison} proteins can be neutralized by Wtf^{antidote} proteins encoded at different loci if the sequences are identical or highly similar (outside of the antidote-specific N-terminal domain; Fig 1A) [17,22,24,26]. Although the examples are limited, similarity at the C-termini of the Wtf poison and antidote proteins may be particularly important for compatibility [15,25,26]. For example, the *wtf18-2* allele encodes an antidote protein that neutralizes the poison produced by the *wtf13* driver [26]. The Wtf18-2^{antidote} and Wtf13^{antidote} proteins are highly similar overall (82% amino acid identity) and identical at their C-termini. Interestingly, the antidote encoded by the reference allele of *wtf18* is not identical to Wtf13^{poison} at the C-terminus and does not neutralize it. In addition, swapping one amino acid for two different amino acids in the C-terminus of Wtf18-2^{antidote} (D366NN mutation) to make it more like the reference Wtf18^{antidote} abolishes the protein's ability to neutralize Wtf13^{poison} [26]. Still, the rules governing poison and antidote compatibility are largely unknown.

While it is clear that a functional *wtf* driver kills about half the spores produced by *wtf*+/*wtf*- heterozygotes, the full impacts of *wtf* gene evolution on the fitness of populations is not clear. Because the *wtf* genes encode the poison and antidote proteins on overlapping coding sequences (Fig 1A), novel poisons can emerge simultaneously with their corresponding antidotes via mutation. This has been observed with a limited number of engineered *wtf* alleles, and one can observe evidence of this divergence in the diversity of extant *wtf* alleles in natural populations [15,19–21,26]. The natural alleles, however, represent a selected population and thus provide a biased sample of the novel *wtf* alleles generated by mutation and recombination. Novel alleles that generate functional drivers are predicted to be favored by the self-selection enabled by drive and be over-represented in natural populations. Conversely, alleles that generate a toxic poison without a compatible antidote would be expected to be under-represented in natural populations due to infertility caused by self-killing.

Major questions remain about the mechanism(s) of Wtf^{poison} toxicity and about the rules of Wtf^{poison} and Wtf^{antidote} compatibility. Our working model is that the toxicity of Wtf^{poison} proteins is tied to their self-assembly [15]. This assembly, however, has only been conclusively demonstrated for the Wtf4 proteins, encoded by the *wtf4* gene from the isolate of *S. pombe* known as *kambucha*. For Wtf^{antidote} function, a working model is that a similar homotypic assembly with the Wtf^{poison} is required to establish a physical connection between the proteins so that the poison is shuttled to the vacuole along with a ubiquitinated antidote [15,24]. The ubiquitination and trafficking of the Wtf antidotes to the vacuole has been demonstrated to be conserved between widely diverged Wtf^{antidote} proteins [19,24]. However, it is not clear if antidote co-assembly with a poison has a functional role in poison neutralization, or if it merely provides a physical link between the proteins to facilitate co-trafficking. It is also unclear if changes in the coding sequence shared by the poison and antidote proteins of a given *wtf* can generate an incompatible set of proteins, or if poisons will always be neutralized by sequence-matched antidotes.

To test these models and to better understand the amino acid sequences that support the Wtf protein functions, we analyzed a panel of natural and engineered Wtf proteins. We found that both well-conserved and poorly conserved amino acid sequences can contribute to protein function. Our analyses revealed broad conservation of Wtf^{poison} self-assembly and suggest that assembly size can affect Wtf^{poison} toxicity, analogous to several other self-assembling toxic proteins [27–29]. This strongly implicates self-assembly as a critical parameter in Wtf^{poison} toxicity. In addition, we found that specific co-assembly with the Wtf^{antidote} is required for efficient Wtf^{poison} neutralization via trafficking to the vacuole. Finally, our analyses identified multiple *wtf* alleles that generate poison proteins that are not efficiently neutralized by their corresponding antidotes. Such alleles are self-destructive and could contribute to sporadic infertility. This work refines our understanding of the functional constraints of Wtf proteins, with important evolutionary implications. More broadly, our observations offer insight into how functional conservation can be maintained despite extreme amino acid sequence divergence and extends our understanding of the limits of protein assembly trafficking mechanisms.

Results

Wtf^{poison} protein self-assembly is broadly conserved.

137 To test the models of Wtf protein functions and to understand how these functions could be
138 supported by extremely diverse protein sequences (e.g., <20% amino acid identity), we
139 generated a large panel of *wtf* variants that represent over 100 million years of divergence [19].
140 We reasoned that functionally important features of the proteins would be conserved in
141 functional variants (i.e. toxic Wtf^{poison} proteins), despite minimal amino acid conservation (Fig
142 1C). Twelve of the variants we assayed are wild-type or mutant alleles of *wtf* genes found in *S.*
143 *octosporus*, *S. osmophilus* or *S. cryophilus* (S1 Fig). One of these genes, *S. octosporus wtf25*,
144 has been previously characterized and found to encode a functional meiotic driver in its
145 endogenous species ([19]; S1 Table). Four additional genes (*S. cryophilus wtf1*, *S. osmophilus*
146 *wtf41*, and *S. octosporus wtf61*) have been shown to encode functional Wtf^{poison} and Wtf^{antidote}
147 proteins in an ectopic *Saccharomyces cerevisiae* assay system ([19]; S1 Table). The *S.*
148 *cerevisiae* system used to study Wtf proteins is well established and reflects phenotypes
149 observed in the endogenous fission yeast species [15,19,24]. Finally, we assayed a panel of
150 new mutant alleles of the previously characterized *wtf4* gene from the *S. kambucha* isolate of *S.*
151 *pombe* [15,22,23] (Fig 1D).
152
153 Our initial model, based on Wtf4^{poison}, was that Wtf^{poison} toxicity is linked to the ability of a Wtf^{poison}
154 to self-assemble [15]. To test this idea, we assayed if other functional Wtf^{poison} proteins besides
155 wild-type Wtf4^{poison} also self-assemble. To do this, we used the Distributed Amphifluoric FRET
156 (DAmFRET) approach, in which proteins are tagged with the photoconvertible mEos3.1
157 fluorophore (referred to as mEos hereafter) and expressed in *S. cerevisiae*. A uniform fraction of
158 the green mEos population is photoconverted to its red form, and protein-protein interactions
159 are then detected as FRET (Fluorescence Resonance Energy Transfer) between the green and
160 red fluorophores within single cells. Monomeric mEos exhibits negligible FRET and is used as a
161 negative control (Fig 2A and 2B) [15,30].
162
163 We first tagged four toxic (*S. cryophilus* Wtf1^{poison}, *S. osmophilus* Wtf41^{poison}, and *S. octosporus*
164 Wtf25^{poison} and Wtf61^{poison}) and one non-toxic (*S. osmophilus* Wtf19^{poison}) Wtf^{poison} protein at the
165 C-terminus with mEos. The tagged proteins retained their toxic/non-toxic phenotypes when
166 expressed in *S. cerevisiae* using a galactose-inducible expression system (Fig 2C) [19]. The
167 assayed proteins all share less than 20% amino acid identity with Wtf4^{poison}, which we use as a
168 positive control (S1B Fig). We found that all five newly tested Wtf^{poison}-mEos proteins, including
169 the nontoxic Wtf19^{poison}-mEos, exhibited self-assembly (Fig 2B). It is important to note, however,
170 that the data reported for Wtf25^{poison}-mEos are limited and we could not reliably assay that

171 protein via DAmFRET. This is because only living cells are considered in DAmFRET and
172 Wtf25^{poison}-mEos kills cells rapidly at low expression (e.g. they die faster than cells expressing
173 Wtf4^{poison}).
174
175 We also assayed DAmFRET in partial deletion alleles of *wtf4^{poison}-mEos* (S2 and S3 Figs).
176 Some of these alleles are described in more detail below, but for this section, we focused on
177 exploring the potential connection between assembly and toxicity. The two toxic mutant
178 Wtf4^{poison} proteins tested, Wtf4-ex5Δ^{poison}-mEos (S2A and S2D-F Fig) and Wtf4Δ$^{20\text{-}poison}$-mEos
179 (S3A-E Fig) both exhibited self-assembly. Of these two proteins, Wtf4Δ$^{20\text{-}poison}$-mEos is more like
180 wild-type Wtf4^{poison}-mEos, in both toxicity and degree of assembly (S2D-F and S3B-E Figs).
181 Most non-toxic Wtf4 mutant proteins (Wtf4-TMD1Δ^{poison}-mEos, Wtf4-ex3Δ^{poison}-mEos, Wtf4-
182 ex4Δ^{poison}-mEos, Wtf4-ex6Δ^{poison}-mEos and Wtf4-consΔ^{poison}-mEos) exhibited reduced assembly
183 compared to the wild-type (S2A-E and S3A-D Figs). We did, however, find one exceptional
184 mutant protein, Wtf4Δ$^{10\text{-}poison}$-mEos. This protein was not toxic but showed similar assembly to
185 the wild-type protein (S3A-D Fig). We could not reliably assay the assembly of some alleles
186 (Wtf4-TMD2Δ^{poison}-mEos, Wtf4-TMD6Δ^{poison}-mEos and Wtf4-ex2Δ^{poison}-mEos) due to low
187 fluorescence signal (S2A, S2B and S4 Figs).
188
189 These results show that Wtf^{poison} self-assembly is broadly conserved (over 100 million years)
190 and can be supported by a wide range of amino acid sequences (e.g., proteins sharing <20%
191 amino acid identity, S1B Fig). Given the broad conservation of self-assembly, that all the toxic
192 alleles exhibited assembly, and that mutant alleles with reduced toxicity also exhibited reduced
193 assembly, our results strongly support an association between self-assembly and toxicity.
194 Importantly, our results also demonstrate that self-assembly alone is insufficient for Wtf^{poison}
195 toxicity, as we found several Wtf^{poison} proteins (Wtf19-mEos and Wtf4Δ$^{10\text{-}poison}$-mEos) that
196 assemble but are not toxic.
197
198 **Deletion alleles demonstrate that both conserved and non-conserved regions contribute**
199 **to Wtf4^{poison} self-assembly and toxicity.**
200 Our deletion mutants in *wtf4^{poison}* encompass both non-conserved and conserved sequences
201 allowing us to test the functional importance of both sequence types (Fig 1; [19-21]). Within *S.*
202 *pombe* Wtf proteins, there is one well conserved 29 base pair segment found at the beginning of
203 exon 3 (Fig 1B; [20]). The Wtf4-consΔ^{poison}-mEos protein lacks this domain and has disrupted

204 self-assembly and is non-toxic, indicating the conserved sequence has a functional role in both
205 Wtf4^{poison} assembly and toxicity (S2C-E Fig).
206
207 We similarly found that several regions that are poorly conserved in Wtf proteins are functionally
208 important in Wtf4^{poison}. For example, exon 4 is not conserved within functional *wtf* genes, even
209 within *S. pombe* [19, 20, 25]. Still, our results demonstrate exon 4 is functionally important in
210 *wtf4* as the Wtf4-ex4Δ^{poison}-mEos protein has disrupted self-assembly and is not toxic (S2A, S2D
211 and S2E Fig). An additional variable feature of *wtf* genes is the number of predicted
212 transmembrane domains, which varies between four and eight within functional Wtf proteins (S2
213 Table). The *wtf4* gene has 6 predicted transmembrane domains and we assayed individual
214 deletions of three (Wtf4-TMD1Δ^{poison}-mEos, Wtf4-TMD2Δ^{poison}-mEos and Wtf4-TMD6Δ^{poison}-
215 mEos). All three transmembrane deletions disrupted toxicity, indicating they are also functionally
216 important (S2B, S2D and S2E Fig).
217
218 An additional set of deletion mutants we queried in a poorly conserved region followed up on an
219 observation by Hu et al [17] in one of the inaugural papers describing *wtf* drivers. In that work,
220 Hu et al [17] described 10 amino acid C-terminal truncations of two *wtf* genes known as *cw9*
221 and *cw27*. These mutant alleles both exhibited disrupted Wtf^{poison}, but not Wtf^{antidote} activity,
222 implicating the C-terminus in Wtf^{poison} function. These proteins share 62% amino acid identity in
223 the C-terminal exon 6 with each other and, at most, 70% with Wtf4. We tested if a similar 10
224 amino acid truncation of *wtf4* would specifically disrupt Wtf4^{poison} activity. This mutation gave us
225 the exceptional *wtf4-Δ^{10}* allele described above that encodes a non-toxic Wtf4Δ$^{10\text{-}poison}$, that
226 surprisingly exhibits wild-type self-assembly (S3A-D Fig). To expand our analyses beyond *wtf4*,
227 we also made 10 amino acid C-terminal truncations of *S. cryophilus* Wtf1*, S. osmophilus* Wtf41*,*
228 *S. octosporus* Wtf61 and Wtf25 poison. These proteins are all significantly smaller than Wtf4
229 (S1C Fig). Surprisingly, we found that these additional truncated proteins all retained toxicity
230 (S3F and S3G Fig) and could be rescued by the corresponding antidotes (S5 Fig) indicating the
231 C-termini are not universally important for Wtf^{poison} function.
232
233 We extended our deletion analyses of the C-terminus of Wtf4 poison and were surprised to find
234 that deleting ten more amino acids than the ten missing in the non-toxic Wtf4Δ$^{10\text{-}poison}$ protein
235 restored toxicity. Specifically, the Wtf4Δ$^{20\text{-}poison}$ protein exhibited robust self-assembly and near
236 wild-type levels of toxicity (S3A-D Fig). A larger deletion of 29 amino acids, Wtf4ex6Δ^{poison},
237 showed reduced self-assembly and was not toxic (S3A-D Fig).

238

239 Together, our results show that even non-conserved sequences can have context-dependent
240 importance within a Wtf^{poison} protein. Specifically, a feature (e.g. the residues encoded in exon 4,
241 or the last 10 amino acids of Wtf4^{poison}) can be functionally important in one Wtf^{poison} protein but
242 be missing or dispensable in another. This, combined with the lack of conservation within Wtf
243 proteins, suggests that the contextually important amino acids (like the last 10 of Wtf4^{poison}) do
244 not have a specific function, but can rather contribute to the overall properties of the protein.
245 Changes in these contextually important regions can be complemented by changes elsewhere
246 in the protein.
247

248 **Intracellular localization of mutant Wtf^{poison} proteins is correlated with toxicity.**
249 We identified self-assembly as one feature shared by functional Wtf^{poison} proteins and suspected
250 that intracellular localization could be another, since we previously found that the toxic *S.*
251 *octosporus* Wtf25^{poison}-mCherry exhibited similar localization to that of toxic Wtf4^{poison} [19].
252 Specifically, both poisons show small puncta broadly distributed in the cytoplasm of *S.*
253 *cerevisiae* cells, with minor localization to what appears to be the endoplasmic reticulum (ER;
254 [15,19]). All functionally confirmed Wtf driver proteins have multiple predicted transmembrane
255 domains (S2 and S3 Tables) and hence, this localization pattern may reflect the poison being
256 trafficked from the ER through the secretory pathway, through the Golgi and trans-Golgi network
257 [24].
258

259 To test the hypothesis that a link exists between the intracellular distribution and toxicity of
260 Wtf^{poison} proteins, we imaged the wild-type Wtf^{poison}-mEos proteins described above in *S.*
261 *cerevisiae* cells. The localization of the *S. octosporus* Wtf25^{poison}-mEos was similar to the
262 previously described Wtf25^{poison}-mCherry described above (Fig 2D). The additional toxic Wtf^{poison}
263 proteins from *S. octosporus*, *S. osmophilus* and *S. cryophilus*, also exhibited dispersed puncta,
264 like the toxic Wtf4^{poison}-mEos control cells (Fig 2D). The nontoxic *S. osmophilus* Wtf19^{poison}-
265 mEos, however, showed a distinct localization pattern with strong signal enrichment in what
266 appears to be the ER (Fig 2D). These data are consistent with our hypothesis that there is a link
267 between intracellular distribution and toxicity with toxic Wtf^{poison} proteins exhibiting distributed
268 puncta.
269

270 To further test our hypothesis, we also assayed the localization of the mutant Wtf4^{poison} proteins
271 mentioned above (S2F and S3E Figs). The most toxic mutant protein, Wtf4Δ^{20poison}-mEos,

localized in distributed puncta like wild-type (S3A-C and S3E Fig). The less toxic Wtf4-ex5Δ^{poison}-mEos protein also formed some distributed puncta, but also exhibited more ER-like localization than wild-type (S2A, S2D and S2F Fig). Most of the non-toxic mutant Wtf4^{poison} proteins (Wtf4-TMD1Δ^{poison}-mEos, Wtf4-TMD2Δ^{poison}-mEos, Wtf4-ex2Δ^{poison}-mEos, Wtf4-ex3Δ^{poison}-mEos, Wtf4-ex4Δ^{poison}-mEos, and Wtf4-consΔ^{poison}-mEos) were less dispersed and exhibited a largely ER-like localization, similar to the non-toxic *S. osmophilus* Wtf19^{poison}-mEos (Fig 2C-D and S2A-D and S2F Fig). One additional non-toxic mutant, Wtf4-TMD6Δ^{poison}-mEos, localized to the vacuole, reminiscent of Wtf^{antidote} protein localization (S2B, S2D and S2F Fig). The non-toxic Wtf4-ex6Δ^{poison}-mEos had a unique localization pattern that combined a diffuse distributed signal with some larger protein assemblies (S3A-C and S3E Fig). Finally, the non-toxic Wtf4Δ$^{10\text{-}poison}$-mEos localization was indistinguishable from wild-type Wtf4^{poison}-mEos (S3A-C and S3E Fig).

In summary, all the toxic Wtf^{poison} proteins show a distributed puncta localization pattern, like Wtf4^{poison}. All except one non-toxic Wtf^{poison} protein showed a distinct localization pattern from Wtf4^{poison}, most often with enhanced ER-like localization. These results parallel our DAmFRET analyses where all toxic Wtf^{poison} proteins assemble and all the nontoxic proteins, except one, show reduced or lack of assembly. In both cases, the exceptional protein is Wtf4Δ$^{10\text{-}poison}$, which is non-toxic, but shows wild-type assembly and localization in cells. Despite the exception, our results show that Wtf^{poison} self-assembly (assayed by DAmFRET) combined with cellular localization patterns are good predictors of Wtf^{poison} protein toxicity (Fig 7A).

Altering assembly properties of Wtf^{poison} proteins affects toxicity.

To further test the model that the toxicity of Wtf^{poison} proteins is tied to their self-assembly, we sought to alter the assembly properties of Wtf4^{poison} using tags. We first aimed to increase the overall size of the Wtf4^{poison} assemblies. To do this, we employed a recently described tool to oligomerize mEos3-fused proteins in trans. Specifically, we expressed a fusion protein consisting of the human ferritin heavy chain protein (FTH1) and a nanobody that recognizes mEos (mEosNB) [31]. The FTH1 domain self assembles to form a 24-mer core and can form supramolecular clusters when fused to self-assembling proteins [32,33]. In our assay, we expressed Wtf4^{poison}-mEos from a galactose inducible promoter and the mEosNB-FTH1 from a doxycycline repressible promoter (Fig 3A and 3B). As expected, we found that Wtf4^{poison}-mEos formed fewer and larger puncta inside cells in the presence of mEosNB-FTH1, consistent with the mEosNB-FTH1 complexes bringing Wtf^{poison}-mEos assemblies into supramolecular clusters

306 (i.e., -Dox panels, Fig 3C). Expression of the mEosNB-FTH1 alone had no effect on yeast
307 growth (Fig 3D, panel (i)). While expression of the Wtf4^{poison}-mEos alone was toxic, co-
308 expression of the mEosNB-FTH1 and Wtf4^{poison}-mEos markedly suppressed the toxicity of the
309 Wtf4^{poison}-mEos (Fig 3D, compare panel (ii) to panel (iii)). We also observed the same
310 suppression of toxicity with four additional toxic Wtf^{poison}-mEos proteins in the presence of the
311 mEosNB-FTH1, indicating the effect was not specific to Wtf4^{poison} (Fig 3C and 3D). These
312 results indicate that these supramolecular Wtf^{poison} assemblies are non-toxic. This effect could
313 be due to altered intracellular localization and/or the reduced exposed surface area of the
314 Wtf^{poison} assemblies.
315
316 We next attempted to increase the solubility Wtf4^{poison} assemblies using a modified N-terminal
317 domain (NT*) tag derived from spidroins, a principal component of spider silk [34]. The NT* tag
318 can decrease protein aggregation, which is the role of the native domain in spiders [35–39]. We
319 added NT* to the N-terminus of the Wtf4^{poison}-mEos to generate NT*-Wtf4^{poison}-mEos (Fig 4A).
320 We found that this protein had a novel combination of assembly and localization not
321 represented in any of our other alleles. Specifically, the NT*-Wtf4^{poison}-mEos protein showed
322 less self-assembly than Wtf4^{poison}-mEos (Fig 4C), but the NT* tag did not visibly alter the
323 localization of the protein within cells (Fig 4E). Interestingly, the NT*-Wtf4^{poison}-mEos protein
324 showed increased toxicity in cells (Fig 4B). To test if the effects of the NT* tag were specific to
325 Wtf4^{poison} or more general, we also tagged *S. octosporus* Wtf25^{poison} with NT* to generate NT*-
326 Wtf25^{poison}-mEos (S6A Fig). As with NT*-Wtf4^{poison}-mEos, we observed unaltered localization
327 and increased toxicity of the NT*-Wtf25^{poison}-mEos protein, relative to wild-type Wtf25^{poison}-mEos
328 (S6B and S6D Fig). We could not, however, quantify NT*-Wtf25^{poison}-mEos assembly by
329 DAmFRET as the high toxicity prevented us from obtaining sufficient viable cells with mEos
330 fluorescence (S4E Fig).
331
332 We also assayed how another solubility tag, the *E. coli* Maltose Binding Protein (MBP), affected
333 Wtf^{poison} toxicity [40–42]. The MBP-tagged Wtf4^{poison} (MBP-Wtf4^{poison}-mEos) had the same
334 phenotype as the NT*-tagged Wtf4^{poison} protein: decreased assembly, increased toxicity,
335 unaltered localization, relative to the wild-type protein (S7 Fig). The phenotype of the MBP-
336 tagged Wtf25^{poison} (MBP-Wtf25^{poison}-mEos) however, did not mirror that of the NT*-tagged
337 protein. Instead, we found that the MBP-Wtf25^{poison}-mEos protein showed reduced, but still high
338 toxicity. The MBP-Wtf25^{poison}-mEos protein also showed an altered, stronger endoplasmic
339 reticulum-like localization, as compared to the wild-type protein (S7A-C Fig). This protein thus

340 adds to those described above in which we see more ER-like localization associated with
341 reduced Wtf^{poison} toxicity. The MBP-Wtf25^{poison}-mEos protein did exhibit self-assembly, but we
342 could not compare it the wild-type protein as high toxicity limited the viable cells we could assay
343 via DAmFRET (S4F and S7D Figs).
344
345 The bulk of our experiments are consistent with a model where the assembly properties and the
346 distribution of Wtf^{poison} proteins within cells affects toxicity, with distributed, punctate assemblies
347 exhibiting more toxicity. Increasing Wtf^{poison} solubility (while maintaining assembly), increases
348 toxicity, unless localization is disrupted. Forcing Wtf^{poison} proteins into large, localized
349 assemblies, suppresses toxicity. The non-toxic Wtf4Δ$^{10\text{-}poison}$ protein that forms distributed
350 assemblies, however, undermines this simple model or at least indicates that there are
351 additional unidentified features that are essential for toxicity.
352
353 An additional possibility that we considered was that the expression levels of the Wtf^{poison}
354 proteins likely contributes to the phenotypes we observed, despite expressing all alleles from a
355 common vector backbone using a common promoter. To assay expression levels, we quantified
356 fluorescence of the mEos tags shared by all alleles. We did not use western blots as that
357 approach is challenging to apply to Wtf^{poison} proteins as they are toxic and highly hydrophobic
358 [15,23]. Instead, we looked at the acceptor (red form of mEos) fluorescence in live cells
359 analyzed in the DAmFRET experiments (S4 Fig; Data from Figs 2B, 4C, S2E and S3D). As
360 expected, based on other studies [43–46], we observed significant fluorescent protein signal
361 heterogeneity within cells expressing the monomer mEos control and each Wtf^{poison} protein
362 tested (S4 Fig). We did not, however, find increased fluorescent signal in cells expressing the
363 most toxic proteins (as determined by growth assays). On the contrary, we tended to observe
364 less signal in the cells expressing the most toxic proteins (e.g., Wtf4^{poison} and NT*-Wtf4^{poison}).
365 These data support a model in which cells expressing the higher levels of toxic proteins are
366 more likely to be removed by death and are not quantified. As mentioned above, however, we
367 also observed low signal in the cells expressing the non-toxic Wtf4-ex2Δ^{poison}, Wtf4-TMD2Δ^{poison},
368 and Wtf4-TMD6Δ^{poison} alleles (S4 Fig). The low levels of Wtf4-TMD6Δ^{poison} could be due to its
369 degradation in the vacuole (S2F Fig). For the other two alleles, it is formally possible the low
370 levels of these proteins in cells could contribute to their lack of toxicity.
371
372 **Limited modularity of the Wtf^{antidote}-specific domain.**

We next wanted to test which protein features affect Wtf4^{antidote} function (Fig 1A and 1B). As described above, the Wtf4^{antidote} shares the resides encoded by exons 2-4 with the Wtf4^{poison} but has an additional N-terminal domain encoded by exon 1. We hypothesized that the amino acids encoded by exon 1 would be insufficient for function and that exons 2-6 would be required for protein self-assembly as they comprise the Wtf4^{poison} protein, which self-assembles [15]. As expected, we found that a protein consisting of only the exon 1-encoded residues linked to a mEos tag (Wtf4 Exon1-mEos) could not self-assemble (S8A and S8B Fig). The Wtf4 Exon1-mEos protein was also not trafficked to the vacuole, despite this protein harboring two PY motifs that promote ubiquitin-mediated trafficking of wild-type Wtf^{antidote} proteins [24] (S8E Fig). Finally, the Wtf4 Exon1-mEos protein could not rescue Wtf4^{poison} toxicity, which parallels recent results using distinct Wtf proteins (S8C and S8F Fig) [24]. These results demonstrate that the antidote-specific domain encoded by *wtf4* exon 1 is insufficient for antidote function.

To test if the exon 1 encoded domain was modular, we generated two mutants *wtf4^{poison}-ex1* and *wtf4^{poison}-ex1^{int}*. The *wtf4^{poison}-ex1* allele moves the antidote-specific domain moved to the C-terminus of the protein (S8A Fig). The *wtf4^{poison}-ex1^{int}* allele moved exon 1 a more central region of the protein (beginning of exon 4). This location is between the last two predicted transmembrane domains and is not predicted to disrupt them (Fig 1B). We found that mEos tagged versions of both Wtf4^{poison}-ex1 and Wtf4^{poison}-ex1^{int} proteins were both non-toxic and trafficked to the vacuole, suggesting they retained at least some antidote functionality (S8D and S8F Fig). Only the Wtf4^{poison}-ex1, however, could neutralize the toxicity of Wtf4^{poison}-mCherry (S8D and S8F Fig). These results demonstrate that the domain encoded by exon 1 is at least partially modular, but that a central location within the polypeptide can disrupt the Wtf^{antidote} protein's ability to neutralize a Wtf^{poison}. We speculate this could be because extensive, continuous, amino acid identity facilitates Wtf^{poison} and Wtf^{antidote} co-assembly.

Wtf^{antidote} requires more than physical linkage to effectively traffic Wtf^{poison} to the vacuole

We next wanted to determine if co-assembly serves merely to link Wtf^{poison} and Wtf^{antidote} proteins to allow for co-trafficking, or if co-assembly serves a more nuanced role in neutralizing Wtf^{poison} toxicity. To test this, we generated Wtf^{poison} and Wtf^{antidote} proteins that were physically linked, but not co-assembled, by artificially tethering Wtf^{poison} proteins to diverged Wtf^{antidote} proteins, with which they cannot co-assemble, using a combination of GFP and GFP-binding protein (GBP) tags (Figs 5A, 5B, S9A and S9B).

407 We first tested if tethering Wtf4^{poison} to *S. octosporus* Wtf61^{antidote} could neutralize the toxic
408 Wtf4^{poison}. We generated Wtf4^{poison}-GBP-mCherry and Wtf61^{antidote}-GFP proteins and found the
409 tags did not disrupt protein function. Specifically, the Wtf4^{poison}-GBP-mCherry protein was toxic,
410 and could be rescued by Wtf4^{antidote} proteins, including Wtf4^{antidote}-GFP. Similarly, the
411 Wtf61^{antidote}-GFP protein was able to rescue Wtf61^{poison}-mCherry (Fig 5C). However, Wtf61^{antidote}-
412 GFP was not able to efficiently traffic Wtf4^{poison}-GBP-mCherry to the vacuole or neutralize its
413 toxicity (Fig 5C and 5D). This failure to rescue is not a failure of the GFP-GBP interaction to link
414 the proteins as we found that the Wtf61^{antidote}-GFP and Wtf4^{poison}-GBP-mCherry proteins largely
415 co-localized, which they did not do in the absence of the GBP tag (Fig 5D). Moreover, the
416 localization of the tethered Wtf61^{antidote}-GFP-Wtf4^{poison}-GBP-mCherry changed relative to the
417 individual proteins: the Wtf61^{antidote}-GFP no longer trafficked to the vacuole and Wtf4^{poison}-GBP-
418 mCherry was less distributed in cells. Effective GFP-GBP linkage is the most parsimonious
419 explanation of these observations. To test if our results were generalizable, we also analyzed a
420 widely diverged, independent pair of Wtf proteins (*S. octosporus* Wtf25^{poison} and *S. cryophilus*
421 Wtf1^{antidote}). Our results with this protein pair mirrored those described above suggesting that
422 specific antidote-poison co-assembly generally promotes proper antidote function (S9 Fig).
423
424 Given that the tethered Wtf61^{antidote}-GFP and Wtf4^{poison}-GBP-mCherry were often adjacent to
425 vacuoles and not totally distributed in cells, as occurs when trafficking of Wtf proteins is
426 disrupted [15], we suspected that the vacuolar targeting was still occurring, but blocked at a late
427 step in the process (e.g., vacuole entry). Consistent with this notion, the assemblies often co-
428 localized with the Rnq-1mCardinal protein, which is a prion protein that marks the insoluble
429 protein deposit (IPOD) [47–49] (Fig 5E). This result was surprising to us because with a different
430 expression system (β-estradiol induction) a considerable amount of the Wtf4^{poison}/Wtf4^{antidote} co-
431 assemblies accumulate at the IPOD are not toxic to cells [15]. It is unclear why GFP/GBP
432 mediated assemblies, but not Wtf/Wtf mediated co-assemblies, would be toxic at the IPOD, but
433 we speculate about this in the discussion.
434
435 Beyond the GFP/GBP tethering experiments, we made additional observations suggesting that
436 a specific nature of co-assembly with Wtf^{poison} is required for Wtf^{antidote} function. When
437 characterizing the toxic NT*-Wtf4^{poison} protein (with the NT* domain that increases solubility), we
438 found that this protein was not effectively rescued by wild-type Wtf4^{antidote}-mCherry (Fig 4D).
439 This drastic reduction in rescue (relative to that observed with the wild-type Wtf4^{poison}) is striking
440 given that the colocalization of NT*-Wtf4^{poison}-mEos with Wtf4^{antidote}-mCherry appears only mildly

441 reduced relative to that observed between wild-type Wtf4 proteins (Figure 4E and 4F). In
442 addition, the localization of the NT*-Wtf4^{poison}-mEos is altered in the presence of Wtf4^{antidote}-
443 mCherry (it becomes less distributed compared to wild type Wtf4 proteins; Fig 4E). These
444 observations suggest the NT*-Wtf4^{poison}-mEos and Wtf4^{antidote}-mCherry proteins interact, but are
445 not efficiently trafficked into the vacuole (Fig 4E). This is analogous to the GFP/GBP linked, but
446 unassembled, Wtf^{poison} and Wtf^{antidote} pairs described above. The effect of the NT* tag on
447 Wtf^{poison}/Wtf^{antidote} compatibility was not, however, universal. We did not observe strong
448 disruption of poison/antidote compatibility caused by the NT* tag on *S. octosporus* Wtf25^{poison}
449 (NT*-Wtf25^{poison} allele, S6 Fig), indicating that factors affecting poison/antidote compatibility can
450 be context dependent.
451
452 Together, our results demonstrate that a physical linkage is insufficient to ensure efficient
453 neutralization of a Wtf^{poison} protein's toxicity by a Wtf^{antidote}. Instead, specific co-assembly of the
454 proteins likely both links compatible Wtf^{poison} and Wtf^{antidote} proteins and facilitates their effective
455 co-trafficking into the vacuole.
456
457 **C-terminal region supports Wtf4^{antdiote} function**
458 As introduced above, Hu et al [17] previously described mutant alleles of two *S. pombe wtf*
459 genes lacking the codons for the last 10 amino acids. Those mutants maintained Wtf^{antidote}
460 activity [17]. To test if the C-terminal amino acids were generally dispensable for antidote
461 function, we made *wtf4^{antidote}* truncation alleles. We found that a 10 amino acid truncation of
462 Wtf4, (Wtf4Δ$^{10\text{-antidote}}$-mCherry) was slightly toxic to cells, as compared to the Wtf4^{antidote}-mCherry
463 and empty vector controls (S10 Fig). A 20 amino acid truncation of the, Wtf4Δ$^{20\text{-antidote}}$-mCherry,
464 showed even more toxicity, although it was still considerably less than the toxicity observed with
465 the Wtf4^{poison}-mCherry. A 29 amino acid truncation, Wtf4-ex6Δ^{antidote}-mCherry, exhibited no
466 toxicity (S10 Fig). These results suggest that the C-terminal 20 amino acids of Wtf4^{antidote} play a
467 role in limiting the toxicity of the Wtf4^{antidote} protein.
468
469 We next tested if the truncation Wtf4^{antidote} proteins could rescue the toxicity of a wild-type
470 Wtf4^{poison}-mEos protein. Neither the Wtf4Δ$^{10\text{-antidote}}$-mCherry or Wtf4-ex6Δ^{antidote}-mCherry proteins
471 appreciably neutralized Wtf4^{poison}-mEos toxicity (S10A and S10B Fig). The Wtf4Δ$^{20\text{-antidote}}$-
472 mCherry protein, however, rescued growth of cells expressing Wtf4^{poison}-mEos to a level
473 comparable to that observed in the cells expressing only Wtf4Δ$^{20\text{-antidote}}$-mCherry. So, despite the
474 slight toxicity of the Wtf4Δ$^{20\text{-antidote}}$-mCherry protein, it still retained some antidote function.

Interestingly, we were surprised to see that the other truncated antidotes Wtf4Δ$^{10\text{-antidote}}$-mCherry and Wtf4-ex6Δ^{antidote}-mCherry could also partially rescue the toxicity of Wtf4Δ$^{20\text{-poison}}$-mEos poison, although it was much less rescue compared to that of the wild-type Wtf4^{antidote}-mCherry protein (S10A and S10B Fig). This demonstrates that these truncated proteins retain some functionality.

Our results indicate that the C-terminus supports Wtf4^{antidote} function, but that some functionality remains even in the absence of the last 29 amino acids. When considered in combination with the results of Hu et al [17], our combined results indicate that the importance of the C-terminus is context dependent. Like our Wtf^{poison} results discussed earlier, these observations, combined with the lack of conservation of Wtf proteins, suggests that Wtf^{antidote} function (outside of the conserved PY motifs) relies on overall properties of the protein (e.g., lack of toxicity and ability to co-assemble with a matching Wtf^{poison}), rather than any functional domain.

Self-killing alleles that encode a functional Wtf^{poison} with an incompatible Wtf^{antidote}

Because Wtf proteins are encoded on largely overlapping coding sequences, a change in the shared coding sequence can simultaneously create a novel Wtf^{poison} protein and a matching novel Wtf^{antidote} protein. Our engineered mutant alleles offered the opportunity to explore if matching proteins are always compatible (i.e., if a novel toxic Wtf^{poison} protein is always neutralized by its corresponding Wtf^{antidote} protein).

We therefore explored poison and antidote compatibility more broadly within the alleles we generated. In many cases, the Wtf^{antidote} proteins were able to rescue their matching Wtf^{poison} alleles (S1 Table). One class of mutants, however, created toxic Wtf^{poison} proteins that were not rescued by the matching Wtf^{antidote}. In *wtf4*, these mutants changed a region of exon 6 that encodes a 7 amino acid repeat found in variable numbers (0-84 base pairs of repeat sequence) within *S. pombe wtf* genes (Fig 6A and 6B) [20]. The repeat region in *wtf4* encodes one complete repeat plus three additional amino acids of the repeat (Fig 6C). We found that mutating this region in Wtf4 by either scrambling the amino acid order (Wtf4-rep2^{sc}) or by replacing the ten amino acids with alanine (Wtf4-rep2^{A} allele) generated toxic Wtf^{poison} proteins that were not neutralized by their matching Wtf^{antidote} proteins (Fig 6D). The Wtf4-rep2$^{\text{sc-antidote}}$-mCherry and Wtf4-rep2$^{\text{A-antidote}}$-mCherry proteins were both trafficked to the vacuole when expressed alone but did not effectively co-traffic their corresponding Wtf^{poison} proteins (Fig 6E).

509 The Wtf4-rep2$^{sc\ antidote}$-mCherry and Wtf4-rep2$^{sc\ poison}$-mEos proteins showed decreased co-
510 localization, relative to wild-type proteins, suggesting the proteins had disrupted co-assembly
511 (Fig 6E and 6F). Alternatively, the Wtf4-rep2$^{A\ antidote}$-mCherry and Wtf4-rep2$^{A\ poison}$-mEos proteins
512 colocalized (Fig 6F) but remained more distributed within cells relative to wild-type (Fig 6E). This
513 distributed localization is a change from the vacuolar localization of Wtf4-rep2$^{A\ antidote}$-mCherry
514 alone, further supporting that the Wtf4-rep2$^{A\ antidote}$-mCherry and Wtf4-rep2$^{A\ poison}$-mEos are
515 interacting. Therefore, the incompatibility of the Wtf4-rep2^{A} proteins adds additional support to
516 our earlier conclusion that a particular form of association is required between Wtf^{antidote} and
517 Wtf^{poison} proteins to ensure the poison is effectively trafficked to the vacuole and neutralized.
518
519 We also assayed the effects of deleting the repeat region of *wtf4* exon 6 alone (*wtf4-rep2Δ*
520 allele), or in combination with deleting another repetitive region found in exon 3 (*wtf4-rep1-2Δ*
521 allele; S11A Fig) [20]. We found that the Wtf4-rep2Δ^{poison}-mEos protein is toxic but is only
522 partially rescued by Wtf4-rep2Δ^{antidote}-mCherry, relative to the rescue observed between wild-
523 type Wtf4 poison and antidote proteins (S11D Fig). We found that the two Wtf4-rep2Δ proteins
524 exhibit decreased colocalization, relative to wild-type proteins, suggesting the limited rescue is
525 due to disrupted poison-antidote interaction (S11E and S11F Fig). Interestingly, we found that
526 the defect in poison-antidote compatibility conferred by the deletion of the exon 6 repeats in the
527 *wtf4-rep2Δ* allele is partially suppressed by also deleting the repetitive region found in exon 3.
528 Specifically, the proteins encoded by the *wtf4-rep1-2Δ* allele, with both regions deleted, have
529 near wild-type phenotypes (S11 Fig). We observed no defects in poison and antidote
530 compatibility in the proteins encoded by an allele (*wtf4-rep1Δ*) lacking only the repetitive region
531 in exon 3 (S11A, S11B, S11D-F Fig).
532
533 Finally, we also tested if the novel mutations we made in this study in the exon 3 or C-terminal
534 repeats affected compatibility with wild-type Wtf proteins. In all cases tested, the repeat mutant
535 Wtf^{poison} proteins were not neutralized by their wild-type Wtf^{antidote} counterparts and vice versa
536 (S12 Fig). For example, Wtf4-rep1Δ^{poison}-mEos is not neutralized by Wtf4^{antidote}-mCherry and
537 Wtf4^{poison}-mEos is not neutralized by Wtf4-rep1Δ^{antidote}-mCherry (S12B Fig).
538
539 The repeats in exon 6, but not in exon 3, are broadly conserved in the *wtf* gene family [19]. We
540 also mutated the homologous region in *S. octosporus wtf25* and found analogous phenotypes
541 as those described above in *wtf4* (S13 Fig). Like *wtf4*, *S. octosporus wtf25* also encodes 10
542 amino acids in this C-terminal region (S13A-C Fig). We generated the *S. octosporus wtf25-*

543 *rep2*^{Sk} allele by swapping the endogenous codons for those of *wtf4*. We found that this allele
544 encoded an incompatible Wtf25-rep2$^{Sk\text{-poison}}$-mCherry and Wtf25-rep2$^{Sk\text{-antidote}}$-mEos pair (S13D
545 Fig). Surprisingly, the individual Wtf25-rep2^{Sk} proteins were compatible with Wtf25 proteins (i.e.,
546 Wtf25-rep2$^{Sk\text{-poison}}$-mCherry was rescued by Wtf25^{antidote}-mEos and vice versa; S13D Fig). We
547 also deleted the repeat region of *S. octosporus wtf25* (to generate the *wtf25-rep2Δ* allele) and
548 again found phenotypes similar to those observed in the analogous *wtf4* mutant (*wtf4-rep2Δ*)
549 (S14 Fig). Specifically, the Wtf25-1^{antidote}-mCherry showed reduced rescue of the Wtf25-
550 rep2Δ^{poison}-mEos toxicity, relative to the wild-type Wtf25 protein pair (S14C Fig).
551
552 Altogether, our results further support a critical role for the repeats in Wtf^{poison} and Wtf^{antidote}
553 compatibility and reveal that mutants in this domain can encode Wtf^{poison} proteins not neutralized
554 by the matching Wtf^{antidote} proteins. Such alleles are important constraints on *wtf* gene evolution
555 as they would contribute to infertility via self-killing.
556
557 **Discussion**
558
559 **Protein assembly plays conserved roles in Wtf protein function.**
560 The mutant analyses provided in this work expands and supports a working model in which 1)
561 Wtf^{poison} toxicity is tied to the homotypic assembly of the proteins [15], 2) Wtf^{antidote} proteins are
562 ubiquitinated and trafficked to the vacuole [15,24] and, 3) Wtf^{antidote} proteins co-assemble with
563 their matching Wtf^{poison} proteins and co-traffic them to the vacuole [15,26]. Recent work has
564 established that ubiquitin-mediated Wtf^{antidote} trafficking and co-trafficking with their
565 corresponding Wtf^{poison} proteins are conserved within the extremely diverse gene family [24]. It
566 was unclear, however, if homotypic protein assembly is a conserved feature of Wtf^{poison} or
567 Wtf^{antidote} protein function.
568
569 The results of this study support the model that homotypic protein assembly plays critical roles
570 in the function of Wtf^{poison} proteins. First, we observed that the ability to self-assemble was
571 conserved amongst functional (i.e., toxic) wild-type Wtf^{poison} proteins from four
572 *Schizosaccharomyces* species (Fig 2). Given that the functional proteins share as little as 20%
573 amino acid identity, these observations likely reflect conserved functional importance of self-
574 assembly. Our mutant analyses of Wtf4^{poison} proteins provided additional support for this model
575 in that all toxic mutant proteins self-assembled (S2 and S3 Figs). Furthermore, we found that
576 the Wtf^{poison} toxicity could be modulated by altering the assembly properties of the protein with

577 tags (Figs 3, 4, S6 and S7). Together, our data suggest that Wtf^{poison} toxicity is tied to protein
578 assembly with distributed, small assemblies showing greater toxicity than localized, larger
579 assemblies (Figs 2-4, 7, S2, S3, S6 and S7). The recent work of Zheng et al. [24] suggests the
580 distributed assemblies may represent localization to the trans-Golgi network.
581
582 Still, it is important to note that the Wtf4Δ$^{10\ poison}$ allele was non-toxic, despite assembling into
583 small, distributed assemblies indistinguishable from those generated by the wild-type protein
584 (S3 Fig). This exceptional protein highlights that even if self-assembly is critical for Wtf^{poison}
585 toxicity, it is not the only factor required. In addition, this allele offers an opportunity for future
586 work to explore features that distinguish toxic from nontoxic protein assemblies.
587
588 Our results also support an expanded, more nuanced role for homotypic protein assembly and
589 trafficking in Wtf^{antidote} function. First, we found that the antidote-specific domain that contains
590 the PY motifs is insufficient to promote vacuole trafficking, suggesting some other features of
591 Wtf proteins are also required (S8 Fig). We posit protein self-assembly could contribute to this
592 function. For Wtf^{antidote} neutralization of a Wtf^{poison}, we initially assumed that co-assembly of
593 Wtf^{antidote} with Wtf^{poison} proteins served only to physically link the proteins, thus enabling the
594 Wtf^{antdiote} to traffic the Wtf^{poison} to the vacuole [15]. We found, however, that physical linkage
595 between a Wtf^{poison} and Wtf^{antidote} can be insufficient to ensure their co-trafficking to the vacuole
596 and neutralization of the Wtf^{poison}'s toxicity. We observed this insufficiency in experiments linking
597 two distinct pairs of non-matching Wtf^{poison} and Wtf^{antidote} proteins with GFP-GBP tags (Figs 5
598 and S9). In addition, we found that the *wtf4-rep2*^{A} and *NT*-wtf4* alleles encode protein pairs in
599 which poison-antidote interaction appeared largely intact, but trafficking into the vacuole and
600 poison neutralization was disrupted (Figs 4 and 6). These experiments suggest that efficient co-
601 trafficking of Wtf^{poison}/ Wtf^{antidote} protein assemblies requires a particular conformation or strong
602 affinity between the interacting proteins not replicated in the ineffective Wtf^{poison}/Wtf^{antidote}
603 combinations mentioned above (Fig 7).
604
605 Moreover, our experiments surprisingly revealed that trafficking toxic Wtf assemblies to the
606 proper destination may not always be sufficient to ensure their neutralization. In previous work
607 using a different induction system than that employed here, we found that much of the trafficked
608 Wtf4^{poison}/Wtf4^{antidote} assemblies accumulated at the insoluble protein deposit (IPOD), in addition
609 to the vacuole [15] and the cells were viable. Similar, but generally smaller, assemblies can be
610 seen accumulating outside of the vacuole (likely the IPOD) in many of the viable cells we image

611 expressing Wtf^{antidote} proteins or compatible Wtf^{poison}/Wtf^{antidote} assemblies using the GAL
612 induction system employed in this study (e.g., Fig 6E panels expressing Wtf4^{antidote} and
613 Wtf4^{antidote}/Wtf4^{poison}). Similarly, Zheng et al [24] found that vacuole localization was not essential
614 for Wtf^{poison} neutralization as they observed that trafficking to the endosome can be sufficient.
615 Here, however, we observed that Wtf4^{poison}-GBP/Wtf61^{antidote}-GFP assemblies (and likely the
616 Wtf25^{poison}-GBP/Wtf1^{antidote}-GFP assemblies) were trafficked to the IPOD, but were still toxic
617 (Figs 5, 7 and S9). These results suggest that factors beyond localization, perhaps assembly
618 conformation, can also affect the toxicity of Wtf proteins.
619
620 **Commonalities between Wtf proteins and other self-assembling proteins.**
621 The Wtf proteins share broad parallels with other nonhomologous proteins that form
622 assemblies. For example, a sequence-independent common oligomeric property may underly
623 the toxicity of unrelated amyloid proteins [50]. While Wtf^{poison} proteins are related to each other,
624 their sequences are extremely diverged. We propose a common feature of their assembled
625 forms is likely responsible for their shared toxicity. Another feature Wtf proteins share with
626 several unrelated proteins is the capacity to form functional assemblies. Multiple amyloidogenic
627 proteins form functional amyloids that perform diverse biological functions, including long term
628 memory in flies [51], epigenetic inheritance in yeast [52] and biofilm formation in bacteria [53–
629 55]. Some functionally aggregating amyloids have also shown to be toxic at intermediate stages
630 of assembly, suggesting that protein toxicity could pose a risk in certain instances [56]. The co-
631 expression of Wtf^{antidote} with the toxic Wtf^{poison} results in a change in its localization and the
632 assembly properties of the Wtf^{poison}-Wtf^{antidote} complex. This suggests that protein-protein
633 interaction within a pair of corresponding Wtf proteins is similar to functional aggregation. While
634 the outcome of functional Wtf protein assembly is different (i.e., successful drive), the delicate
635 interplay between toxic and non-toxic protein assemblies is similar to functional aggregating
636 amyloids.
637
638 The use of E3 ubiquitin ligases to direct protein trafficking is an additional theme Wtf proteins
639 share with other self-assembling proteins acting in diverse cell signaling processes, including
640 immune response [57,58], prion disease [59] and other neurodegenerative disorders [60–66]. In
641 multiple cases, ubiquitination of a key protein results in its aggregation, differential trafficking to
642 specific intracellular locations or degradation, suggesting that this is a common mechanism for
643 enabling downstream signaling processes. Additionally, a lack of ubiquitination by the ligase

644 often results in toxic aggregates [59,62,65] or reduced functionality of the key protein [57,58],
645 which are very reminiscent of the Wtf^{poison}/Wtf^{antidote} assemblies discussed above.
646
647 **Rapidly evolving coding sequence repeats can affect Wtf^{poison}-Wtf^{antidote} compatibility.**
648 Most *S. pombe wtf* genes contain varying copy numbers of a sequence repeat in exon 3 [20].
649 The potential role of the exon 3 repeats was unclear, but all functionally validated *S. pombe wtf*
650 drivers contain the exon 3 repeats (S2 Table). One *wtf* gene (*wtf23* from the CBS5557 strain)
651 that lacks the exon 3 repeats has been tested in *S. pombe* and failed to cause drive in two strain
652 backgrounds, although it was not determined if the encoded proteins were non-functional or if
653 the driver was effectively suppressed [20,25]. Previous work also found that a mismatch of
654 repeat numbers in exon 3 between a Wtf13^{poison} (five repeats) and Wtf18-2^{antidote} (four repeats)
655 could still produce a compatible poison and antidote pair [26]. In this work, we found that
656 deleting the exon 3 repeats in *wtf4* (*wtf4-rep1Δ* allele) produced a functional, compatible Wtf^{poison}
657 and Wtf^{antidote} pair. The Wtf4-rep1Δ^{poison}, however, was not neutralized by the wild-type
658 Wtf4^{antidote}, which has two repeats (S12B Fig). This indicates that the exon 3 repeats can affect
659 Wtf^{poison} and Wtf^{antidote} compatibility in a context dependent fashion.
660
661 Many *S. pombe wtf* genes also contain a sequence repeat in exon 6 [20]. Repeats homologous
662 to those found in *S. pombe* exon 6 can also be found in the C-termini of many genes in *S.*
663 *octosporus* and *S. osmophilus* [19]. All functionally validated drivers contain repeats in *S.*
664 *octosporus*, but one functional *S. pombe* driver (*wtf35* from FY29033) lacks the repeats (S5
665 Table) [19,25]. Previous work demonstrated that a mismatch in the number of exon 6 repeats
666 could affect Wtf^{poison} and Wtf^{antidote} compatibility in *S. pombe* Wtf proteins [15,26]. This current
667 work extends previous work by showing with additional alleles of *wtf4* and novel alleles of *S.*
668 *octosporus wtf25* that copy number mismatches in this region disrupt Wtf^{poison} and Wtf^{antidote}
669 compatibility.
670
671 Overall, our results support the model that the rapid copy number evolution of the repeats found
672 in *wtf* genes contribute to rapid innovation of novel Wtf^{poison} and Wtf^{antidote} pairs [19,20]. These
673 highly evolvable sequences have likely contributed to the long-term evolutionary success of *wtf*
674 drivers, as generating novel alleles allows frequent generation of novel drivers likely to be
675 heterozygous (and thus drive) in crosses. Frequent driver turnover may also complicate the
676 evolution of drive suppressors that are not other *wtf* genes. Still, this work reveals that these

677 hypermutable regions come with a burden as they contain the potential to generate self-killing
678 alleles, which are discussed below.
679
680 **Wtf fitness landscape likely includes self-killing alleles.**
681 Our analyses of mutations in the repeats found in exon 6 of *S. pombe* genes revealed a novel
682 self-killing phenotype in which a *wtf* allele can encode a toxic Wtf^{poison} that is not effectively
683 neutralized by its corresponding $Wtf^{antidote}$. Such an allele is expected to lead to a dominant loss
684 of fertility, analogous to mutations where the antidote protein expression or function is disrupted
685 [17,22,24]. This phenotype was strongest in mutants that changed the sequence of the repeats
686 (i.e., *wtf4-rep2*^{sc}, *wtf4-rep2*^{A} and *wtf25-rep*^{Sk}). These mutations are rather dramatic and have a
687 low probability of arising spontaneously in nature.
688
689 A weaker version of the self-killing phenotype was, however, also observed in mutations that
690 deleted the repeats. Interestingly, the deleterious effects of removing the exon 6 repeats in *wtf4*
691 (*wtf4-rep2Δ* allele) could be suppressed by also deleting the exon 3 repeats (*wtf4-rep1-2Δ*
692 allele) (S12C and S12D Fig). This suppression, in addition to the one functional driver known to
693 lack the exon 6 repeats, shows that changes in other regions of the protein can compensate for
694 the missing repeats. Still, the existence of *wtf* genes without the repeats, and extensive gene
695 conversion within the family, suggests that novel deleterious repeat deletion mutations are likely
696 to arise recurrently in natural populations [19–21].
697
698 We may have also fortuitously sampled one largely self-killing allele from a natural population
699 that did not have disrupted repeats, suggesting there are multiple paths to generating such
700 alleles. The *wtf41* gene from *S. osmophilus* encodes a toxic $Wtf41^{poison}$ that is not efficiently
701 neutralized by the corresponding $Wtf41^{antidote}$ protein (S5C Fig, [19]). All together, we propose
702 self-killing *wtf* alleles could contribute to recurrent, spontaneous sub-fertility or infertility. We
703 propose this spontaneous sub-fertility could be a persistent burden on the population fitness of
704 all *Schizosaccharomyces* species carrying *wtf* drivers.
705
706 **Rapid evolution and the risk of self-killing alleles.**
707 Beyond *wtf* genes, there are many known killer meiotic drivers [3,5,6,8,9,11]. There are also
708 likely many more yet to be discovered, given their accelerated pace of discovery in recent years.
709 Although the genes causing drive in different systems are not homologous, they often share
710 mechanistic and evolutionary themes [13,14,67]. Those themes include production of

711 poisons/killer elements and rapid evolution. The *wtf* genes have illustrated that high evolvability,
712 via nonallelic gene conversion and mutable coding sequence repeats, can facilitate the
713 evolutionary success of meiotic drivers [19,21,68]. This work reveals that rapid evolution of killer
714 elements also presents the risk of generating self-killing alleles. There is no reason to suppose
715 such risks would be specific to the *wtf* killers. Instead, we posit that such self-killing alleles may
716 be a widespread source of recurrent, spontaneous infertility in eukaryotes.
717
718 **Materials and Methods**
719
720 **Cloning**
721
722 We confirmed all the vectors described in this study by Sanger sequencing or by Nanopore
723 sequencing via Plasmidsaurus. The specifics for the yeast strains used in this study are listed in
724 S4 Table, plasmids are in S5 Table and the oligos are in S6 Table.
725
726 ***S. cerevisiae* vectors:**
727
728 *Generation of a Gal-inducible GFP vector to tag alleles:* We amplified GFP-ADH1 terminator
729 from a previously published plasmid, pSZB464 [15] with oligos 3744+3743. We digested this
730 product with SacI and SpeI and cloned it into pDK20 [69] to generate pSZB1528. We then
731 isolated the Gal promoter-GFP-ADH1T after digestion with SacI and KpnI and cloned it into a
732 SacI-KpnI digested pRS316 [70] to generate pSZB1540.
733
734 *Generation of a Gal-inducible mCherry vector to tag alleles:* We amplified mCherry-ADH1
735 terminator from pFA6a-mCherry-kanMX6 [71] with oligos 3745+3743. We digested this product
736 with SacI and SpeI and cloned it into pDK20 [69] to generate pSZB1526. We then isolated the
737 Gal promoter-mCherry-ADH1T after digestion with SacI and KpnI and cloned it into a SacI-KpnI
738 digested pRS314 [70] to generate pSZB1537.
739
740 *Generation of a Gal-inducible mEos3.1 vector to tag alleles:* We digested V08 [30] with SacI and
741 KpnI to release the fragment with Gal promoter- 4x(EAAAR) linker-mEos3.1. We then cloned
742 this into SacI-KpnI digested pRS316 [70] to generate pSZB1460.
743

744 *Generation of a monomer mEos3.1 in an ARS/CEN plasmid:* We cut out Gal-monomer
745 mEos3.1-cyc1T from RHX0935 [30] with SacI and KpnI, and cloned into SacI, KpnI cut pRS316
746 [70] to generate pSZB1514.
747
748 *Generation of Gal-inducible wtf alleles:*
749
750 *S. kambucha wtf4 exon 1:* The 136 base pairs that makes up exon 1 of *S. kambucha wtf4* was
751 synthesized and cloned into pSZB1460 by IDT to generate pSZB1552.
752
753 *S. kambucha wtf4-rep1Δ:* We deleted 66 base pairs (bases 313-378 of poison coding
754 sequence) that make up the exon 3 coding sequence repeats in *S. kambucha wtf4*^{poison} and
755 cloned it into pSZB1460 to generate pSZB1565. We repeated the same deletion in *S.*
756 *kambucha wtf4*^{antidote} (bases 439-504 of antidote coding sequence) and this construct was
757 synthesized and cloned it into pSZB1537 by IDT to generate pSZB1736.
758
759 *S. kambucha wtf4-rep2Δ:* We deleted 30 base pairs (bases 802-831 of poison coding
760 sequence) that make up the exon 6 repeats in *S. kambucha wtf4* and this construct was
761 synthesized and cloned it into pSZB1460 to generate pSZB1566 by IDT. To construct the
762 mutant antidote, we deleted bases 928-957 of the antidote coding sequence and this construct
763 was synthesized and cloned it into pSZB1537 by IDT generate pSZB1737.
764
765 *S. kambucha wtf4-rep1-2Δ:* We deleted 66 base pairs (bases 313-378 of poison coding
766 sequence) and 30 base pairs (bases 802-831 of poison coding sequence) to delete both the
767 exon 3 and 6 coding sequence repeats in *S. kambucha wtf4.* This construct was synthesized
768 and cloned into pSZB1460 to generate pSZB1670. To construct the mutant antidote, we deleted
769 66 base pairs (bases 439-504 of antidote coding sequence) and 33 base pairs (bases 928-957
770 of antidote coding sequence). This construct was synthesized and cloned it into pSZB1537 by
771 IDT generate pSZB1738.
772
773 *S. kambucha wtf4-rep2*^{sc}*:* We randomly scrambled the 10 amino acids that make up the exon 6
774 coding sequence repeats in *S. kambucha wtf4*^{poison} and then reordered the codons to match the
775 amino acids. We then replaced the wild-type 30 base pairs with the scrambled 30 base pairs
776 (TTTGGGAGAGCGAGAGGGATAGGTAATATA) and this construct was synthesized and
777 cloned into pSZB1460 to generate pSZB1742. To construct the mutant antidote, we replaced

778 the exon 6 coding sequence repeats with the same scrambled 30 base pairs, and this construct
779 was synthesized and cloned into pSZB1537 by IDT to generate pSZB1740.
780
781 *S. kambucha wtf4-rep2^{A}:* We replaced the 30 base pairs that make up the exon 6 coding
782 sequence repeats with alanine codons (GCAGCGGCTGCCGCTGCAGCTGCCGCAGCG) in *S.*
783 *kambucha wtf4^{poison}* and this construct was synthesized and was cloned into pSZB1460 to
784 generate pSZB1743. To construct the mutant antidote, we replaced the exon 6 coding
785 sequence repeats with the same alanine codons, and this construct was synthesized and
786 cloned into pSZB1537 by IDT to generate pSZB1741.
787
788 *S. kambucha wtf4^{poison}-ex1^{int}:* We inserted exon 1 in between exons 3 and 4 of *S. kambucha*
789 *wtf4^{poison}* and this construct was synthesized and cloned into pSZB1460 by IDT to generate
790 pSZB1616. To maintain the in-frame codons, we inserted exon 1 at 541 base pairs of the poison
791 coding sequence, which is one base pair before exon 3 ends.
792
793 *S. kambucha wtf4^{poison}-ex1:* We inserted exon 1 before the stop codon of *S. kambucha wtf4^{poison}*
794 coding sequence and this construct was synthesized and cloned into pSZB1460 by IDT to
795 generate pSZB1555.
796
797 *S. kambucha wtf4-TMD1Δ*: We used TMHMM2.0 [71,72] to predict transmembrane topology
798 (see S3 Table for a detailed description). With these predictions as guidance, we deleted the
799 first predicted transmembrane domain (bases 121-186 of poison coding sequence) from in *S.*
800 *kambucha wtf4^{poison}* and this construct was synthesized and cloned into pSZB1460 by IDT to
801 generate pSZB1561.
802
803 *S. kambucha wtf4-TMD2Δ:* We deleted the second predicted transmembrane domain (bases
804 232-291 of poison coding sequence) of *S. kambucha wtf4^{poison}* coding sequence and this
805 construct was synthesized and cloned into pSZB1460 by IDT to generate pSZB1562.
806
807 *S. kambucha wtf4-TMD6Δ:* We deleted the sixth predicted transmembrane domain (bases 580-
808 648 of poison coding sequence) of *S. kambucha wtf4^{poison}* coding sequence and this construct
809 was synthesized and cloned into pSZB1460 by IDT to generate pSZB1563.
810

811 *S. kambucha wtf4-ex2Δ*: We deleted exon 2 (bases 11-283) of *S. kambucha wtf4*^{poison} coding
812 sequence and this construct was synthesized and cloned into pSZB1460 by IDT to generate
813 pSZB1556.
814
815 *S. kambucha wtf4-ex3Δ:* We deleted exon 3 (bases 284-541) of *S. kambucha wtf4*^{poison} coding
816 sequence and this construct was synthesized and cloned into pSZB1460 by IDT to generate
817 pSZB1557.
818
819 *S. kambucha wtf4- ex4Δ:* We deleted exon 4 (bases 542-733) of *S. kambucha wtf4*^{poison} coding
820 sequence and this construct was synthesized and cloned into pSZB1460 by IDT to generate
821 pSZB1558.
822
823 *S. kambucha wtf4-ex5Δ:* We deleted exon 5 (bases 734-796) of *S. kambucha wtf4*^{poison} coding
824 sequence and this construct was synthesized and cloned into pSZB1460 by IDT to generate
825 pSZB1559.
826
827 *S. kambucha wtf4-ex6Δ:* We deleted exon 6 (bases 797-885) of *S. kambucha wtf4*^{poison} coding
828 sequence and this construct was synthesized and cloned into pSZB1460 by IDT to generate
829 pSZB1560. To construct the mutant antidote, we deleted exon 6 and this construct was
830 synthesized and cloned into pSZB1537 by IDT to generate pSZB1899.
831
832 *S. kambucha wtf4-consΔ:* From previous analysis of *S. pombe wtf* genes, a conserved region
833 within exon 3 was identified [20]. This conserved region within exon 3 was 29 base pairs long
834 (bases 284-312) in *S. kambucha wtf4*^{poison} coding sequence. To maintain in-frame codons, we
835 included one base pair upstream the conserved region, and made a 30 base pairs deletion
836 (bases 283-312) in *S. kambucha wtf4*^{poison} coding sequence and this construct was synthesized
837 and cloned into pSZB1460 by IDT to generate pSZB1617.
838
839 *S. kambucha wtf4-Δ*$^{10\text{-}poison}$*-mEos:* We amplified a 10 amino acid truncated poison from
840 pSZB464 [15] with oligos 3183+3186 and cloned this into V08 [30] via Golden Gate assembly
841 (New England Biolabs) to generate pSZB1402. We digested this with SacI and KpnI and cloned
842 the insert into SacI, KpnI digested pRS316 [70] to generate pSZB1505.
843

844 *S. kambucha wtf4-Δ$^{10\text{-antidote}}$-mCherry:* We amplified 10 amino acid truncated antidote from
845 pSZB708 [15] with oligos 1402+3138, and mCherry-cyc1T from pSZB708 [15] with oligos
846 3139+2170. We then stitched these pieces with oligos 1402+2170. We cut this fragment with
847 XhoI, BamHI and cloned this into XhoI, BamHI cut pDK20 [69] to generate pSZB1416. We cut
848 this plasmid with KpnI and XhoI and cloned the insert into KpnI, XhoI cut pRS314 [70] to
849 generate pSZB1550.
850
851 *S. kambucha wtf4-Δ$^{20\text{-poison}}$-mEos:* We amplified 20 amino acid truncated poison from pSZB464
852 [15] with oligos 3183+3282 and cloned this into V08 [30] via Golden Gate assembly (New
853 England Biolabs) to generate pSZB1444. We digested this with SacI and KpnI and cloned the
854 insert into SacI, KpnI digested pRS316 [70] to generate pSZB1507.
855
856 *S. kambucha wtf4-Δ$^{20\text{-antidote}}$-mCherry:* We amplified 20 amino acid truncated antidote from
857 pSZB708 [15] with oligos 1402+3829. We digested this fragment with XhoI and BamHI and
858 cloned the insert into XhoI, BamHI cut pSZB1537 to generate pSZB1567.
859
860 *S. kambucha wtf4^{poison}-mCherry:* We amplified *S. kambucha wtf4^{poison}-mCherry-cyc1T* from
861 pSZB708 [15] with oligos 2625+964. This product was cut with BamHI and XhoI and cloned into
862 BamHI, XhoI cut pDK20 [69] to generate pSZB1374. We cut this plasmid with KpnI and XhoI
863 and cloned the insert into KpnI, XhoI cut pRS314 [70] to generate pSZB1381.
864
865 *S. kambucha wtf4^{poison}-mEos:* We digested RHX1389 [15] with KpnI, SacI and ligated the insert
866 with KpnI, SacI cut pRS316 [70] to generate pSZB1455. This plasmid had the start site of the
867 poison mutated to TAG, which was then corrected to ATG by GenScript to generate pSZB1476.
868
869 *S. kambucha wtf4^{poison}-GBP-mCherry:* We added the GFP-binding protein sequence from
870 Addgene plasmid #89068 [74] at the end of *S. kambucha wtf4^{poison}* and this construct was
871 synthesized and cloned into pSZB1537 by IDT to generate pSZB1748.
872
873 *S. kambucha NT*-wtf4^{poison}-mEos*: We added the mutated N-terminal domain (D40K, K65D)
874 from the flagelliform spidroin 1A variant 1 from *Trichonephila clavipes*, NT* [34,35], followed by
875 a TEV cleavage site (ENLYFQS) [75] at the N-terminus of *S. kambucha wtf4^{poison}* coding
876 sequence, which was synthesized and cloned into pSZB1460 by IDT to generate pSZB1900.
877

878 *S. kambucha MBP-wtf4^{poison}-mEos*: We added the *S. cerevisiae* codon-optimized *E. coli* Maltose
879 Binding Protein (MBP) coding sequence [76,77] followed by a 4X(GGGS)-GG linker to the N-
880 terminus of *S. kambucha wtf4^{poison}* coding sequence, which was synthesized and cloned into
881 pSZB1460 by IDT to generate pSZB1949.
882
883 *S. kambucha wtf4^{antidote}-GFP*: We ordered *S. kambucha wtf4^{antidote}* which was synthesized and
884 cloned into pSZB1540 by IDT to generate pSZB1874.
885
886 *S. kambucha wtf4^{antidote}-mCherry*: We amplified *S. kambucha wtf4^{antidote}-mCherry-cyc1T* from
887 pSZB1005 [15] with oligos 1402+2170. This product was digested with BamHI and XhoI and
888 cloned into BamHI, XhoI cut pDK20 [69] to generate pSZB1699. This plasmid was digested with
889 KpnI, XhoI and ligated with KpnI, XhoI cut pRS314 [70] to generate pSZB1774.
890
891 *S. kambucha wtf4^{antidote}-mEos*: We digested pSZB1120 [7] with KpnI, SacI and ligated the insert
892 into KpnI, SacI cut pRS316 [70] to generate pSZB1453. This plasmid had the start site of the
893 antidote mutated to TAG, which was then corrected to ATG by GenScript to generate
894 pSZB1477.
895
896 *S. octosporus wtf25^{poison}-mEos:* We amplified *S. octosporus wtf25^{poison}* from pSZB1353 [19] with
897 oligos 3841+3840 and cloned this into V08 [30] via Golden Gate assembly (New England
898 Biolabs) to generate pSZB1548. We digested this with SacI and KpnI and cloned the insert into
899 SacI, KpnI digested pRS316 [70] to generate pSZB1585.
900
901 *S. octosporus wtf25^{poison}-mCherry:* We ordered *S. octosporus wtf25^{poison}* coding sequence was
902 synthesized and cloned into pSZB1537 by IDT to generate pSZB1807.
903
904 *S. octosporus wtf25^{poison}-GBP-mCherry:* We added the GFP-binding protein sequence from
905 Addgene plasmid #89068 [74] at the end of *S. octosporus wtf25^{poison}* coding sequence and this
906 construct was synthesized and cloned into pSZB1537 by IDT to generate pSZB1868.
907
908 *S. octosporus wtf25^{antidote}-mCherry:* We ordered *S. octosporus wtf25^{antidote}* coding sequence was
909 synthesized and cloned into pSZB1537 by IDT to generate pSZB1746.
910

911 *S. octosporus wtf25^{antidote}-mEos:* We ordered *S. octosporus wtf25^{antidote}* coding sequence was
912 synthesized and cloned into pSZB1460 by IDT to generate pSZB1806.
913
914 *S. octosporus wtf25^{antidote}-mEos in pRS314*: We amplified *S. octosporus wtf25^{antidote}* from
915 pSZB1347 [19] with oligos 3839+3840. This insert was cloned into V08 [30] via Golden Gate
916 cloning (New England Biolabs) to generate pSZB1593. We digested this with KpnI, SacI and
917 cloned the insert into pRS314 [70] to generate pSZB1598.
918
919 *S. octosporus wtf25^{antidote}-GFP:* We ordered *S. octosporus wtf25^{antidote}* coding sequence was
920 synthesized and cloned into pSZB1540 by IDT to generate pSZB1869.
921
922 *S. octosporus wtf25-repΔ:* We deleted 30 base pairs (bases 505-534) that make up the exon 4
923 repeats in *S. octosporus wtf25^{poison}* and was synthesized and cloned into pSZB1460 by IDT to
924 generate pSZB1687. To construct the mutant antidote, we deleted bases 640-669 of the
925 antidote coding sequence and this construct was synthesized and cloned it into pSZB1540 by
926 IDT generate pSZB1739.
927
928 *S. octosporus wtf25-rep^{Sk}:* To swap the coding sequence repeats between *S. kambucha wtf4*
929 exon 6 and *S. octosporus wtf25* exon 4, we replaced the 30 base pairs from *wtf25*
930 (ATAGGAAACGGTGCACGGCATAGGAAAT) with 30 base pairs from *wtf4*
931 (ATAGGGAATATAGGGAGAGCGTTTAGAGGT) in *S. octosporus wtf25*. The mutant poison
932 was synthesized and cloned into pSZB1537 by IDT to generate pSZB1732. The mutant antidote
933 was synthesized and cloned into pSZB1460 by IDT to generate pSZB1731.
934
935 *S. octosporus wtf25Δ$^{10\text{-}poison}$-mEos:* We amplified a 10 amino acid C-terminal truncated
936 *wtf25^{poison}* from pSZB1353 [19] with oligos 4173+4174 and cloned this into V08 [30] via Golden
937 Gate assembly (New England Biolabs) to generate pSZB1675. We then cut out the tagged
938 poison with SacI and KpnI and ligated it with cut pRS316 [70] to generate pSZB1694.
939
940 *S. octosporus NT*-wtf25^{poison}:* We added the mutated N-terminal domain (D40K, K65D) from the
941 flagelliform spidroin 1A variant 1 from *Trichonephila clavipes*, NT* [33,34], followed by a TEV
942 cleavage site (ENLYFQS) [75] at the N-terminus of *S. octosporus wtf25^{poison}* coding sequence,
943 which was synthesized and cloned into pSZB1460 by IDT to generate pSZB1927.
944

945 *S. octosporus MBP-wtf25^{poison}-mEos*: We added the *S. cerevisiae* codon-optimized *E. coli*
946 Maltose Binding Protein (MBP) coding sequence [76,77] followed by a 4X(GGGS)-GG linker to
947 the N-terminus of *S. octosporus wtf25^{poison}* coding sequence, which was synthesized and cloned
948 into pSZB1460 by IDT to generate pSZB1950.
949
950 *S. octosporus wtf61^{poison}-mEos:* We amplified *S. osmophilus wtf61^{poison}* from pSZB1040 [19] with
951 oligos 3837+3838 and cloned this into V08 [30] via Golden Gate assembly (New England
952 Biolabs) to generate pSZB1569. We digested this with SacI and KpnI and cloned the insert into
953 SacI, KpnI digested pRS314 [70] to generate pSZB1583.
954
955 *S. octosporus wtf61^{poison}-mCherry:* We amplified *S. osmophilus wtf61^{poison}* from pSZB1040 [19]
956 with oligos 4193+4194. We digested this product with XhoI, BamHI and cloned this into XhoI,
957 BamHI cut pSZB1537 to generate pSZB1706.
958
959 *S. octosporus wtf61^{antidote}-GFP:* We amplified *S. osmophilus wtf61^{antidote}* from pSZB1095 [19] with
960 oligos 4192+4194. We digested this product with XhoI, BamHI and cloned this into with XhoI,
961 BamHI cut pSZB1540 to generate pSZB1708.
962
963 *S. octosporus wtf61^{antidote}-mEos:* We amplified *S. osmophilus wtf61^{antidote}* from pSZB1095 [19]
964 with oligos 3836+3837 and cloned into V08 [30] via Golden Gate assembly (New England
965 Biolabs) to generate pSZB1645. We then digested pSZB1645 with KpnI and SacI and ligated it
966 with KpnI, BamHI cut pRS314 to generate pSZB1647.
967
968 *S. cryophilus wtf1^{poison}-mEos*: We amplified *S. cryophilus wtf1^{poison}* from pSZB1122 [19] with
969 oligos 3844+3843 and cloned this into V08 [30] via Golden Gate assembly (New England
970 Biolabs) to generate pSZB1544. We digested this with SacI and KpnI and cloned the insert into
971 SacI, KpnI digested pRS316 [70] to generate pSZB1575.
972
973 *S. cryophilus wtf1^{poison}-mCherry*: We ordered *S. cryophilus wtf1^{poison}* which was synthesized and
974 cloned into pSZB1537 by IDT to generate pSZB1870.
975
976 *S. cryophilus wtf1^{antidote}-mEos*: We amplified *S. cryophilus wtf1^{antidote}* from pSZB1192 [19] with
977 oligos 3843+3842 and cloned this into V08 [30] via Golden Gate assembly (New England

978 Biolabs) to generate pSZB1605. We digested this with SacI and KpnI and cloned the insert into
979 SacI, KpnI digested pRS314 [70] to generate pSZB1612.
980
981 *S. cryophilus wtf1^{antidote}-GFP*: We ordered *S. cryophilus wtf1^{antidote}* which was synthesized and
982 cloned into pSZB1540 by IDT to generate pSZB1871.
983
984 *S. cryophilus wtf1Δ$^{10\text{-}poison}$:* We amplified a 10 amino acid C-terminal truncated *wtf1^{poison}* from
985 pSZB1122 [19] and oligos 4177+4178 and cloned this into V08 [30] via Golden Gate assembly
986 (New England Biolabs) to generate pSZB1673. We then cut out the tagged poison with SacI,
987 KpnI and cloned into cut pRS316 [70] to generate pSZB1692.
988
989 *S. osmophilus wtf41^{poison}-mEos:* We cloned *S. osmophilus wtf41^{poison}* from pSZB1327 [19] with
990 oligos 3361+3362 and cloned this into V08 [30] via Golden Gate assembly (New England
991 Biolabs) to generate pSZB1533. We then cut out the tagged poison with SacI, KpnI and cloned
992 into cut pRS316 [70] to generate pSZB1581.
993
994 *S. osmophilus wtf41Δ$^{10\text{-}poison}$-mEos:* We cloned C-terminus 10 amino acid truncated *S.*
995 *osmophilus wtf41^{poison}* from pSZB1325 [19] with oligos 4175+4176 and cloned this into V08 [30]
996 via Golden Gate assembly (New England Biolabs) to generate pSZB1676. We then cut out the
997 tagged poison with SacI, KpnI and cloned into cut pRS316 [70] to generate pSZB1696.
998
999 *S. osmophilus wtf41^{antidote}-mEos:* We amplified *S. osmophilus wtf41^{antidote}* from pSZB1325 [19]
1000 with oligos 3832+3362 and cloned this into V08 [30] via Golden Gate assembly (New England
1001 Biolabs) to generate pSZB1599. We then cut out the tagged poison with SacI, KpnI and cloned
1002 into cut pRS314 [70] to generate pSZB1607.
1003
1004 *S. osmophilus wtf19^{poison}-mEos:* We amplified *S. osmophilus wtf19^{poison}* from pSZB1324 [19] with
1005 oligos 3835+3834 and cloned this into V08 [30] via Golden Gate assembly (New England
1006 Biolabs) to generate pSZB1546. We then cut out the tagged poison with SacI, KpnI and cloned
1007 into cut pRS316 [70] to generate pSZB1579.
1008
1009 **Strain construction**
1010
1011 *S. cerevisiae strains with Galactose and β-estradiol inducible systems:*

1012

1013 We used the previously published strain, SZY1637 [15] and an independently constructed
1014 isolates of SZY1637, SZY1639 or SZY5807, to construct the strains in this study by
1015 transforming in the appropriate vectors. These strains have the lexA-ER-haB42 transcription
1016 factor integrated at *HIS3* [78]. In general, we used a protocol, modified from [79], to transform
1017 the vectors into these strains. Briefly, we incubated a mixture of 276μL of PLATE solution, 50μL
1018 of boiled salmon sperm DNA, 30μL of water, 1-4μL of vector DNA and a match-head sized
1019 amount of yeast at 30°C overnight and plated on selective media on the following day to select
1020 for transformants. We used Synthetic Complete (SC) media (Yeast Nitrogen Base from VWR
1021 #291940 and SC Supplement mix from SunSci) with the appropriate dropouts of the selective
1022 components to maintain vectors in the strains as in [15]. In some cases, transformants did not
1023 express the construct when induced. To ensure proper testing of genotypes, we screened
1024 multiple transformants via cytometry or microscopy to ensure that strains express the
1025 fluorescently tagged construct(s).
1026

1027 *Construction of S. cerevisiae strain with mEosNB-FTH1:*

1028

1029 We mated RHY3171 [31] to BY4741 [80] to obtain the progeny (SZY6594) that contained the
1030 *hoΔ::natMX::tTa{Off}tet07^mEosNB-(G4s)3-FTH1* construct, but lacked the *pGal-WHI5::hphMX*
1031 construct.
1032

1033 **Spot assays**

1034

1035 For spot assays, we first grew the strains for each experiment in the appropriate SC dropout
1036 media overnight at 30°C. The next day, we measured the OD600 of each strain and normalized
1037 the OD of all the strains to an OD of ~1. We then serially diluted these normalized cultures 10-
1038 fold (up to the dilution of 10^{-5}) in water and plated 5μL of each dilution on both SC dropout
1039 media and SC Galactose dropout media. We imaged the plates post 72h of growth at 30°C,
1040 except in the case of Figs 4B, S6B and S6C, where plates were grown for an additional day at
1041 30°C to clearly visualize differences in poison toxicity.
1042

1043 For the spot assays presented in Fig 3D, we first grew the strains in 5mL SC-URA (uracil) media
1044 overnight at 30°C. The next day, we pelleted overnight cultures and resuspended in 1mL of

1045 sterile water. We then used 100μL of this as the first in the dilution series. This was diluted 5-
1046 fold, up to eleven dilutions in order to observe the toxicity/suppression clearly. We plated 5μL of
1047 each dilution on SC-URA media, SC Galactose-URA media and SC Galactose-URA media with
1048 40mg/L Doxycycline (Calbiochem #324385). We imaged the plates post 72h of growth at 30°C.
1049
1050 For the spot assays presented in S7B Fig, we first grew the strains in 5mL SC-TRP-URA media
1051 overnight at 30°C. The next day, we pelleted overnight cultures and resuspended in 1mL of
1052 sterile water. We then used 100μL of this as the first in the dilution series. This was diluted 5-
1053 fold, up to 11 dilutions in order to observe the toxicity clearly. We plated 5μL of each dilution on
1054 SC-TRP-URA media and SC Galactose-TRP-URA media. We imaged the plates post 72h of
1055 growth at 30°C.
1056
1057 **Microscopy**
1058
1059 The appropriate strains for each experiment were first grown in 5mL of the appropriate SC
1060 dropout media overnight at 30°C. The next day, we inoculated 3mL of SC Raffinose dropout
1061 media with 1mL of the saturated overnight cultures and let them grow overnight at 30°C. On the
1062 following day, we pelleted the cultures and resuspended the cells in 3mL SC Galactose dropout
1063 media and incubated at 30°C. Cells were induced for 4-6 hours on SC Galactose dropout media
1064 and then imaged on a Zeiss LSM 980 confocal microscope which consisted of an Axio Observer
1065 Z1 base, through a 40x C-Apochromat (NA = 1.2) water immersion objective. The GFP and
1066 mCherry tagged proteins were excited at 488 and 561 nm, respectively. Emission was collected
1067 in channel mode onto a GaAsP detector in photon counting mode through a 491-544 nm
1068 bandpass for GFP and a 570-632 nm bandpass for mCherry. Transmitted light was also
1069 collected. Image fields of view were zoomed optically to a ~26 μm square with 512 pixels in
1070 each dimension.
1071
1072 For imaging cells expressing *S. octosporus* Wtf61^{antidote}-GFP, *S. kambucha* Wtf4^{poison}-GBP-mCh
1073 and Rnq1-mCardinal, we first grew cells in SC-Trp-Ura-Leu media. The next day, we inoculated
1074 3mL of SC Raffinose-Trp-Ura-Leu media with 1mL of the saturated overnight cultures and let
1075 them grow overnight at 30°C. The following day, we pelleted the cultures and resuspended the
1076 cells in 3mL SC Galactose-Trp-Ura-Leu + 500nM β-estradiol (VWR, # #AAAL03801-03) media
1077 and incubated at 30°C. Cells were induced for 4 hours and then imaged as described above,

1078 except that we also excited mCardinal tagged proteins at 640nm and collected the emission on
1079 channel mode onto a 650-700 nm bandpass detector of the Zeiss LSM 980 confocal
1080 microscope.
1081
1082 **Spectral unmixing for mEosNB-FTH1 strains**
1083
1084 For imaging the mEosNB-FTH1 strains, we first grew the strains in 5mL SC-URA+40mg/L
1085 Doxycycline. The next day, we inoculated 3mL of both SC Raffinose-URA and SC Raffinose-
1086 URA+40mg/L Doxycycline media with 1mL of the saturated overnight cultures and let them
1087 grow overnight at 30°C. The following day, we pelleted the cultures and resuspended the cells
1088 in 3mL of both SC Galactose-URA and SC Galactose-URA+40mg/L Doxycycline and incubated
1089 at 30°C. The rest of the methodology was as described in the section above.
1090
1091 The background fluorescence for strains constructed with SZY6594 had high autofluorescence
1092 in the GFP channel. To distinguish autofluorescence from true mEos signal, we spectrally
1093 unmixed the images. First, we captured spectral images with the lambda mode on the detector
1094 of the Zeiss LSM 980 confocal microscope (same settings as above), exciting the cells at 488
1095 nm and collecting emission over the entire visual spectrum. We then made reference spectra for
1096 mEos and autofluorescence from control cells, and then spectrally unmixed images using an in-
1097 house written plugin on ImageJ (https://research.stowers.org/imagejplugins/). The data
1098 presented in Fig 3C has transmitted light images collected on the channel mode with GFP
1099 excitation, and the spectrally unmixed images collected on lambda mode.
1100
1101 **Image analysis to quantify colocalization of mEos and mCherry signals in tagged**
1102 **constructs**
1103
1104 Cell regions of interest (ROIs) were found based on the transmitted light only using Cellpose
1105 (https://www.cellpose.org/) in Python using the “cyto” model and a diameter of 200. Pixels from
1106 these ROIs were then background subtracted using an average background signal from an ROI
1107 placed away from any cell. The Scipy Pearson Correlation for each cell ROI was then calculated
1108 for all pixels in each cell. Dead cells and aberrant ROIs were hand filtered out using Fiji
1109 (https://fiji.sc/). Find the raw data for these analyses in S1 Data.
1110
1111 **DAmFRET**

1112

1113 We performed the analysis similar to the methods in [15], with a few exceptions. We grew the
1114 strains in the same method described for microscopy, however, we induced the cells for 5-6
1115 hours. We then photoconverted the cells post induction for 5 minutes, using the OmniCure
1116 S2000 Elite UV lamp for photoconversion. The total power over 5 minutes of exposure amounts
1117 to 12.048 J/cm^2. The sample collection and data analysis were similar to methods described in
1118 [15] with a few exceptions. We included an empty vector strain in each experiment to effectively
1119 exclude auto fluorescent cell populations. All the cells for each experiment were induced at the
1120 same time, for the same amount of time, and were grown in the same 96-well plate. Three
1121 technical replicates were included for each sample.

1122

1123 There was only one fluorescent population that was independent of expression level for each
1124 construct analyzed. In order to clearly visualize AmFRET values across the cells expressing
1125 different constructs, we analyzed cells above a certain Acceptor fluorescence intensity threshold
1126 set for each experiment. For each set of experimental data, the median of the Wtf4^{poison}-mEos
1127 AmFRET values was calculated. The difference of this median value from 1 was then added to
1128 all the datasets within an experiment. For visualizing the results of the DAmFRET experiments,
1129 plots of AmFRET values were generated using GraphPad Prism 10 (Version 10.2.3 (347)).

1130

1131 Statistical analysis for the DAmFRET experiments involved pooling the technical replicates and
1132 performing pairwise t-tests comparing these values to either the wild-type Wtf4^{poison}-mEos
1133 dataset, or the monomer dataset. For each DAmFRET experiment, we then did a multiple
1134 sampling correction (Bonferroni correction) by dividing the p value cutoff (0.05) by the number of
1135 tests performed. Find the raw data and statistical analysis for each DAmFRET experiment in S4
1136 Data.

1137

1138 We used GraphPad Prism 10 (Version 10.2.3 (347)) to visualize acceptor fluorescence intensity
1139 values of live cells expressing the relevant Wtf^{poison} constructs presented in S6 Fig. Three
1140 technical replicates of each isolate were plotted, with the median included. Find the raw data for
1141 this analysis in S2 Data.

1142

1143 **Figure legends**

1144

1145 **Figure 1. Features of *wtf4* and mutant alleles.**

1146 **A.** A cartoon of *S. kambucha wtf4* coding sequence (CDS). Wtf4^{antidote} coding sequence is
1147 shown in magenta, which includes exons 1-6. The Wtf4^{poison} coding sequence is shown in cyan,
1148 which includes 21 base pairs from intron 1 (in grey), and exons 2-6. **B.** Features of Wtf4^{antidote}
1149 and Wtf4^{poison} proteins. Row 1 shows predicted secondary structure domains and functional
1150 motifs, including PY motifs (in mustard) and predicted transmembrane domains (in red). Row 2
1151 shows the coding sequence repeats in exon 3 and exon 6. Row 3 highlights a well-conserved
1152 region 9 amino acids long. Row 4 is the normalized hydrophobicity of the Wtf4 proteins from
1153 ProtScale, with the Kyle and Doolittle Hydropathy scale [81]. The higher the number on the
1154 scale, the higher the hydrophobicity of the amino acid. See S5 and S6 Tables for detailed
1155 descriptions. **C.** Percentage amino acid identity of Wtf^{antidotes} from 33 *wtf* driver genes from four
1156 isolates of *S. pombe* [20]. The antidote sequences were aligned using Geneious Prime
1157 (2023.0.4) and the percentage amino acid identity is depicted as a heatmap, with yellow being
1158 100% identity. *S. kambucha wtf4* CDS is shown below for comparison, with the exons labeled
1159 corresponding to the consensus. Labeled areas within exons 3 and 6, where identity is low,
1160 represent the expansion and contraction of the coding sequence repeats of different *wtf* genes.
1161 **D.** Cartoon of *wtf4* mutants constructed in this study. Each mutant category was constructed
1162 based on a specific feature mentioned above. The categories are depicted with a wild type *wtf4*
1163 allele at the top. See S1 Table for a comprehensive overview of the alleles and their
1164 phenotypes.
1165
1166 **Figure 2. Extremely diverged toxic Wtf^{poison} proteins exhibit similar self-assembly and**
1167 **intracellular localization**.
1168 **A**. Cartoon illustrating the Distributed Amphifluoric FRET (DAmFRET) assay (modified from
1169 [30]). AmFRET values for individual cells were calculated by dividing the acceptor fluorescence
1170 by the FRET fluorescence, both measured via cytometry. **B.** Combined AmFRET values for
1171 three technical replicates of the specified Wtf^{poison}-mEos proteins and monomer-mEos (negative
1172 control). X^{P} represents the WtfX poison proteins tested here. The median is indicated with a
1173 solid line and the bars represent the interquartile range. For easier comparison, the values were
1174 normalized so that Wtf4^{poison} had a median of 1 in each experiment. The data shown here do not
1175 include outliers. See S2 Data for the complete dataset and p-values. Statistical significance:
1176 *p<0.01; t-tests with Bonferroni correction. **C.** A spot assay of cells serially diluted and plated on
1177 SC-TRP-URA and SC Gal-TRP-URA plates. Each strain carries an empty [*TRP1*] plasmid, and
1178 either an empty [*URA3*] plasmid (EV) or the indicated *wtf^{poison}-mEos* allele under the control of a
1179 galactose-inducible promoter. The plates were grown at 30˚C for 3 days. **D.** Representative

1180 images of the same strains depicted in C were induced in galactose media for 4 hours at 30˚C to
1181 express the indicated mEos-tagged proteins. The images are not at the same brightness and
1182 contrast settings to clearly show localization of tagged proteins. Yellow arrows indicate
1183 endoplasmic reticulum-like localization. TL is transmitted light, and the scale bar is 4 μm.
1184
1185 **Figure 3. Increasing poison assembly with tags suppresses Wtf^{poison} toxicity.**
1186 **A.** A cartoon of the constructs used in this experiment (C-D). The mEosNB-FTH1 construct was
1187 integrated into the genome and is under the control of a doxycycline-repressible promoter.
1188 mEosNB is a nanobody that binds mEos. The *wtf^{poison}* alleles are carried on a [*URA3*] plasmid
1189 and are under the control of a galactose-inducible promoter. **B.** Cartoon of the constructs
1190 expressed on each medium used: SC-Ura, SC Galactose-Ura + 40 mg/L doxycycline, and SC
1191 Galactose-Ura. FTH1 is a 24-mer but is depicted as an 8-mer core. **C.** Representative images of
1192 cells induced with galactose media (with or without 40mg/L Doxycycline) for 4 hours at 30˚C to
1193 express the indicated Wtf^{poison}mEos proteins. The cells induced without Doxycycline (-Dox) also
1194 express mEosNB-FTH1. This strain background exhibits high autofluorescence, so we
1195 spectrally unmixed the signal to remove autofluorescence (See Methods). The images are not
1196 at the same brightness and contrast settings to clearly show localization of tagged proteins. TL
1197 is transmitted light, and the scale bar is 4 μm. **D.** A spot assay of cells carrying the constructs
1198 illustrated in A-C serially diluted on SC-Ura, SC Galactose-Ura + 40mg/L Doxycycline and SC
1199 Galactose-Ura plates and grown at 30˚C for 3 days. Each strain carries either an empty [*URA3*]
1200 plasmid (EV) or the indicated *wtf^{poison}-mEos* allele. These media induce the expression of
1201 mEosNB-FTH1 (i), the indicated Wtf^{poison}-mEos protein (ii), or both (iii), respectively. The
1202 horizontal break in the image of each plate is due to rearrangements of the images to facilitate
1203 easy comparison. All strains within a panel were grown on the same plates (i.e., one SC-TRP-
1204 URA or SC Gal-TRP-URA or SC Gal-TRP-URA + 40mg/L Doxycycline plate).
1205
1206 **Figure 4. Reducing Wtf4^{poison} assembly with NT* tag increases toxicity and affects its**
1207 **rescue by Wtf4^{antidote}.**
1208 **A.** Cartoon of alleles used in this experiment (B-F). The NT* tag has a general anti-aggregation
1209 property [34]. **B.** A spot assay of cells serially diluted and plated on SC-TRP-URA and SC Gal-
1210 TRP-URA plates and grown at 30˚C for 4 days. Each strain carries both a [*URA3*] and a [*TRP1*]
1211 plasmid. The plasmids are either empty (EV) or carry the indicated *wtf4* alleles under the control
1212 of galactose-inducible promoters. The horizontal break in the image for each plate is due to a
1213 rearrangement of the image to facilitate easy comparison. All strains were grown on the same

1214 plates (i.e., one SC-TRP-URA or SC Gal-TRP-URA plate). **C.** AmFRET values for three
1215 technical replicates of the specified Wtf4^{poison}-mEos alleles and monomer-mEos (negative
1216 control). The median is indicated with a solid line and the bars represent the interquartile range.
1217 For easier comparison, the values were normalized so that Wtf4^{poison} had a median of 1 in each
1218 experiment. Since Wtf4-20^{poison}-mEos cells were very low in number, we pooled two biological
1219 replicates (n=6 technical replicates). The data shown here do not include outliers. See S2 Data
1220 for the complete dataset and p-values. Statistical significance: *p<0.025, t-tests with Bonferroni
1221 correction. **D.** A spot assay of cells serially diluted and plated on SC-TRP-URA and SC Gal-
1222 TRP-URA plates and grown at 30˚C for 3 days. Each strain carries both a [*URA3*] and a [*TRP1*]
1223 plasmid. The plasmids are either empty (EV) or carry the indicated *wtf4* alleles under the control
1224 of galactose-inducible promoters. All strains were grown on the same plates (i.e., one SC-TRP-
1225 URA or SC Gal-TRP-URA plate). **E.** Representative images of the same strains depicted in D
1226 were induced with galactose media for 4 hours at 30˚C to express the indicated Wtf4^{poison}-mEos
1227 proteins and/or Wtf4^{antidote}-mCherry. The images are not at the same brightness and contrast
1228 settings to clearly show localization of tagged proteins. 4^{P} indicates Wtf4^{poison}, 4^{A} indicates
1229 Wtf4^{antidote}, TL is transmitted light, and the scale bar is 4 µm. **F**. Pearson's Correlation between
1230 mCherry and mEos signal in cells from E expressing the specified proteins. N>100, *** p<0.001,
1231 t-test.
1232
1233 **Figure 5. Effective neutralization of Wtf4^{poison} requires more than a physical connection to**
1234 **a Wtf^{antidote}.**
1235 **A.** Cartoon of constructs used in this experiment. *S. kambucha wtf4^{poison}* was tagged at the C-
1236 terminus with either mCherry or GBP-mCherry (GBP: GFP-binding protein). *S. kambucha*
1237 *wtf4^{antidote}* was tagged with mEos or GFP. *S. octosporus wtf61^{antidote}* was tagged with GFP. *S.*
1238 *octosporus wtf61^{poison}* was tagged with mCherry. **B.** Experimental set up and summary of the
1239 results shown in C and D. In a matching Wtf protein pair (top), poison-antidote interaction and
1240 rescue of poison toxicity is observed. In the mismatched pair (bottom), interaction between GFP
1241 and GBP results in a forced interaction between the poison and the antidote (shown in D). This
1242 interaction is insufficient to rescue the mismatched poison (shown in C). **C.** Spot assay of cells
1243 serially diluted and plated on SC-TRP-URA and SC Gal-TRP-URA plates and grown at 30˚C for
1244 3 days. Each strain carries both a [*URA3*] and a [*TRP1*] plasmid. The plasmids are either empty
1245 (EV) or carry the indicated *wtf* alleles under the control of galactose-inducible promoters. The
1246 horizontal break in the image of each plate is due to rearrangements of the images to facilitate
1247 easy comparison. All strains within a panel were grown on the same plates (i.e., one SC-TRP-

1248 URA or SC Gal-TRP-URA plate). **D.** Representative images of the same strains shown in C
1249 were induced in galactose for 4 hours at 30˚C to express the indicated Wtf proteins. **E.**
1250 Representative images of cells induced with galactose and 500nM β-estradiol for 4 hours at
1251 30˚C to produce the indicated proteins. Rnq1-mCardinal marks the insoluble protein deposit
1252 (IPOD) that is associated with the vacuole [46–48]. In D-E, the images are not at the same
1253 brightness and contrast settings to clearly show localization of tagged proteins. 4^{P} indicates
1254 $Wtf4^{poison}$, 4^{A} indicates $Wtf4^{antidote}$, 61^{P} indicates $Wtf61^{poison}$, 61^{A} indicates $Wtf61^{antidote}$, TL is
1255 transmitted light, and the scale bar is 4 µm.
1256
1257 **Figure 6. Modification of *wtf4* exon 6 CDS repeats can disrupt antidote rescue.**
1258 **A.** Cartoon of two coding sequence repeat mutants of *S. kambucha wtf4*. **B**. Logo representing
1259 the amino acids encoded by the repeats found in exon 6 of *S. pombe wtf* genes from [20]. **C.**
1260 The amino acids encoded by the exon 6 repeats in *S. kambucha wtf4* and the *wtf4-rep2*^{sc} and
1261 *wtf4-rep2*^{A} mutant alleles. **D.** Spot assay of cells serially diluted and plated on SC-TRP-URA
1262 and SC Gal-TRP-URA plates and grown at 30˚C for 3 days. Each strain carries both a [*URA3*]
1263 and a [*TRP1*] plasmid. The plasmids are either empty (EV) or carry the indicated *wtf4* alleles
1264 under the control of galactose-inducible promoters. The horizontal breaks in the image of each
1265 plate are due to rearrangements of the images to facilitate easy comparison. All strains within a
1266 panel were grown on the same plates (i.e., one SC-TRP-URA or SC Gal-TRP-URA plate). **E.**
1267 Representative images the same strains depicted in D were induced in galactose for 4 hours at
1268 30˚C to express the indicated Wtf proteins. The images are not at the same brightness and
1269 contrast settings to clearly show localization of tagged proteins. The arrows in the TL panels
1270 highlight vacuoles. 4^{P} indicates $Wtf4^{poison}$, 4^{A} indicates $Wtf4^{antidote}$, TL indicates transmitted light,
1271 and the scale bar is 4 µm. **F**. Pearson's Correlation between mEos and mCherry signal in cells
1272 expressing the specified constructs from E. N>100, ***p<0.001, t-test.
1273
1274 **Figure 7. Analyses of Wtf proteins reveal additional functional constraints.**
1275 **A.** A dispersed Wtf^{poison} localization and poison-poison assembly can be observed across
1276 greatly diverged proteins and are associated with Wtf^{poison} toxicity. However, assembly and/or
1277 localization alone are insufficient to cause toxicity. In multiple examples of non-toxic proteins (an
1278 example is included in each panel), we observe either an endoplasmic reticulum-like localization
1279 or vacuolar localization. **B.** Modulating Wtf^{poison} assembly with exogenous tags affects its
1280 toxicity. While increasing Wtf^{poison} assembly via tethering to mEosNB-FTH1 suppresses toxicity,
1281 increasing solubility with NT* (or MBP in the case of *S. kambucha* $Wtf4^{poison}$) increases the

1282 toxicity. **C.** Multiple modalities of ineffective antidote rescue. Effective rescue of a Wtf^{poison} by the
1283 corresponding Wtf^{antidote} (e.g., Wtf4 proteins) is supported by specific co-assembly and vacuolar
1284 localization. Artificial tethering of a mismatched Wtf^{poison} and Wtf^{antidote} does not result in effective
1285 rescue. Disruption of poison-antidote co-localization (e.g., Wtf4-rep2^{sc} proteins) or vacuolar
1286 targeting of co-localized poison-antidote proteins (e.g., Wtf4-rep2^{A} proteins) also results in
1287 ineffective rescue.
1288
1289 **Supplemental Information**
1290
1291 **S1 Figure. Wtf proteins share limited amino acid identity but have common features**
1292 **A.** A cartoon of *S. octosporus wtf25* coding sequence (CDS). Wtf25^{antidote} coding sequence is
1293 shown in purple, which includes exons 1-5. The Wtf4^{poison} coding sequence is shown in navy,
1294 which begins at the 27th base pair of exon 2 and extends through exon 5. Row 4 depicts the
1295 predicted transmembrane domains (in red) and PY motif (in mustard). Row 5 depicts the CDS
1296 repeats found in exon 4 (in cobalt). Row 6 depicts the normalized hydrophobicity of Wtf25
1297 proteins from ProtScale, with the Kyle and Doolittle Hydropathy scale [81]. The higher the
1298 number on the scale, the higher the hydrophobicity of the amino acid. See S2 and S3 Tables for
1299 more detailed descriptions. **B.** Pairwise amino acid identity of the 6 Wtf^{antidote} proteins shown.
1300 The amino acid sequences were aligned using Geneious Prime (2023.0.4), and the percentage
1301 amino acid identity is depicted as a heatmap, with yellow being 100% identity. **C.** Depiction of
1302 CDS repeats and lengths of 6 *wtf^{antidote}* CDSs. The CDS repeats found in exon 6 of *S. kambucha*
1303 *wtf4* are homologous to those found in exon 4 of the other *wtf* genes [19]. The scale bar
1304 represents 108 base pairs (bp). **D-E.** *S. octosporus wtf25* (**D**), *S. cryophilus wtf1*, and *S.*
1305 *osmophilus wtf41* (**E**) mutants constructed in this study. The categories have their respective
1306 wild type allele shown on top. See S1 Table for a comprehensive overview of the alleles and
1307 their phenotypes.
1308
1309 **S2 Figure. Deletion mutants affect Wtf4^{poison} toxicity, self-assembly and localization.**
1310 Cartoon of *S. kambucha wtf4* exon deletion mutants (**A**), predicted transmembrane domain
1311 (TMD) deletion mutants (**B**) and a mutant that deletes a 9 amino acid conserved region encoded
1312 in exon 3 (**C**). **D.** A spot assay of cells serially diluted and plated on SC-LEU-URA and SC Gal-
1313 LEU-URA plates and grown at 30˚C for 3 days. Each strain carries an empty [*LEU2*] plasmid,
1314 and either an empty [*URA3*] plasmid (EV) or the indicated *wtf4^{poison}-mEos* alleles under the
1315 control of a galactose-inducible promoter. The horizontal break in the image for each plate is

1316 due to rearrangement of the image to facilitate easy comparison. All strains were grown on the
1317 same plates (i.e., one SC-LEU-URA or SC Gal-LEU-URA plate). **E.** AmFRET values for three
1318 technical replicates of the specified Wtf4^{poison}-mEos proteins and monomer-mEos (negative
1319 control). The median is indicated with a solid line and the bars represent the interquartile range.
1320 For easier comparison, the values were normalized so that Wtf4^{poison} had a median of 1 in each
1321 experiment. The data shown here do not include outliers. See S2 Data for the complete dataset
1322 and p-values. Statistical significance: *p<0.008, **p<0.0008, t-tests between the means of each
1323 replicate, with Bonferroni correction. **F.** Representative images of the same strains depicted in D
1324 were induced in galactose media for 4 hours at 30˚C to express the indicated mEos-tagged
1325 proteins. The images are not at the same brightness and contrast settings to clearly show
1326 localization of tagged proteins. Yellow arrows indicate endoplasmic reticulum-like localization.
1327 4^{P} indicates Wtf4^{poison}, TL is transmitted light, and the scale bar is 4 µm.
1328
1329 **S3 Figure. C-terminal truncations have inconsistent effects on Wtf^{poison} protein toxicity.**
1330 **A.** Cartoon of C-terminal truncation mutants of *S. kambucha wtf4*. **B.** Cartoon illustrating the
1331 amino acids lost with the C-terminal truncation alleles of *wtf4*. The amino acids comprising the
1332 exon 6 coding sequence repeats are highlighted in pink. **C.** A spot assay of cells serially diluted
1333 and plated on SC-TRP-URA and SC Gal-TRP-URA plates and grown at 30˚C for 3 days. Each
1334 strain carries both an empty [*TRP1*] plasmid (EV) and a [*URA3*] plasmid that is either empty or
1335 carries the indicated *wtf4^{poison}-mEos* allele under the control of a galactose inducible promoter.
1336 **D.** AmFRET values for three technical replicates of the specified Wtf4^{poison}-mEos alleles and
1337 monomer-mEos (negative control). The median is indicated with a solid line and the bars
1338 represent the interquartile range. For easier comparison, the values were normalized so that
1339 Wtf4^{poison} had a median of 1 in each experiment. The data shown here do not include outliers.
1340 See S2 Data for the complete dataset and p-values. Statistical significance: *p<0.0125, t-test
1341 with Bonferroni correction. **E.** Representative images of the same strains depicted in C were
1342 induced with galactose media for 4 hours at 30˚C to express the indicated mEos-tagged
1343 proteins. The images are not at the same brightness and contrast settings to clearly show
1344 localization of tagged proteins. 4^{P} indicates Wtf4^{poison}, TL is transmitted light, and the scale bar is
1345 4 µm. **F.** Cartoons of C-terminal truncation mutants of *S. cryophilus wtf1* (*wtf1-Δ^{10}*), *S.*
1346 *osmophilus wtf41* (*wtf41-Δ^{10}*), and *S. octosporus wtf25* (*wtf25-Δ^{10}*). **G.** Spot assays of cells
1347 serially diluted and plated on SC-TRP-URA and SC Gal-TRP-URA plates and grown at 30˚C for
1348 3 days. Each strain carries both an empty [*TRP1*] plasmid (EV) and an empty [*URA3*] plasmid
1349 (EV), or the indicated *wtf^{poison}-mEos* allele under the control of a galactose-inducible promoter.

1350 The horizontal breaks in the images for each plate are due to rearrangements of the image to
1351 facilitate easy comparison. All strains were grown on the same plates (i.e., one SC-TRP-URA or
1352 SC Gal-TRP-URA plate).
1353
1354 **S4 Figure. The fluorescence signal intensity of expressed Wtf^{poison} proteins does not**
1355 **correlate with toxicity.**
1356 **A-F** Acceptor fluorescence intensity (in arbitrary units, a.u.) of similarly sized live cells across all
1357 Wtf DAmFRET experiments in this study, with the line indicating the median of the population.
1358 Data represented here is from the following experiments: A corresponds to Fig 2B, B
1359 corresponds to S2E Fig, C corresponds to S3D Fig, D corresponds to Fig 4C, E corresponds
1360 alleles in S6 Fig, and F corresponds to S7D Fig. The Y-axis is scaled to a log10 scale. The data
1361 are color coded, with toxic poisons in teal, and non-toxic alleles in orange.
1362
1363 **S5 Figure. C-terminus truncation alleles of diverged Wtf^{poison}s are rescued by their**
1364 **corresponding wild type Wtf^{antidote}s.**
1365 **A.** Cartoon of *S. cryophilus wtf1*, *S. osmophilus wtf41*, and *S. octosporus wtf25* C-terminal
1366 truncation mutants. **B-D.** Spot assays of cells serially diluted on SC-TRP-URA and SC Gal-TRP-
1367 URA plates and grown at 30˚C for 3 days. Each strain carries both a [*URA3*] and a [*TRP1*]
1368 plasmid. The plasmids are either empty (EV) or carry the indicated *wtf* alleles under the control
1369 of galactose-inducible promoters. The horizontal breaks in the images within a panel are due to
1370 rearrangements of the images to facilitate easy comparison. All strains within a panel were
1371 grown on the same plates (i.e., one SC-TRP-URA or SC Gal-TRP-URA plate).
1372
1373 **S6 Figure**. **Reducing assembly with NT* tag increases Wtf25^{poison} toxicity.**
1374 **A.** Cartoon of alleles used in this experiment (B-E). The NT* tag has a general anti-aggregation
1375 property [34]. **B-C.** Spot assays of cells serially diluted on SC-TRP-URA and SC Gal-TRP-URA
1376 plates and grown at 30˚C for 4 days. Each strain carries both a [*URA3*] and a [*TRP1*] plasmid.
1377 The plasmids are either empty (EV) or carry the indicated *wtf25* alleles under the control of
1378 galactose-inducible promoters. In B, the horizontal break in the image of each plate is due to a
1379 rearrangement of the image to facilitate easy comparison. All strains within a panel were grown
1380 on the same plates (i.e., one SC-TRP-URA or SC Gal-TRP-URA plate for panel B). **D.**
1381 Representative images of the same strains shown in C were induced with galactose media for 4
1382 hours at 30˚C to express the indicated Wtf25^{poison}-mEos proteins and/or Wtf25^{antidote}-mCherry.
1383 The images are not at the same brightness and contrast settings to clearly show localization of

1384 tagged proteins. 25^{P} indicates Wtf25^{poison}, 25^{A} indicates Wtf25^{antidote}, TL is transmitted light, and
1385 the scale bar is 4 μm. **E**. Pearson's Correlation between mCherry and mEos signal in cells from
1386 D expressing the specified proteins. N>100, p>0.05, t-test.
1387
1388 **S7 Figure. Reducing Wtf^{poison} assembly with MBP tag affects toxicity.**
1389 **A.** Cartoon of alleles used in this experiment (B-C). MBP is the *E. coli* Maltose Binding Protein
1390 [76]. **B.** Spot assay of cells serially diluted and plated on SC-TRP-URA and SC Gal-TRP-URA
1391 plates and grown at 30˚C for 4 days. Each strain carries both an empty [*TRP1*] plasmid and a
1392 [*URA3*] plasmid that is either empty (EV) or carries the indicated *wtf^{poison}-mEos* allele under the
1393 control of a galactose-inducible promoter. The horizontal break in the image of each plate is due
1394 to rearrangement of the image to facilitate easy comparison. All strains were grown on the same
1395 plates (i.e., one SC Gal-TRP-URA plate or SC-Trp-Ura). **C.** Representative images of the same
1396 strains depicted in B induced with galactose media for 4 hours at 30˚C to express the indicated
1397 mEos-tagged proteins. The images are not at the same brightness and contrast settings to
1398 clearly show localization of tagged proteins. Yellow arrows indicate endoplasmic reticulum-like
1399 localization. 4^{P} indicates Wtf4^{poison}, 25^{P} indicates Wtf25^{poison}, TL is transmitted light, and the
1400 scale bar is 4 μm. **D.** AmFRET values for three technical replicates of the specified Wtf^{poison}-
1401 mEos alleles and monomer-mEos (negative control). The median is indicated with a solid line
1402 and the bars represent the interquartile range. For easier comparison, the values were
1403 normalized so that Wtf4^{poison} had a median of 1 in each experiment. The data shown do not
1404 include outliers. See S2 Data for the complete dataset and p-values. Statistical significance:
1405 *p<0.016, t-test with Bonferroni correction.
1406
1407 **S8 Figure. Limited modularity of the Wtf4^{antidote}-specific domain.**
1408 **A.** Cartoon of *wtf4^{antidote}* exon 1 and mutants that relocate, or both relocate and mutate the exon.
1409 **B.** AmFRET values for three technical replicates of the specified mEos-tagged proteins and
1410 monomer-mEos (negative control). The median is indicated with a solid line and the bars
1411 represent 1.5 times the interquartile range. For easier comparison, the values were normalized
1412 so that Wtf4^{poison} had a median of 1 in each experiment. The data shown do not include outliers.
1413 See S2 Data for the complete dataset and p-values. Statistical significance: *p<0.0125, t-tests
1414 with Bonferroni correction. **C-D.** Spot assays of cells serially diluted on SC-TRP-URA and SC
1415 Gal-TRP-URA plates and grown at 30˚C for 3 days. Each strain carries both a [*URA3*] and a
1416 [*TRP1*] plasmid. The plasmids are either empty (EV) or carry the indicated *wtf4* alleles under the
1417 control of galactose-inducible promoters. The horizontal breaks in the images of each plate in

1418 panels C and D are due to rearrangements of the images to facilitate easy comparison. All
1419 strains within a panel were grown on the same plates (i.e., one SC-TRP-URA or SC Gal-TRP-
1420 URA plate for panel C). **E.** Representative images of the same strains shown in C induced with
1421 galactose media for 4 hours at 30˚C to express the Wtf4^{poison}-mEos, Wtf4 exon1-mCherry, or
1422 both proteins. **F.** Representative images of the same strains shown in D were induced with
1423 galactose media for 4 hours at 30˚C to the indicated *wtf4* alleles. In E-F, arrows in the
1424 transmitted light images indicate vacuoles. The images are not at the same brightness and
1425 contrast settings to clearly show localization of the tagged proteins. 4^{P} indicates Wtf4^{poison}, 4^{A}
1426 indicates Wtf4^{antidote}, Ex1 is Wtf4 exon1, TL is transmitted light, and the scale bar is 4 µm.
1427

1428 **S9 Figure. Effective neutralization of Wtf25^{poison} requires more than a physical connection**
1429 **to a Wtf^{antidote}.**

1430 **A.** Cartoon of constructs used in this experiment. *S. octosporus* Wtf25^{poison} was tagged at the C-
1431 terminus with either mCherry or GBP-mCherry (GBP: GFP-binding protein). *S. octosporus*
1432 Wtf25^{antidote} was tagged with mEos or GFP. *S. cryophilus* Wtf1^{antidote} was tagged with GFP. *S.*
1433 *cryophilus* Wtf1^{poison} was tagged with mCherry. **B.** Experimental set up and summary of the
1434 results shown in C and D. In a matching Wtf protein pair (top), poison-antidote interaction and
1435 rescue of poison toxicity is observed. In the mismatched pair (bottom), interaction between GFP
1436 and GBP results in a forced interaction between the poison and the antidote (shown in D). This
1437 interaction is insufficient to rescue the mismatched poison (shown in C). **C.** Spot assay of cells
1438 serially diluted and plated on SC-TRP-URA and SC Gal-TRP-URA plates and grown at 30˚C for
1439 3 days. Each strain carries both a [*URA3*] and a [*TRP1*] plasmid. The plasmids are either empty
1440 (EV) or carry the indicated *wtf* alleles under the control of galactose-inducible promoters. The
1441 horizontal breaks in the images of each plate are due to rearrangements of the image to
1442 facilitate easy comparison. All strains within a panel were grown on the same plates (i.e., one
1443 SC-TRP-URA or SC Gal-TRP-URA plate). **D.** Representative images the strains depicted in C
1444 were induced in galactose for 4 hours at 30˚C to express the indicated Wtf proteins. The images
1445 are not at the same brightness and contrast settings to clearly show localization of tagged
1446 proteins. The arrows in the transmitted light images indicate vacuoles. 25^{P} indicates Wtf25^{poison},
1447 25^{A}- indicates Wtf25^{antidote}, 1^{P} indicates Wtf1^{poison}, 1^{A} indicates Wtf1^{antidote}, TL indicates
1448 transmitted light, and the scale bar is 4 µm.
1449

1450 **S10 Figure. Idiosyncratic poison and antidote compatibility between wild-type and**
1451 **truncation alleles of *wtf4*.**

1452 **A.** Cartoon of *S. kambucha wtf4* C-terminal truncation mutants. **B.** Spot assay of cells serially
1453 diluted and plated on SC-TRP-URA and SC Gal-TRP-URA plates and grown at 30˚C for 3 days.
1454 Each strain carries both a [*URA3*] and a [*TRP1*] plasmid. The plasmids are either empty (EV) or
1455 carry the indicated *wtf4* alleles under the control of galactose-inducible promoters. The
1456 horizontal breaks in the images are due to rearrangements of the images to facilitate easy
1457 comparison. All strains within a panel were grown on the same plates (i.e., one SC-TRP-URA or
1458 SC Gal-TRP-URA plate). **C.** Representative images the strains depicted in B were induced in
1459 galactose for 4 hours at 30˚C to express the indicated Wtf4 proteins. The images are not at the
1460 same brightness and contrast settings to clearly show localization of tagged proteins. The
1461 arrows in the TL panels highlight vacuoles. 4^P indicates $Wtf4^{poison}$, 4^A indicates $Wtf4^{antidote}$, TL
1462 indicates transmitted light, and the scale bar is 4 µm.
1463
1464 **S11 Figure. *wtf4* coding sequence repeats are dispensable, but can affect antidote**
1465 **rescue. A.** Cartoon of exon 3 and exon 6 coding sequence repeat deletion mutants of *S.*
1466 *kambucha wtf4*. **B-C.** Logo for amino acids encoded by the repeats found in exon 3 (B) and
1467 exon 6 (C) of *S. pombe wtf* genes from [20]. The sequence of the amino acids encoded in each
1468 repeat region in *S. kambucha wtf4* is shown below each logo. **D.** Spot assay of cells serially
1469 diluted and plated on SC-TRP-URA and SC Gal-TRP-URA plates and grown at 30˚C for 3 days.
1470 Each strain carries both a [*URA3*] and a [*TRP1*] plasmid. The plasmids are either empty (EV) or
1471 carry the indicated *wtf4* alleles under the control of galactose-inducible promoters. The
1472 horizontal break in the image of each plate is due to rearrangements of the images to facilitate
1473 easy comparison. All strains within a panel were grown on the same plates (i.e., one SC-TRP-
1474 URA or SC Gal-TRP-URA plate). **E.** Representative images of the same strains as depicted in D
1475 were induced in galactose for 4 hours at 30˚C to express the indicated Wtf4 proteins. The
1476 images are not at the same brightness and contrast settings to clearly show localization of
1477 tagged proteins. The arrows in the TL panels highlight vacuoles. 4^P indicates $Wtf4^{poison}$, 4^A
1478 indicates $Wtf4^{antidote}$, TL indicates transmitted light, and the scale bar is 4 µm. **F**. Pearson's
1479 Correlation between mEos and mCherry signal in cells expressing the specified constructs from
1480 E. N>100, ***p<0.001, t-test.
1481
1482 **S12 Figure. Coding sequence repeat mutant proteins do not interact with wildtype Wtf4**
1483 **proteins functionally.**
1484 **A.** Cartoon of coding sequence repeat mutants of *S. kambucha wtf4.* **B-H.** Spot assays of cells
1485 serially diluted on SC-TRP-URA and SC Gal-TRP-URA plates and grown at 30˚C for 3 days.

1486 Each strain carries both a [*URA3*] and a [*TRP1*] plasmid. The plasmids are either empty (EV) or
1487 carry the indicated *wtf4* alleles under the control of galactose-inducible promoters. The
1488 horizontal breaks in the images in within a panel are due to rearrangements of the images to
1489 facilitate easy comparison. All strains within a panel were grown on the same plates (i.e., one
1490 SC-TRP-URA or SC Gal-TRP-URA plate in panel B).
1491
1492 **S13 Figure. Swapping *wtf* CDS repeats across species affects Wtf25 antidote rescue.**
1493 **A.** Cartoon of a coding sequence repeat mutant of *S. octosporus wtf25*. **B**. Logo representing
1494 the amino acids encoded by the repeats found in exon 4 of *S. octosporus wtf* genes from [19].
1495 **C.** The amino acids encoded by the exon 4 repeats of *S. octosporus wtf25* and by the exon 6
1496 repeats of *S. kambucha wtf4*. **D.** Spot assay of cells serially diluted and plated on SC-TRP-URA
1497 and SC Gal-TRP-URA plates and grown at 30˚C for 3 days. Each strain carries both a [*URA3*]
1498 and a [*TRP1*] plasmid. The plasmids are either empty (EV) or carry the indicated *wtf25* alleles
1499 under the control of galactose-inducible promoters. The horizontal breaks in the images are due
1500 to rearrangements of the images to facilitate easy comparison. All strains within a panel were
1501 grown on the same plates (i.e., one SC-TRP-URA or SC Gal-TRP-URA plate). **E.**
1502 Representative images of the same strains depicted in D were induced in galactose for 4 hours
1503 at 30˚C to express the indicated Wtf25 proteins. The images are not at the same brightness and
1504 contrast settings to clearly show localization of tagged proteins. The arrows in the TL panel
1505 highlight vacuoles. Yellow arrows indicate endoplasmic reticulum-like localization. 25^{P} indicates
1506 $Wtf25^{poison}$, 25^{A} indicates $Wtf25^{antidote}$, TL indicates transmitted light, and the scale bar is 4 µm.
1507
1508 **S14 Figure. *S. octosporus wtf25* coding sequence repeats are functionally dispensable**
1509 **for poison toxicity but promote antidote rescue.**
1510 **A.** Cartoon of *S. octosporus wtf25* exon 4 coding sequence repeat deletion mutant. **B.** Logo for
1511 the amino acids encoded by the repeats found in exon 4 of *S. octosporus wtf* genes from [19] **C.**
1512 Spot assay of cells serially diluted and plated on SC-TRP-URA and SC Gal-TRP-URA plates
1513 and grown at 30˚C for 4 days. Each strain carries both a [*URA3*] and a [*TRP1*] plasmid. The
1514 plasmids are either empty (EV) or carry the indicated *wtf25* alleles under the control of
1515 galactose-inducible promoters. The horizontal breaks in the images are due to rearrangements
1516 of the images to facilitate easy comparison. All strains within a panel were grown on the same
1517 plates (i.e., one SC-TRP-URA or SC Gal-TRP-URA plate). **D.** Representative images the same
1518 strains depicted in C were induced in galactose for 4 hours at 30˚C to express the indicated
1519 Wtf25 proteins. The images are not at the same brightness and contrast settings to clearly show

1520 localization of tagged proteins. The arrows in the TL panels highlight vacuoles. Yellow arrows
1521 indicate endoplasmic reticulum-like localization. 25^{P} indicates $Wtf25^{poison}$, 25^{A} indicates
1522 $Wtf25^{antidote}$, TL indicates transmitted light, and the scale bar is 4 μm.
1523
1524 **S1 Table. Overview of *wtf* alleles and their phenotypes in this study**. Columns 1-2 describe
1525 the allele names and their construction. Columns 3-4 describe the toxicity of the poison and
1526 antidote proteins encoded by the corresponding allele. Column 5 notes if the mutant antidote
1527 can rescue the corresponding poison allele. Column 6-7 note if the specific antidote allele can
1528 rescue the wild-type poison (Column 6), or if the specific poison can be rescued by the wild-type
1529 antidote (Column 7). Column 8 notes if the corresponding antidote can rescue other poison
1530 alleles. Column 9 notes the AmFRET values are comparable to the wild-type $Wtf4^{poison}$-mEos or
1531 monomer-mEos. Finally, column 10 notes the figures/supplemental figures where these alleles
1532 can be found. Rows are separated based on the wild-type allele that the mutants were
1533 constructed from, where applicable. ND indicates that the specified experiment was not done.
1534
1535 **S2 Table. Overview of features across *wtf* driver genes.** Column 1 denotes the *wtf* driver
1536 gene, and columns 2-8 describe specific features of each gene and their encoded proteins.
1537 Column 2 notes if the gene has been shown to drive in fission yeast or been shown to encode
1538 for functional Wtf poison and antidote proteins in *S. cerevisiae*. Column 3 notes the number of
1539 exons in the gene, and column 4 notes the size of the $Wtf^{antidote}$ protein in amino acids. If the
1540 antidote sequence had a predicted coiled-coil domain, column 5 notes the size and location in
1541 the antidote protein as described in [15]. Column 6 notes the numbers of PY motifs (L/PPXY;
1542 [24]) in exon 1. While some $Wtf^{antidote}$ proteins also have an additional PY motif in exon 2, we did
1543 not include that information here since those motifs are shared by the corresponding poison
1544 proteins as well. Column 7 notes the number of predicted transmembrane domains predicted by
1545 TMHMM2.0 [72,73]. Column 8 notes the length of the exon 3 coding sequence repeats (if
1546 present) in amino acids. Column 9 notes the length of the exon 4/6 coding sequence repeats (if
1547 present) in amino acids. NA (not applicable) here indicates that the repeats were not present in
1548 the Wtf protein. Column 10 mentions the reference(s) where these genes/encoded proteins
1549 were characterized.
1550
1551 **S3 Table. Overview of predicted transmembrane domains of $Wtf^{antidote}$ proteins.** The
1552 results from the TMHMM2.0 [72,73] analysis of $Wtf^{antidote}$ proteins encoded by *wtf* driver genes in
1553 S2 table are detailed here. Find the specific results of the analyses, including the number of

amino acids in the predicted transmembrane domains, probability of the N-terminal being internal to the membrane (N-in), the specific location and the length of the predicted transmembrane domains.

S4 Table. Yeast strains used in this study. Column 1 is the figure where these strains were used, Column 2 is the name of the yeast strain and column 3 is the genotype of the strain. If the strain was constructed in this study, column 4 has the details on how the strain was constructed. If the strain was constructed in another study, column 5 notes the references for the same.

S5 Table. Plasmids used in this study. Column 1 denotes if the plasmids were used for strain construction or cloning, and the specific wild-type alleles that the plasmids correspond to. Column 2 is the name of the plasmid and column 3 is a short description of the plasmid. If the plasmid was not constructed in this study, column 4 references the studies the plasmids were constructed in.

S6 Table. Oligos used in this study. Column 1 denotes the name of the oligo and column 2 has the sequence of the oligos. If the oligo was not constructed in this study, column 3 references the studies the oligos were used in.

S1 Data. Raw Data for Pearson's Correlation tests performed in this study. Each sheet contains the raw data for the Pearson's Correlation tests and the statistical analysis corresponding to the tests performed in Figs 4F, S6E, 6F and S11F, respectively. See Methods for how this analysis was performed.

S2 Data. Raw Data for AmFRET plots presented in this study. Each sheet contains the raw data and the statistical analysis for the AmFRET plots of different Wtf^{poison}-mEos proteins, Wtf4^{antidote}-mEos, *S. kambucha wtf4* Exon1-mEos and monomer-mEos proteins in Figs 2B, S2E, S3D, Fig 4C, S6 Fig, S7D and S8B, respectively. The corresponding raw data for the Acceptor fluorescence intensity presented in S4 Fig for each of these experiments are found next to the relevant AmFRET data. See Methods for how this analysis was performed.

Acknowledgements

We thank the members of the Zanders lab, the Halfmann lab and the Core facilities at Stowers Institute for their help and guidance throughout the stages of development of this paper.

1588

1589 **References**

1590

1591 1. Burt A, Trivers R. Genes in Conflict. Harvard University Press; 2006.
1592 https://doi.org/10.2307/J.CTVJHZRC6.
1593 2. Sandler L, Novitski E. Meiotic Drive as an Evolutionary Force. Am Nat 1957;91:105–10.
1594 3. Bravo Núñez MA, Nuckolls NL, Zanders SE. Genetic Villains: Killer Meiotic Drivers.
1595 Trends in Genetics 2018;34:424–33. https://doi.org/10.1016/j.tig.2018.02.003.
1596 4. Zanders SE, Unckless RL. Fertility Costs of Meiotic Drivers. Current Biology
1597 2019;29:R512–20. https://doi.org/10.1016/j.cub.2019.03.046.
1598 5. Wang C, Wang J, Lu J, Wang H, Wu C, Xiong Y, et al. A natural gene drive system
1599 confers reproductive isolation in rice. Cell 2023;186:3577–92.
1600 https://doi.org/10.1016/j.cell.2023.06.023.
1601 6. Xie Y, Shen R, Chen L, Liu YG. Molecular mechanisms of hybrid sterility in rice. Sci
1602 China Life Sci 2019;62:737–43. https://doi.org/10.1007/S11427-019-9531-7.
1603 7. Li J, Zhou J, Zhang Y, Yang Y, Pu Q, Tao D. New Insights into the Nature of
1604 Interspecific Hybrid Sterility in Rice. Front Plant Sci 2020;11.
1605 https://doi.org/10.3389/FPLS.2020.555572.
1606 8. Myint ZM, Koide Y, Takanishi W, Ikegaya T, Kwan C, Hikichi K, et al. OlCHR, encoding
1607 a chromatin remodeling factor, is a killer causing hybrid sterility between rice species *Oryza*
1608 *sativa* and *O. longistaminata*. IScience 2024;27. https://doi.org/10.1016/J.ISCI.2024.109761.
1609 9. Saupe SJ, Johannesson H. On the Mechanistic Basis of Killer Meiotic Drive in Fungi.
1610 Annu Rev Microbiol 2022; 76:305–23. https://doi.org/10.1146/ANNUREV-MICRO-041320-
1611 113730.
1612 10. Simon M, Durand S, Ricou A, Vrielynck N, Mayjonade B, Gouzy J, et al. APOK3, a
1613 pollen killer antidote in *Arabidopsis thaliana*. Genetics 2022;221.
1614 https://doi.org/10.1093/GENETICS/IYAC089.
1615 11. Wang D, Wang H, Xu X, Wang M, Wang Y, Chen H, et al. Two complementary genes in
1616 a presence-absence variation contribute to *indica-japonica* reproductive isolation in rice. Nat
1617 Commun 2023;14. https://doi.org/10.1038/S41467-023-40189-X.
1618 12. You S, Zhao Z, Yu X, Zhu S, Wang J, Lei D, et al. A toxin-antidote system contributes to
1619 interspecific reproductive isolation in rice. Nat Commun 2023;14.
1620 https://doi.org/10.1038/S41467-023-43015-6.

1621 13. Courret C, Wei X, Larracuente AM. New perspectives on the causes and consequences
1622 of male meiotic drive. Curr Opin Genet Dev 2023;83.
1623 https://doi.org/10.1016/J.GDE.2023.102111.
1624 14. Lai EC, Vogan AA. Proliferation and dissemination of killer meiotic drive loci. Curr Opin
1625 Genet Dev 2023;82. https://doi.org/10.1016/J.GDE.2023.102100.
1626 15. Nuckolls NL, Mok AC, Lange JJ, Yi K, Kandola TS, Hunn AM, et al. The *wtf4* meiotic
1627 driver utilizes controlled protein aggregation to generate selective cell death. Elife 2020; 9:1–35.
1628 https://doi.org/10.7554/eLife.55694.
1629 16. Urquhart AS, Gardiner DM. A Natural Fungal Gene Drive Enacts Killing via DNA
1630 Disruption. MBio 2023;14. https://doi.org/10.1128/MBIO.03173-22.
1631 17. Hu W, Jiang Z Di, Suo F, Zheng JX, He WZ, Du LL. A large gene family in fission yeast
1632 encodes spore killers that subvert Mendel's law. Elife 2017;6.
1633 https://doi.org/10.7554/ELIFE.26057.
1634 18. Brysch-Herzberg M, Jia GS, Sipiczki M, Seidel M, Li W, Assali I, et al.
1635 *Schizosaccharomyces lindneri* sp. nov., a fission yeast occurring in honey. Yeast 2023; 40:237–
1636 53. https://doi.org/10.1002/YEA.3857.
1637 19. De Carvalho M, Jia GS, Nidamangala Srinivasa A, Billmyre RB, Xu YH, Lange JJ, et al.
1638 The *wtf* meiotic driver gene family has unexpectedly persisted for over 100 million years. Elife
1639 2022;11. https://doi.org/10.7554/eLife.81149.
1640 20. Eickbush MT, Young JM, Zanders SE. Killer meiotic drive and dynamic evolution of the
1641 *wtf* gene family. Mol Biol Evol 2019; 36:1201–14. https://doi.org/10.1093/molbev/msz052.
1642 21. Xu Y-H, Suo F, Zhang X-R, Du T-Y, Hua Y, Jia G-S, et al. Evolutionary modes of *wtf*
1643 meiotic driver genes in *Schizosaccharomyces pombe*. BioRxiv 2024:2024.05.30.596636.
1644 https://doi.org/10.1101/2024.05.30.596636.
1645 22. Nuckolls NL, Núñez MAB, Eickbush MT, Young JM, Lange JJ, Yu JS, et al. *wtf* genes
1646 are prolific dual poison-antidote meiotic drivers. Elife 2017;6.
1647 https://doi.org/10.7554/ELIFE.26033.
1648 23. Nuckolls NL, Nidamangala Srinivasa A, Mok AC, Helston RM, Núñez MAB, Lange JJ, et
1649 al. *S. pombe wtf* drivers use dual transcriptional regulation and selective protein exclusion from
1650 spores to cause meiotic drive. PLoS Genet 2022;18.
1651 https://doi.org/10.1371/JOURNAL.PGEN.1009847.
1652 24. Zheng JX, Du TY, Shao GC, Ma ZH, Jiang Z Di, Hu W, et al. Ubiquitination-mediated
1653 Golgi-to-endosome sorting determines the toxin-antidote duality of fission yeast *wtf* meiotic
1654 drivers. Nat Commun 2023;14. https://doi.org/10.1038/S41467-023-44151-9.

1655 25. Bravo Nuñez MA, Sabbarini IM, Eickbush MT, Liang Y, Lange JJ, Kent AM, et al.
1656 Dramatically diverse *Schizosaccharomyces pombe wtf* meiotic drivers all display high gamete-
1657 killing efficiency. PLoS Genet 2020;16. https://doi.org/10.1371/journal.pgen.1008350.
1658 26. Bravo Núñez MA, Lange JJ, Sarah ZE. A suppressor of a *wtf* poison-antidote meiotic
1659 driver acts via mimicry of the driver's antidote. PLoS Genet 2018;14.
1660 https://doi.org/10.1371/journal.pgen.1007836.
1661 27. Mannini B, Mulvihill E, Sgromo C, Cascella R, Khodarahmi R, Ramazzotti M, et al.
1662 Toxicity of protein oligomers is rationalized by a function combining size and surface
1663 hydrophobicity. ACS Chem Biol 2014; 9:2309–17.
1664 https://doi.org/10.1021/CB500505M/SUPPL_FILE/CB500505M_SI_001.PDF.
1665 28. Ries HM, Nussbaum-Krammer C. Shape matters: The complex relationship between
1666 aggregation and toxicity in protein-misfolding diseases. Essays Biochem 2016; 60:181–90.
1667 https://doi.org/10.1042/EBC20160008.
1668 29. Bucciantini M, Giannoni E, Chiti F, Baroni F, Taddei N, Ramponi G, et al. Inherent
1669 toxicity of aggregates implies a common mechanism for protein misfolding diseases. Nature
1670 2002 416:6880 2002; 416:507–11. https://doi.org/10.1038/416507a.
1671 30. Khan T, Kandola TS, Wu J, Venkatesan S, Ketter E, Lange JJ, et al. Quantifying
1672 Nucleation In Vivo Reveals the Physical Basis of Prion-like Phase Behavior. Mol Cell 2018;
1673 71:155-168.e7. https://doi.org/10.1016/j.molcel.2018.06.016.
1674 31. Kimbrough H, Jensen J, Weber C, Miller T, Maddera LE, Babu V, et al. A tool to dissect
1675 heterotypic determinants of homotypic protein phase behavior. bioRxiv 2025;
1676 https://doi.org/10.1101/2025.01.01.631016.
1677 32. Bellapadrona G, Elbaum M. Supramolecular Protein Assemblies in the Nucleus of
1678 Human Cells. Angewandte Chemie International Edition 2014; 53:1534–7.
1679 https://doi.org/10.1002/ANIE.201309163.
1680 33. Bracha D, Walls MT, Wei MT, Zhu L, Kurian M, Avalos JL, et al. Mapping Local and
1681 Global Liquid Phase Behavior in Living Cells Using Photo-Oligomerizable Seeds. Cell 2018;
1682 175:1467-1480.e13. https://doi.org/10.1016/J.CELL.2018.10.048.
1683 34. Schellhaus AK, Xu S, Gierisch ME, Vornberger J, Johansson J, Dantuma NP. A spider
1684 silk-derived solubility domain inhibits nuclear and cytosolic protein aggregation in human cells.
1685 Communications Biology 2022 5:1 2022; 5:1–8. https://doi.org/10.1038/s42003-022-03442-5.
1686 35. Kronqvist N, Sarr M, Lindqvist A, Nordling K, Otikovs M, Venturi L, et al. Efficient protein
1687 production inspired by how spiders make silk. Nat Commun 2017;8.
1688 https://doi.org/10.1038/NCOMMS15504.

1689 36. Askarieh G, Hedhammar M, Nordling K, Saenz A, Casals C, Rising A, et al. Self-
1690 assembly of spider silk proteins is controlled by a pH-sensitive relay. Nature 2010 465:7295
1691 2010; 465:236–8. https://doi.org/10.1038/nature08962.
1692 37. Abelein A, Chen G, Kitoka K, Aleksis R, Oleskovs F, Sarr M, et al. High-yield Production
1693 of Amyloid-β Peptide Enabled by a Customized Spider Silk Domain. Scientific Reports 2020
1694 10:1 2020; 10:1–10. https://doi.org/10.1038/s41598-019-57143-x.
1695 38. Jaudzems K, Askarieh G, Landreh M, Nordling K, Hedhammar M, Jörnvall H, et al. pH-
1696 Dependent Dimerization of Spider Silk N-Terminal Domain Requires Relocation of a Wedged
1697 Tryptophan Side Chain. J Mol Biol 2012; 422:477–87.
1698 https://doi.org/10.1016/J.JMB.2012.06.004.
1699 39. Andersson M, Chen G, Otikovs M, Landreh M, Nordling K, Kronqvist N, et al. Carbonic
1700 Anhydrase Generates CO2 and H+ That Drive Spider Silk Formation Via Opposite Effects on
1701 the Terminal Domains. PLoS Biol 2014;12: e1001921.
1702 https://doi.org/10.1371/JOURNAL.PBIO.1001921.
1703 40. Brumbaugh-Reed EH, Aoki K, Toettcher JE, Toettcher J. Rapid and reversible
1704 dissolution of biomolecular condensates using light-controlled recruitment of a solubility tag.
1705 BioRxiv 2024:2024.01.16.575860. https://doi.org/10.1101/2024.01.16.575860.
1706 41. Raran-Kurussi S, Keefe K, Waugh DS. Positional effects of fusion partners on the yield
1707 and solubility of MBP fusion proteins. Protein Expr Purif 2015; 110:159.
1708 https://doi.org/10.1016/J.PEP.2015.03.004.
1709 42. Raran-Kurussi S, Sharwanlal SB, Balasubramanian D, Mote KR. A comparison between
1710 MBP- and NT* as N-terminal fusion partner for recombinant protein production in E. coli. Protein
1711 Expr Purif 2022; 189:105991. https://doi.org/10.1016/J.PEP.2021.105991.
1712 43. Blake WJ, Kærn M, Cantor CR, Collins JJ. Noise in eukaryotic gene expression. Nature
1713 2003 422:6932 2003; 422:633–7. https://doi.org/10.1038/nature01546.
1714 44. Elowitz MB, Levine AJ, Siggia ED, Swain PS. Stochastic gene expression in a single
1715 cell. Science (1979) 2002; 297:1183–6. https://doi.org/10.1126/SCIENCE.1070919/
1716 45. Ozbudak EM, Thattai M, Kurtser I, Grossman AD, Van Oudenaarden A. Regulation of
1717 noise in the expression of a single gene 2002. https://doi.org/10.1038/ng869.
1718 46. Nordholt N, Van Heerden J, Kort R, Bruggeman FJ. Effects of growth rate and promoter
1719 activity on single-cell protein expression. Scientific Reports 2017 7:1 2017; 7:1–11.
1720 https://doi.org/10.1038/s41598-017-05871-3.
1721 47. Rothe S, Prakash A, Tyedmers J. The Insoluble Protein Deposit (IPOD) in Yeast. Front
1722 Mol Neurosci 2018; 11:385163. https://doi.org/10.3389/FNMOL.2018.00237/

1723 48. Tyedmers J, Treusch S, Dong J, McCaffery JM, Bevis B, Lindquist S. Prion induction
1724 involves an ancient system for the sequestration of aggregated proteins and heritable changes
1725 in prion fragmentation. Proc Natl Acad Sci U S A 2010; 107:8633–8.
1726 https://doi.org/10.1073/PNAS.1003895107/
1727 49. Kaganovich D, Kopito R, Frydman J. Misfolded proteins partition between two distinct
1728 quality control compartments. Nature 2008 454:7208 2008; 454:1088–95.
1729 https://doi.org/10.1038/nature07195.
1730 50. Kayed R, Head E, Thompson JL, McIntire TM, Milton SC, Cotman CW, et al. Common
1731 structure of soluble amyloid oligomers implies common mechanism of pathogenesis. Science
1732 (1979) 2003; 300:486–9. https://doi.org/10.1126/SCIENCE.1079469/
1733 51. Majumdar A, Cesario WC, White-Grindley E, Jiang H, Ren F, Khan MR, et al. Critical
1734 role of amyloid-like oligomers of *Drosophila* Orb2 in the persistence of memory. Cell 2012;
1735 148:515–29. https://doi.org/10.1016/J.CELL.2012.01.004.
1736 52. Alberti S, Halfmann R, King O, Kapila A, Lindquist S. A systematic survey identifies
1737 prions and illuminates sequence features of prionogenic proteins. Cell 2009; 137:146.
1738 https://doi.org/10.1016/J.CELL.2009.02.044.
1739 53. Perov S, Lidor O, Salinas N, Golan N, Tayeb-Fligelman E, Deshmukh M, et al. Structural
1740 Insights into Curli CsgA Cross-β Fibril Architecture Inspire Repurposing of Anti-amyloid
1741 Compounds as Anti-biofilm Agents. PLoS Pathog 2019;15.
1742 https://doi.org/10.1371/JOURNAL.PPAT.1007978.
1743 54. Yan Z, Yin M, Chen J, Li X. Assembly and substrate recognition of curli biogenesis
1744 system. Nature Communications 2020 11:1 2020; 11:1–10. https://doi.org/10.1038/s41467-019-
1745 14145-7.
1746 55. Sheng J, Olrichs NK, Gadella BM, Kaloyanova D V., Bernd Helms J. Regulation of
1747 Functional Protein Aggregation by Multiple Factors: Implications for the Amyloidogenic Behavior
1748 of the CAP Superfamily Proteins. Int J Mol Sci 2020; 21:1–23.
1749 https://doi.org/10.3390/IJMS21186530.
1750 56. Jackson MP, Hewitt EW. Why Are Functional Amyloids Non-Toxic in Humans?
1751 Biomolecules 2017;7. https://doi.org/10.3390/BIOM7040071.
1752 57. Kong L, Sui C, Chen T, Zhang L, Zhao W, Zheng Y, et al. The ubiquitin E3 ligase
1753 TRIM10 promotes STING aggregation and activation in the Golgi apparatus. Cell Rep 2023;42.
1754 https://doi.org/10.1016/j.celrep.2023.112306.

1755 58. Liu B, Zhang M, Chu H, Zhang H, Wu H, Song G, et al. The ubiquitin E3 ligase TRIM31
1756 promotes aggregation and activation of the signaling adaptor MAVS through Lys63-linked
1757 polyubiquitination. Nat Immunol 2017; 18:214–24. https://doi.org/10.1038/ni.3641.
1758 59. Masperone L, Codrich M, Persichetti F, Gustincich S, Zucchelli S, Legname G. The E3
1759 Ubiquitin Ligase TRAF6 Interacts with the Cellular Prion Protein and Modulates Its Solubility and
1760 Recruitment to Cytoplasmic p62/SQSTM1-Positive Aggresome-Like Structures. Mol Neurobiol
1761 2022; 59:1577–88. https://doi.org/10.1007/S12035-021-02666-6/
1762 60. Zhang ZY, Harischandra DS, Wang R, Ghaisas S, Zhao JY, McMonagle TP, et al.
1763 TRIM11 protects against tauopathies and is down-regulated in Alzheimer's disease. Science
1764 (1979) 2023;381. https://doi.org/10.1126/science.add6696.
1765 61. Davidson JM, Wu SSL, Rayner SL, Cheng F, Duncan K, Russo C, et al. The E3
1766 Ubiquitin Ligase SCF Cyclin F Promotes Sequestosome-1/p62 Insolubility and Foci Formation
1767 and is Dysregulated in ALS and FTD Pathogenesis. Mol Neurobiol 2023; 60:5034–54.
1768 https://doi.org/10.1007/s12035-023-03355-2.
1769 62. Watabe K, Kato Y, Sakuma M, Murata M, Niida-Kawaguchi M, Takemura T, et al. Praja1
1770 RING-finger E3 ubiquitin ligase suppresses neuronal cytoplasmic TDP-43 aggregate formation.
1771 Neuropathology 2020; 40:570–86. https://doi.org/10.1111/neup.12694.
1772 63. Won SY, Park JJ, You ST, Hyeun JA, Kim HK, Jin BK, et al. p21-activated kinase 4
1773 controls the aggregation of α-synuclein by reducing the monomeric and aggregated forms of α-
1774 synuclein: involvement of the E3 ubiquitin ligase NEDD4-1. Cell Death Dis 2022;13.
1775 https://doi.org/10.1038/s41419-022-05030-1.
1776 64. Watabe K, Niida-Kawaguchi M, Tada M, Kato Y, Murata M, Tanji K, et al. Praja1 RING-
1777 finger E3 ubiquitin ligase is a common suppressor of neurodegenerative disease-associated
1778 protein aggregation. Neuropathology 2022; 42:488–504. https://doi.org/10.1111/neup.12840.
1779 65. Nadel CM, Thwin AC, Callahan M, Lee K, Connelly E, Craik CS, et al. The E3 Ubiquitin
1780 Ligase, CHIP/STUB1, Inhibits Aggregation of Phosphorylated Proteoforms of Microtubule-
1781 associated Protein Tau (MAPT). J Mol Biol 2023;435.
1782 https://doi.org/10.1016/j.jmb.2023.168026.
1783 66. Yan C, Gong L, Chen L, Xu M, Abou-Hamdan H, Tang M, et al. PHB2 (prohibitin 2)
1784 promotes PINK1-PRKN/Parkin-dependent mitophagy by the PARL-PGAM5-PINK1 axis 2020.
1785 https://doi.org/10.1080/15548627.2019.1628520.
1786 67. Lindholm AK, Dyer KA, Firman RC, Fishman L, Forstmeier W, Holman L, et al. The
1787 Ecology and Evolutionary Dynamics of Meiotic Drive. Trends Ecol Evol 2016; 31:315–26.
1788 https://doi.org/10.1016/j.tree.2016.02.001.

1789 68. Hernández JFL, Rubinstein BY, Unckless RL, Zanders SE. Modeling the Evolution of
1790 Populations with Multiple Killer Meiotic Drivers. BioRxiv 2023:2023.09.28.560003.
1791 https://doi.org/10.1101/2023.09.28.560003.
1792 69. Dasgupta SK, Jain S, Kaushal D, Tyagi AK. Expression Systems for Study of
1793 Mycobacterial Gene Regulation and Development of Recombinant BCG Vaccines. Biochem
1794 Biophys Res Commun 1998; 246:797–804. https://doi.org/10.1006/BBRC.1998.8724.
1795 70. Sikorski RS, Hieter P. A system of shuttle vectors and yeast host strains designed for
1796 efficient manipulation of DNA in Saccharomyces cerevisiae. Genetics 1989; 122:19–27.
1797 https://doi.org/10.1093/GENETICS/122.1.19.
1798 71. Snaith HA, Samejima I, Sawin KE. Multistep and multimode cortical anchoring of tea1p
1799 at cell tips in fission yeast. EMBO J 2005; 24:3690. https://doi.org/10.1038/SJ.EMBOJ.7600838.
1800 72. Sonnhammer ELL, Von Heijne G, Krogh A. A hidden Markov model for predicting
1801 transmembrane helices in protein sequences. AAAI Press; 1998.
1802 73. Krogh A, Larsson B, Von Heijne G, Sonnhammer ELL. Predicting transmembrane
1803 protein topology with a hidden Markov model: Application to complete genomes. J Mol Biol
1804 2001; 305:567–80. https://doi.org/10.1006/jmbi.2000.4315.
1805 74. Chen Y hui, Wang G yuan, Hao H chao, Chao C jiang, Wang Y, Jin Q wen. Facile
1806 manipulation of protein localization in fission yeast through binding of GFP-binding protein to
1807 GFP. J Cell Sci 2017; 130:1003–15. https://doi.org/10.1242/JCS.198457.
1808 75. Sanchez MI, Ting AY. Directed evolution improves the catalytic efficiency of TEV
1809 protease. Nature Methods 2019 17:2 2019; 17:167–74. https://doi.org/10.1038/s41592-019-
1810 0665-7.
1811 76. Kapust RB, Waugh DS. *Escherichia coli* maltose-binding protein is uncommonly
1812 effective at promoting the solubility of polypeptides to which it is fused. Protein Sci 1999;
1813 8:1668. https://doi.org/10.1110/PS.8.8.1668.
1814 77. Fox JD, Routzahn KM, Bucher MH, Waugh DS. Maltodextrin-binding proteins from
1815 diverse bacteria and archaea are potent solubility enhancers. FEBS Lett 2003; 537:53–7.
1816 https://doi.org/10.1016/S0014-5793(03)00070-X.
1817 78. Ottoz DSM, Rudolf F, Stelling J. Inducible, tightly regulated and growth condition-
1818 independent transcription factor in *Saccharomyces cerevisiae*. Nucleic Acids Res 2014;42.
1819 https://doi.org/10.1093/nar/gku616.
1820 79. R Elble. A simple and efficient procedure for transformation of yeasts. Biotechniques
1821 1992.

1822 80. Winston F, Dollard C, Ricupero-Hovasse SL. Construction of a set of convenient
1823 *Saccharomyces cerevisiae* strains that are isogenic to S288C. Yeast 1995;11:53–5.
1824 https://doi.org/10.1002/YEA.320110107.
1825 81. Gasteiger E, Hoogland C, Gattiker A, Duvaud S, Wilkins MR, Appel RD, et al. Protein
1826 Identification and Analysis Tools on the ExPASy Server. The Proteomics Protocols Handbook
1827 2005:571–607. https://doi.org/10.1385/1-59259-890-0:571.
1828
1829

Figure 1

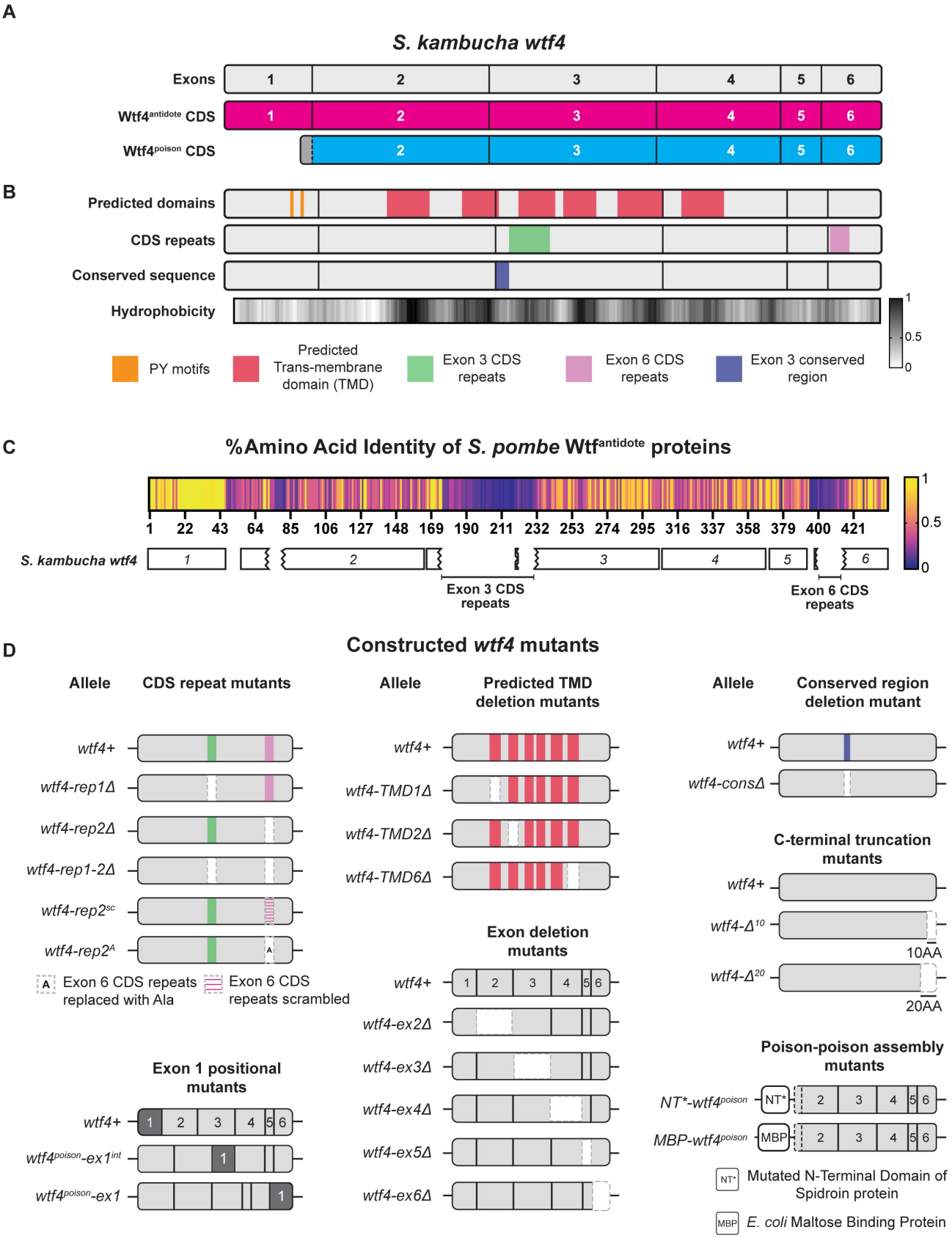
A
S. kambucha wtf4
Exons
1
2
3
4
5
6
Wtf4antidote CDS
Wtf4poison CDS
B
Predicted domains
CDS repeats
Conserved sequence
Hydrophobicity
1
0.5
0
PY motifs
Predicted Trans-membrane domain (TMD)
Exon 3 CDS repeats
Exon 6 CDS repeats
Exon 3 conserved region
C
%Amino Acid Identity of S. pombe Wtfantidote proteins
1 22 43 64 85 106 127 148 169 190 211 232 253 274 295 316 337 358 379 400 421
S. kambucha wtf4
Exon 3 CDS repeats
Exon 6 CDS repeats
D
Constructed wtf4 mutants
Allele
CDS repeat mutants
wtf4+
wtf4-rep1Δ
wtf4-rep2Δ
wtf4-rep1-2Δ
wtf4-rep2sc
wtf4-rep2A
Exon 6 CDS repeats replaced with Ala
Exon 6 CDS repeats scrambled
Exon 1 positional mutants
wtf4poison-ex1int
wtf4poison-ex1
Predicted TMD deletion mutants
wtf4-TMD1Δ
wtf4-TMD2Δ
wtf4-TMD6Δ
Exon deletion mutants
wtf4-ex2Δ
wtf4-ex3Δ
wtf4-ex4Δ
wtf4-ex5Δ
wtf4-ex6Δ
Conserved region deletion mutant
wtf4-consΔ
C-terminal truncation mutants
wtf4-Δ10
10AA
wtf4-Δ20
20AA
Poison-poison assembly mutants
NT*-wtf4poison
MBP-wtf4poison
Mutated N-Terminal Domain of Spidroin protein
E. coli Maltose Binding Protein

Figure 2

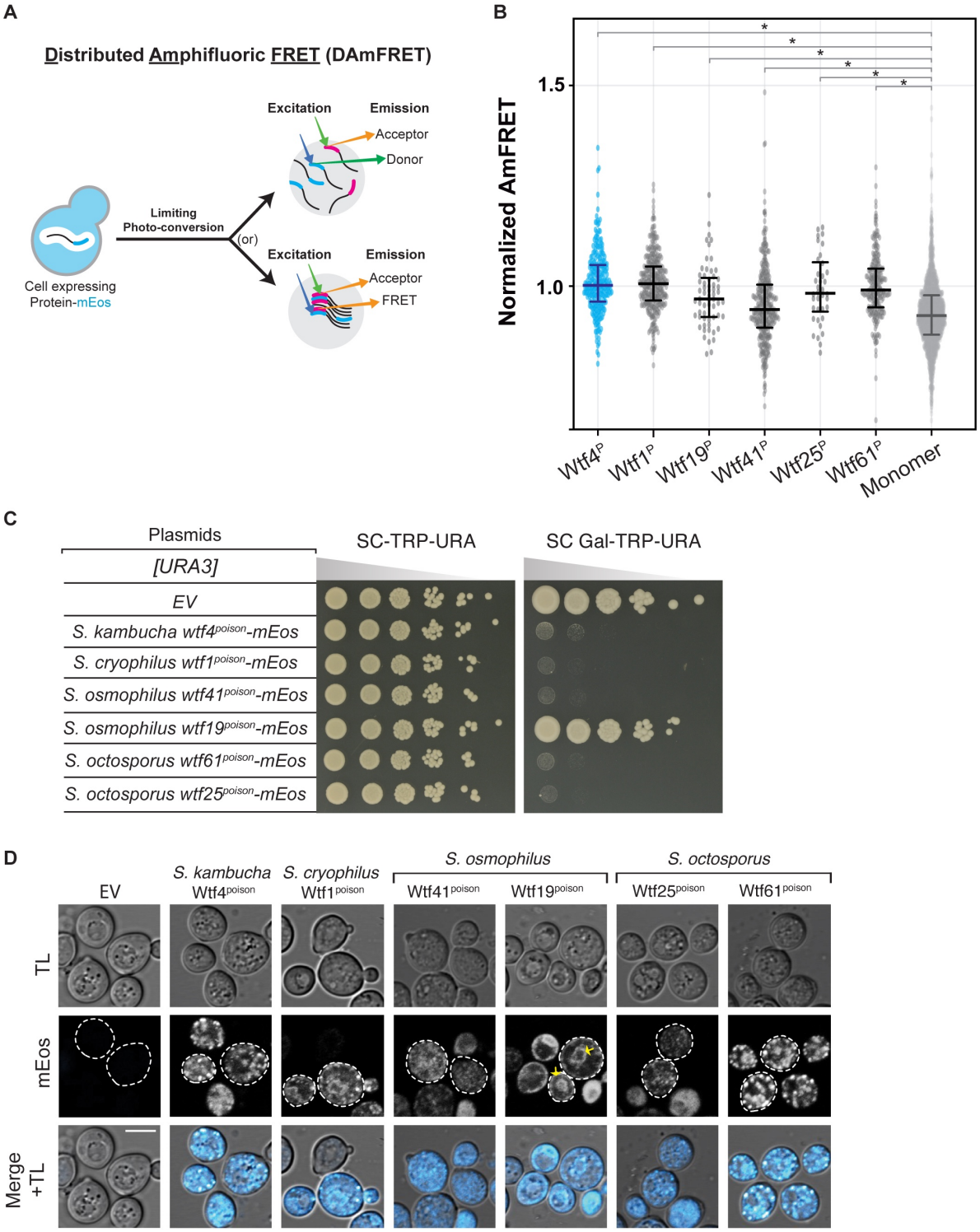
A
Distributed Amphifluoric FRET (DAmFRET)
Excitation
Emission
Acceptor
Donor
Limiting
Photo-conversion
(or)
Excitation
Emission
Acceptor
FRET
Cell expressing
Protein-mEos
B
Normalized AmFRET
1.5
1.0
Wtf4P
Wtf1P
Wtf19P
Wtf41P
Wtf25P
Wtf61P
Monomer
C
Plasmids
SC-TRP-URA
SC Gal-TRP-URA
[URA3]
EV
S. kambucha wtf4poison-mEos
S. cryophilus wtf1poison-mEos
S. osmophilus wtf41poison-mEos
S. osmophilus wtf19poison-mEos
S. octosporus wtf61poison-mEos
S. octosporus wtf25poison-mEos
D
EV
S. kambucha Wtf4poison
S. cryophilus Wtf1poison
S. osmophilus
Wtf41poison
Wtf19poison
S. octosporus
Wtf25poison
Wtf61poison
TL
mEos
Merge +TL

Figure 3

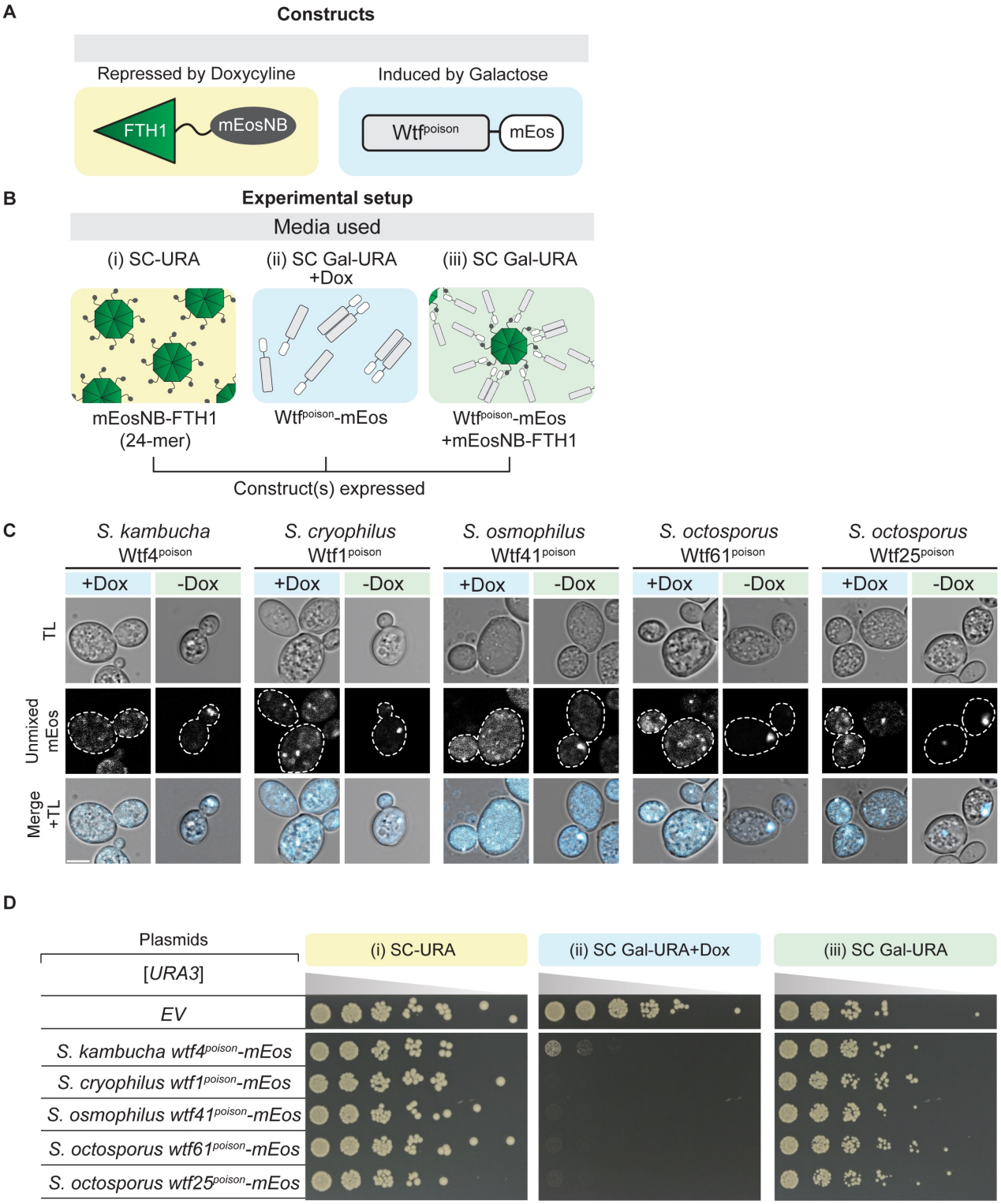
A
Constructs
Repressed by Doxycyline
Induced by Galactose
FTH1
mEosNB
Wtf poison
mEos
B
Experimental setup
Media used
(i) SC-URA
(ii) SC Gal-URA +Dox
(iii) SC Gal-URA
mEosNB-FTH1 (24-mer)
Wtf poison-mEos
Wtf poison-mEos +mEosNB-FTH1
Construct(s) expressed
C
S. kambucha Wtf4 poison
S. cryophilus Wtf1 poison
S. osmophilus Wtf41 poison
S. octosporus Wtf61 poison
S. octosporus Wtf25 poison
+Dox
-Dox
TL
Unmixed mEos
Merge +TL
D
Plasmids
[URA3]
EV
S. kambucha wtf4 poison-mEos
S. cryophilus wtf1 poison-mEos
S. osmophilus wtf41 poison-mEos
S. octosporus wtf61 poison-mEos
S. octosporus wtf25 poison-mEos
(i) SC-URA
(ii) SC Gal-URA+Dox
(iii) SC Gal-URA

Figure 4

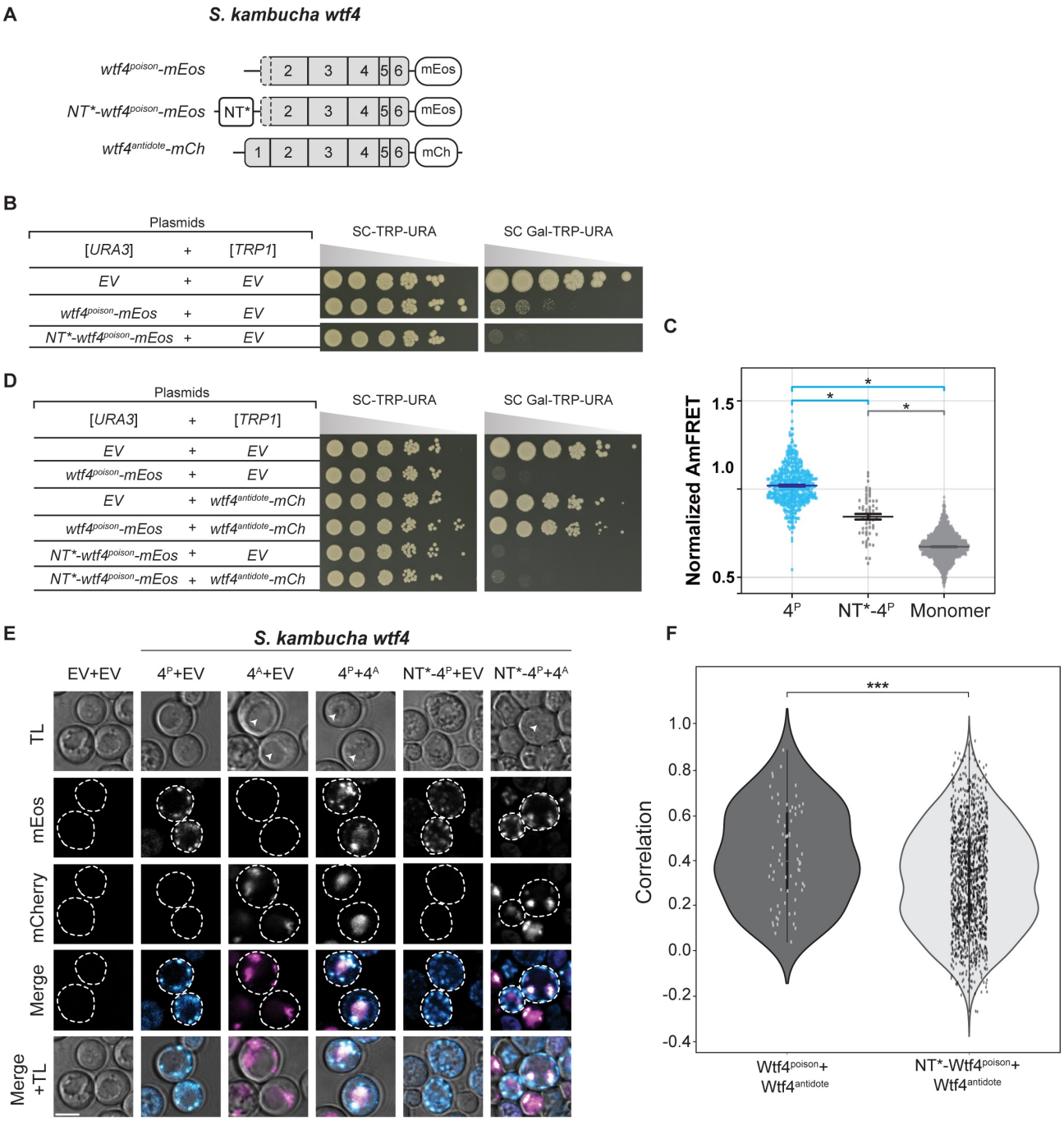
A
S. kambucha wtf4
wtf4poison-mEos
NT*-wtf4poison-mEos
wtf4antidote-mCh
NT*
mEos
mCh
B
Plasmids
[URA3] + [TRP1]
EV + EV
wtf4poison-mEos + EV
NT*-wtf4poison-mEos + EV
SC-TRP-URA
SC Gal-TRP-URA
C
Normalized AmFRET
4P
NT*-4P
Monomer
D
wtf4antidote-mCh
E
S. kambucha wtf4
EV+EV
4P+EV
4A+EV
4P+4A
NT*-4P+EV
NT*-4P+4A
TL
mEos
mCherry
Merge
Merge +TL
F
Correlation
Wtf4poison+ Wtf4antidote
NT*-Wtf4poison+ Wtf4antidote

Figure 5

A

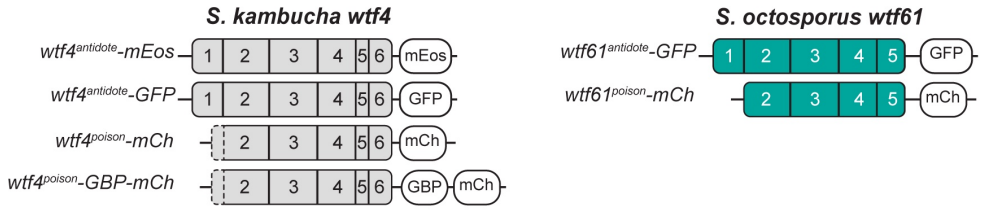

C

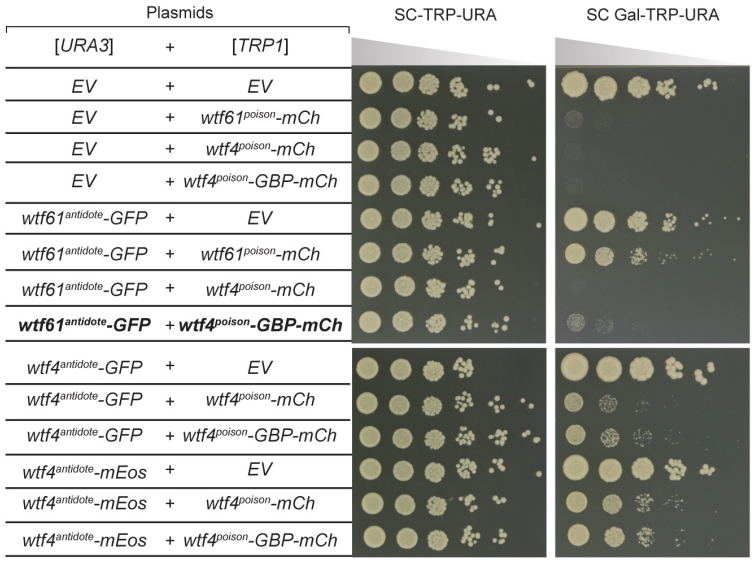

B

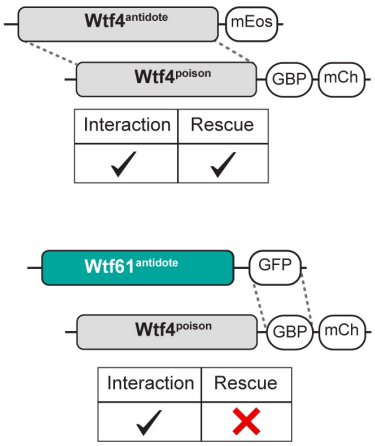

D

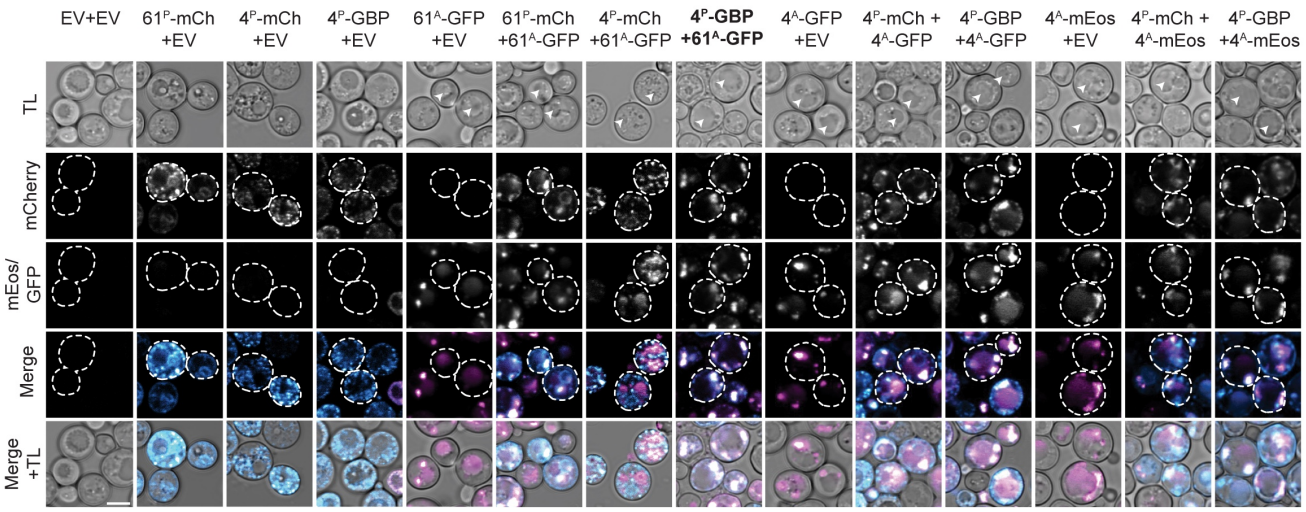

E

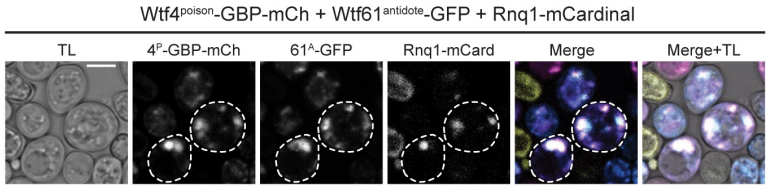

Figure 6

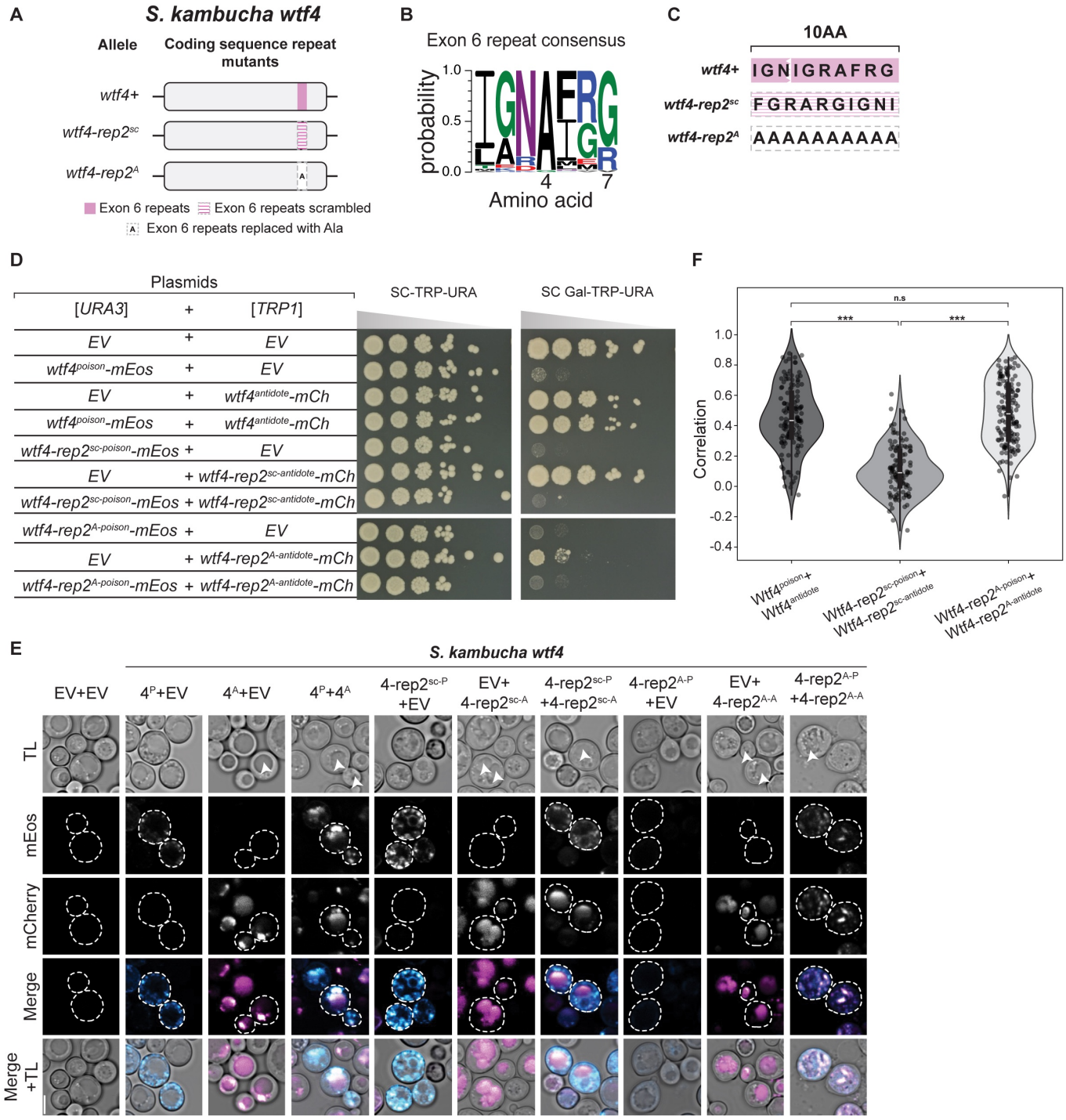
A
S. kambucha wtf4
Allele
Coding sequence repeat mutants
wtf4+
wtf4-rep2sc
wtf4-rep2A
Exon 6 repeats
Exon 6 repeats scrambled
Exon 6 repeats replaced with Ala
B
Exon 6 repeat consensus
probability
1.0
0.5
0.0
4
7
Amino acid
C
10AA
wtf4+ IGNIGRAFRG
wtf4-rep2sc FGRARGIGNI
wtf4-rep2A AAAAAAAAAA
D
Plasmids
[URA3] + [TRP1]
SC-TRP-URA
SC Gal-TRP-URA
EV + EV
wtf4poison-mEos + EV
EV + wtf4antidote-mCh
wtf4poison-mEos + wtf4antidote-mCh
wtf4-rep2sc-poison-mEos + EV
EV + wtf4-rep2sc-antidote-mCh
wtf4-rep2sc-poison-mEos + wtf4-rep2sc-antidote-mCh
wtf4-rep2A-poison-mEos + EV
EV + wtf4-rep2A-antidote-mCh
wtf4-rep2A-poison-mEos + wtf4-rep2A-antidote-mCh
F
n.s
***
***
Correlation
1.0
0.8
0.6
0.4
0.2
0.0
-0.2
-0.4
Wtf4poison+ Wtf4antidote
Wtf4-rep2sc-poison+ Wtf4-rep2sc-antidote
Wtf4-rep2A-poison+ Wtf4-rep2A-antidote
E
S. kambucha wtf4
EV+EV
4P+EV
4A+EV
4P+4A
4-rep2sc-P +EV
EV+ 4-rep2sc-A
4-rep2sc-P +4-rep2sc-A
4-rep2A-P +EV
EV+ 4-rep2A-A
4-rep2A-P +4-rep2A-A
TL
mEos
mCherry
Merge
Merge +TL

Figure 7

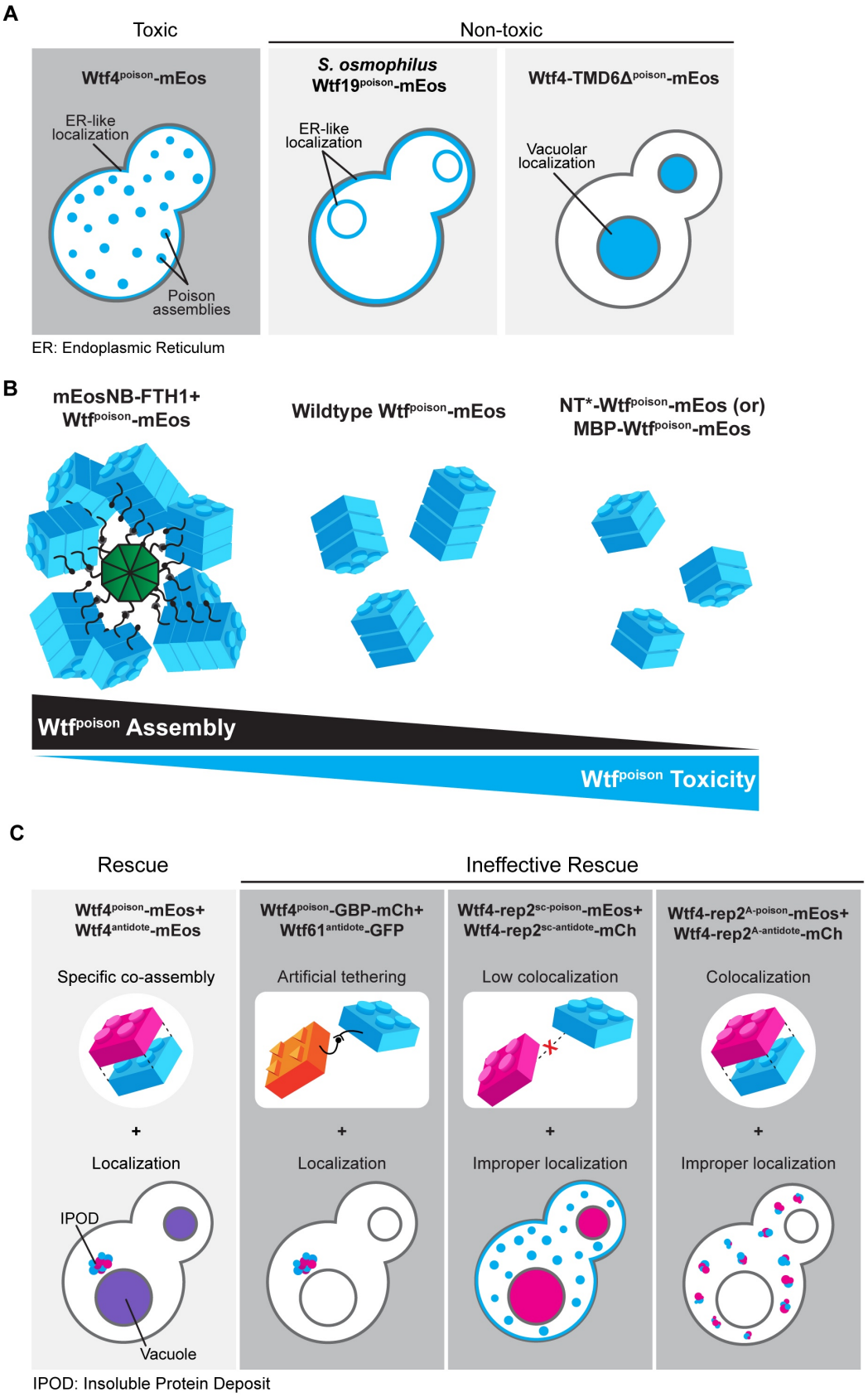
A
Toxic
Non-toxic
Wtf4poison-mEos
ER-like localization
Poison assemblies
S. osmophilus Wtf19poison-mEos
ER-like localization
Wtf4-TMD6Δpoison-mEos
Vacuolar localization
ER: Endoplasmic Reticulum
B
mEosNB-FTH1+ Wtfpoison-mEos
Wildtype Wtfpoison-mEos
NT*-Wtfpoison-mEos (or) MBP-Wtfpoison-mEos
Wtfpoison Assembly
Wtfpoison Toxicity
C
Rescue
Ineffective Rescue
Wtf4poison-mEos+ Wtf4antidote-mEos
Specific co-assembly
+
Localization
IPOD
Vacuole
Wtf4poison-GBP-mCh+ Wtf61antidote-GFP
Artificial tethering
+
Localization
Wtf4-rep2sc-poison-mEos+ Wtf4-rep2sc-antidote-mCh
Low colocalization
+
Improper localization
Wtf4-rep2A-poison-mEos+ Wtf4-rep2A-antidote-mCh
Colocalization
+
Improper localization
IPOD: Insoluble Protein Deposit

S1 Figure

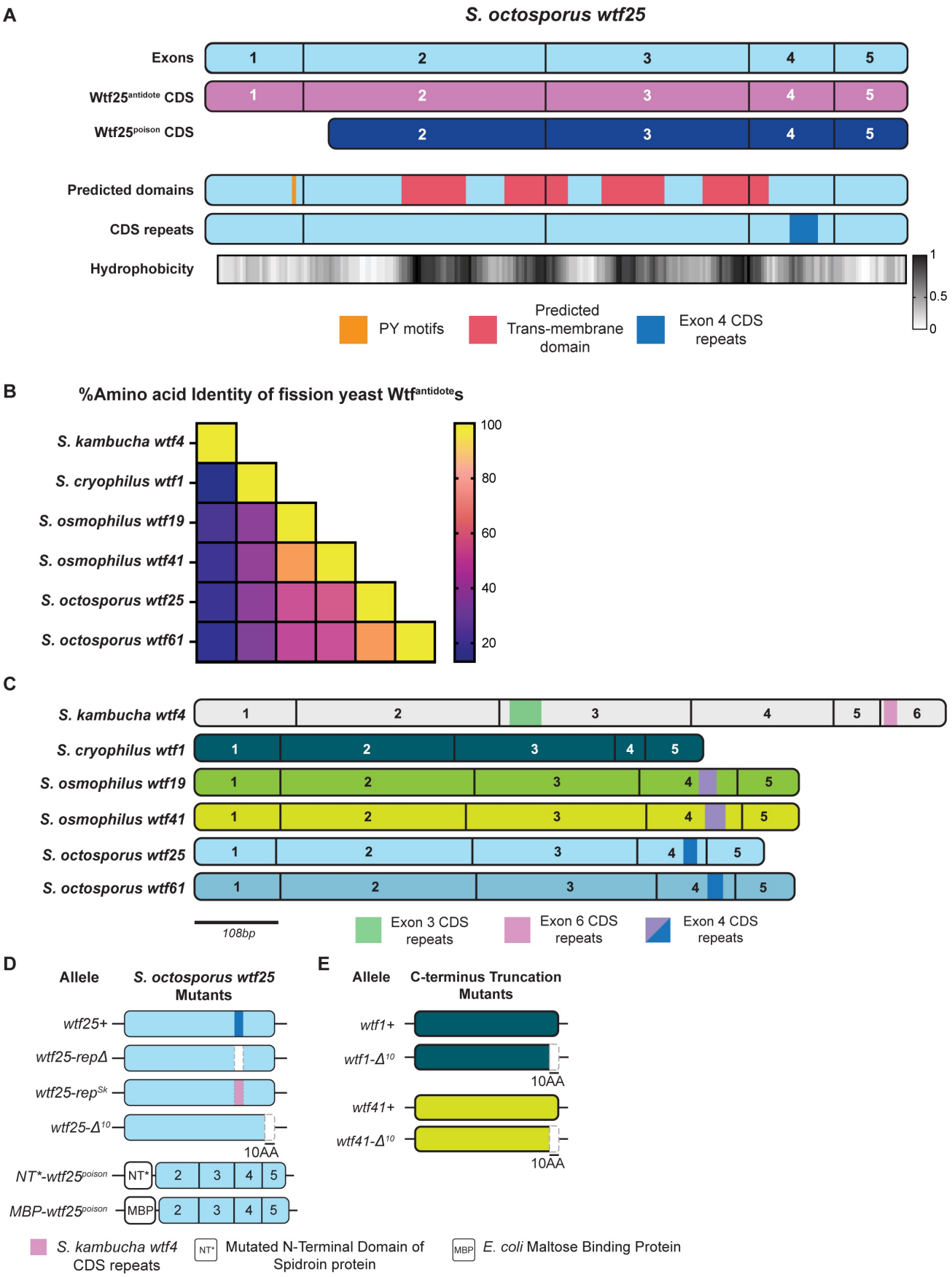
A
S. octosporus wtf25
Exons
Wtf25antidote CDS
Wtf25poison CDS
Predicted domains
CDS repeats
Hydrophobicity
PY motifs
Predicted Trans-membrane domain
Exon 4 CDS repeats
B
%Amino acid Identity of fission yeast Wtfantidotes
S. kambucha wtf4
S. cryophilus wtf1
S. osmophilus wtf19
S. osmophilus wtf41
S. octosporus wtf25
S. octosporus wtf61
C
108bp
Exon 3 CDS repeats
Exon 6 CDS repeats
Exon 4 CDS repeats
D
Allele
S. octosporus wtf25 Mutants
wtf25+
wtf25-repΔ
wtf25-repSk
wtf25-Δ10
10AA
NT*-wtf25poison
MBP-wtf25poison
S. kambucha wtf4 CDS repeats
Mutated N-Terminal Domain of Spidroin protein
E. coli Maltose Binding Protein
E
Allele
C-terminus Truncation Mutants
wtf1+
wtf1-Δ10
wtf41+
wtf41-Δ10

S2 Figure

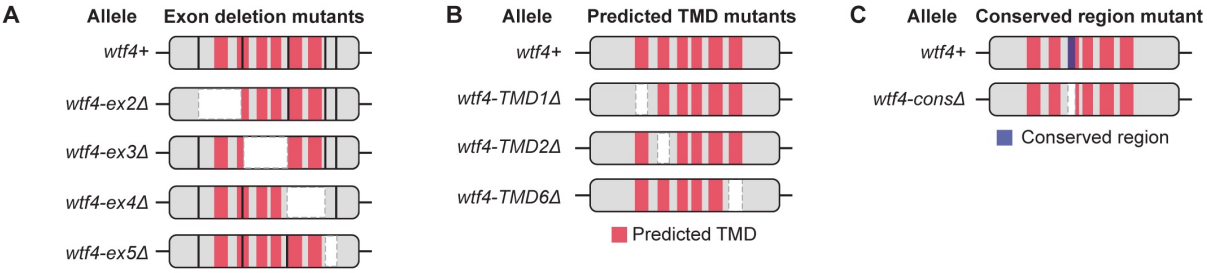
A
Allele
Exon deletion mutants
wtf4+
wtf4-ex2Δ
wtf4-ex3Δ
wtf4-ex4Δ
wtf4-ex5Δ
B
Allele
Predicted TMD mutants
wtf4+
wtf4-TMD1Δ
wtf4-TMD2Δ
wtf4-TMD6Δ
Predicted TMD
C
Allele
Conserved region mutant
wtf4+
wtf4-consΔ
Conserved region

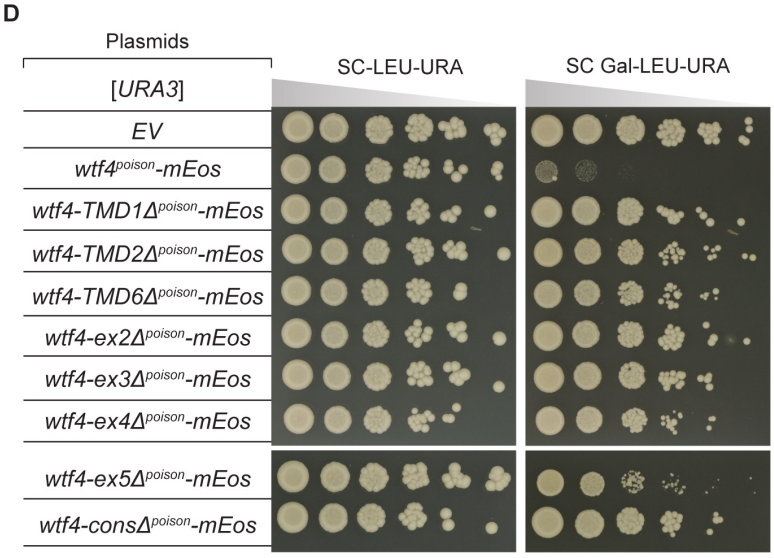
D
Plasmids
SC-LEU-URA
SC Gal-LEU-URA
[URA3]
EV
wtf4poison-mEos
wtf4-TMD1Δpoison-mEos
wtf4-TMD2Δpoison-mEos
wtf4-TMD6Δpoison-mEos
wtf4-ex2Δpoison-mEos
wtf4-ex3Δpoison-mEos
wtf4-ex4Δpoison-mEos
wtf4-ex5Δpoison-mEos
wtf4-consΔpoison-mEos

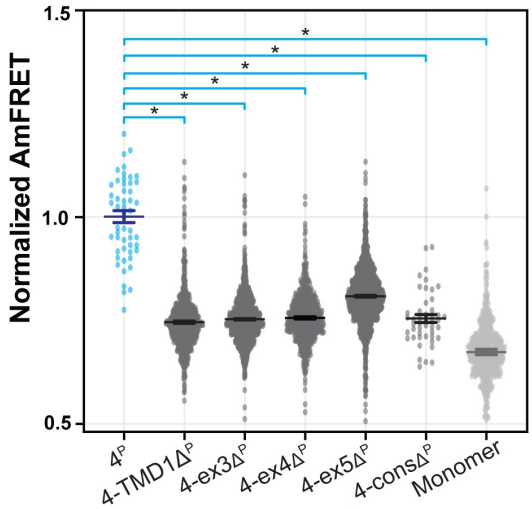
E
Normalized AmFRET
1.5
1.0
0.5
*
4P
4-TMD1ΔP
4-ex3ΔP
4-ex4ΔP
4-ex5ΔP
4-consΔP
Monomer

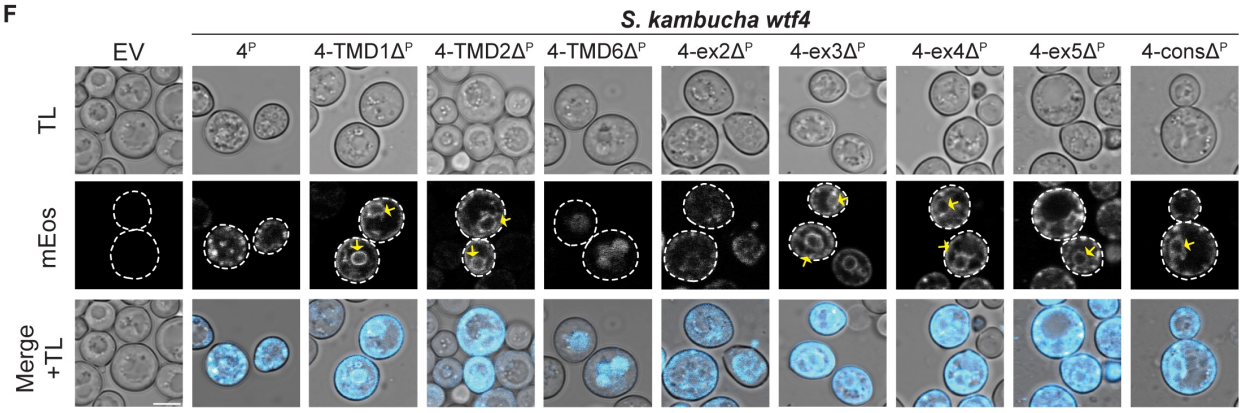
F
S. kambucha wtf4
EV
4P
4-TMD1ΔP
4-TMD2ΔP
4-TMD6ΔP
4-ex2ΔP
4-ex3ΔP
4-ex4ΔP
4-ex5ΔP
4-consΔP
TL
mEos
Merge +TL

S3 Figure

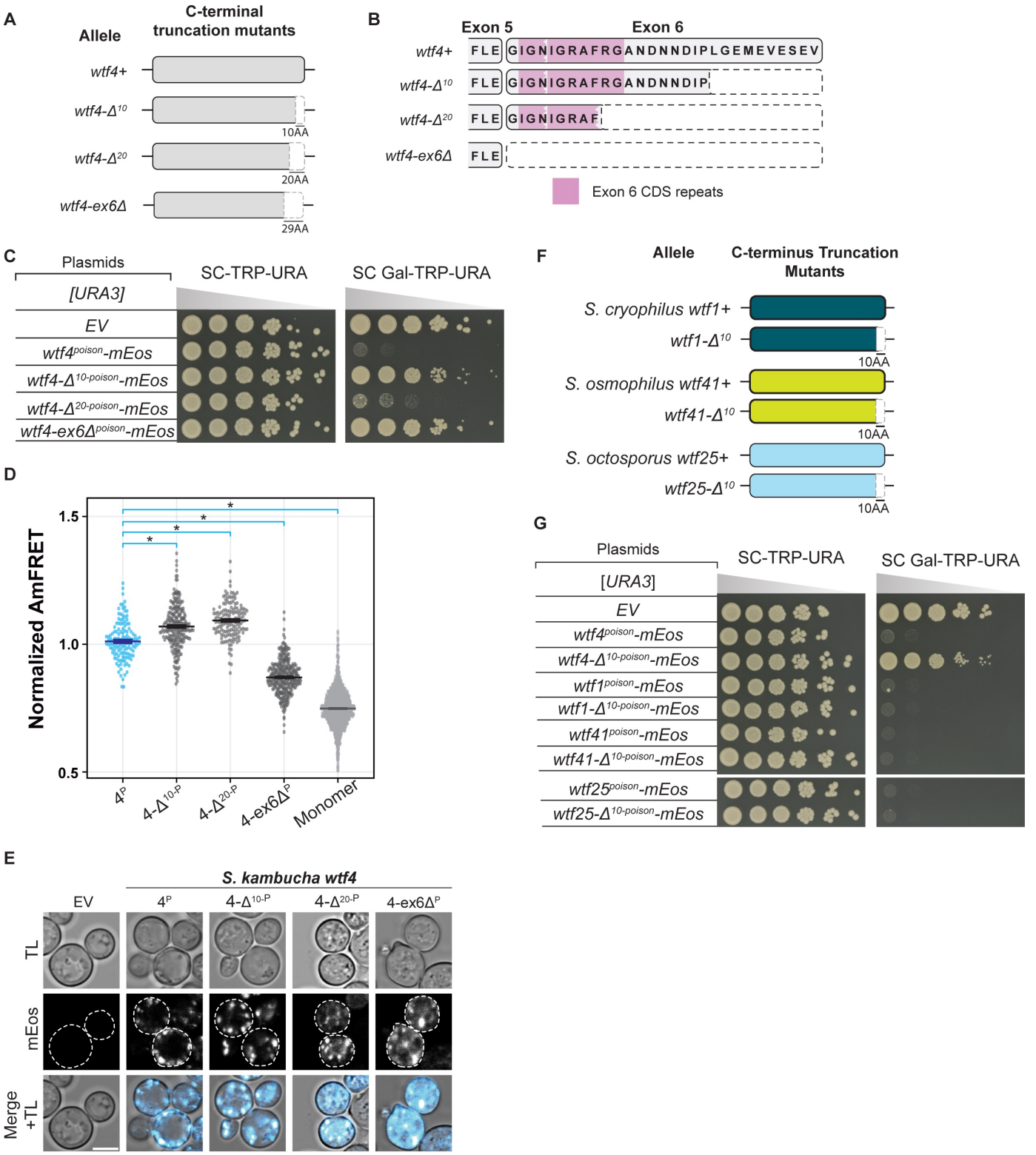
A
Allele
C-terminal truncation mutants
wtf4+
wtf4-Δ10
10AA
wtf4-Δ20
20AA
wtf4-ex6Δ
29AA
B
Exon 5
Exon 6
wtf4+
FLE GIGNIGRAFRGANDNNDIPLGEMEVESEV
wtf4-Δ10
FLE GIGNIGRAFRGANDNNDIP
wtf4-Δ20
FLE GIGNIGRAF
wtf4-ex6Δ
FLE
Exon 6 CDS repeats
C
Plasmids
SC-TRP-URA
SC Gal-TRP-URA
[URA3]
EV
wtf4poison-mEos
wtf4-Δ10-poison-mEos
wtf4-Δ20-poison-mEos
wtf4-ex6Δpoison-mEos
D
Normalized AmFRET
1.5
1.0
0.5
4P
4-Δ10-P
4-Δ20-P
4-ex6ΔP
Monomer
E
S. kambucha wtf4
EV
4P
4-Δ10-P
4-Δ20-P
4-ex6ΔP
TL
mEos
Merge +TL
F
Allele
C-terminus Truncation Mutants
S. cryophilus wtf1+
wtf1-Δ10
10AA
S. osmophilus wtf41+
wtf41-Δ10
10AA
S. octosporus wtf25+
wtf25-Δ10
10AA
G
Plasmids
SC-TRP-URA
SC Gal-TRP-URA
[URA3]
EV
wtf4poison-mEos
wtf4-Δ10-poison-mEos
wtf1poison-mEos
wtf1-Δ10-poison-mEos
wtf41poison-mEos
wtf41-Δ10-poison-mEos
wtf25poison-mEos
wtf25-Δ10-poison-mEos

S4 Figure

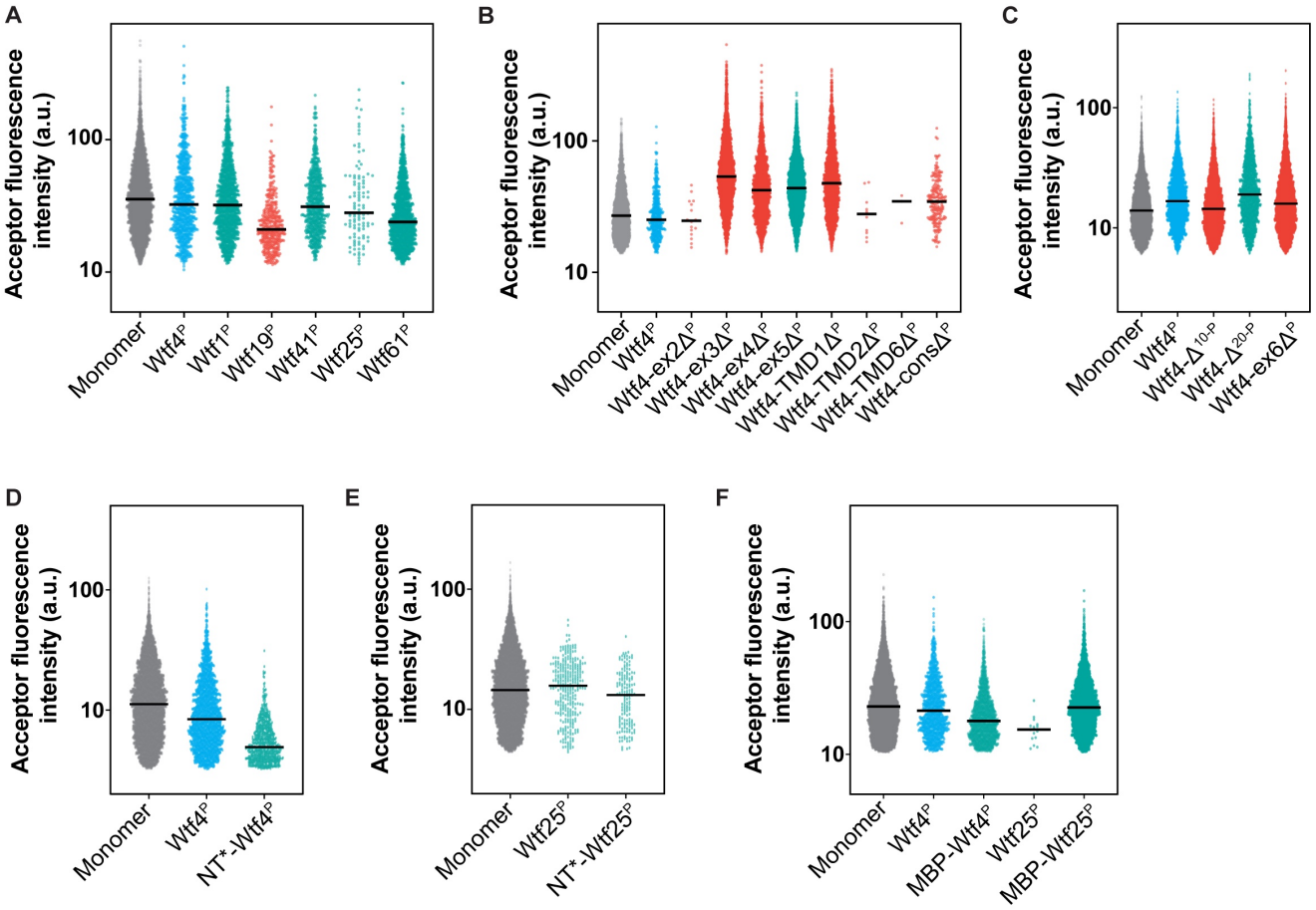
A
Acceptor fluorescence intensity (a.u.)
100
10
Monomer
Wtf4P
Wtf1P
Wtf19P
Wtf41P
Wtf25P
Wtf61P
B
Acceptor fluorescence intensity (a.u.)
100
10
Monomer
Wtf4P
Wtf4-ex2ΔP
Wtf4-ex3ΔP
Wtf4-ex4ΔP
Wtf4-ex5ΔP
Wtf4-TMD1ΔP
Wtf4-TMD2ΔP
Wtf4-TMD6ΔP
Wtf4-consΔP
C
Acceptor fluorescence intensity (a.u.)
100
10
Monomer
Wtf4P
Wtf4-Δ10-P
Wtf4-Δ20-P
Wtf4-ex6ΔP
D
Acceptor fluorescence intensity (a.u.)
100
10
Monomer
Wtf4P
NT*-Wtf4P
E
Acceptor fluorescence intensity (a.u.)
100
10
Monomer
Wtf25P
NT*-Wtf25P
F
Acceptor fluorescence intensity (a.u.)
100
10
Monomer
Wtf4P
MBP-Wtf4P
Wtf25P
MBP-Wtf25P

S5 Figure

A

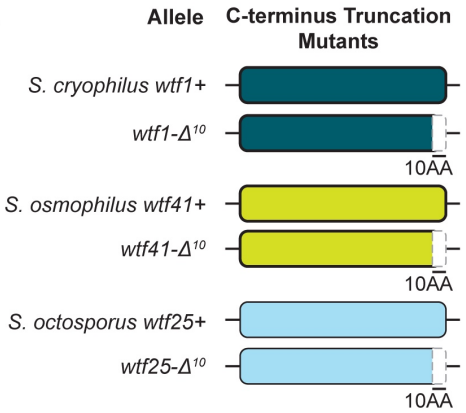

B

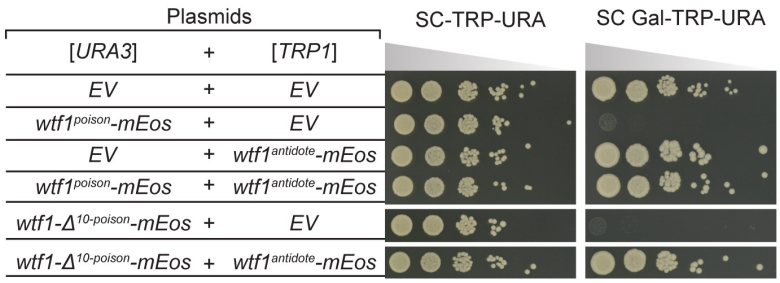

C

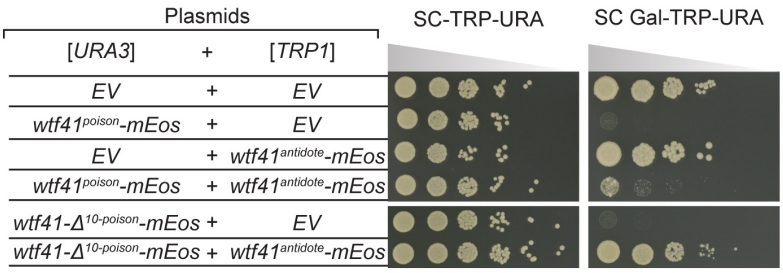

D

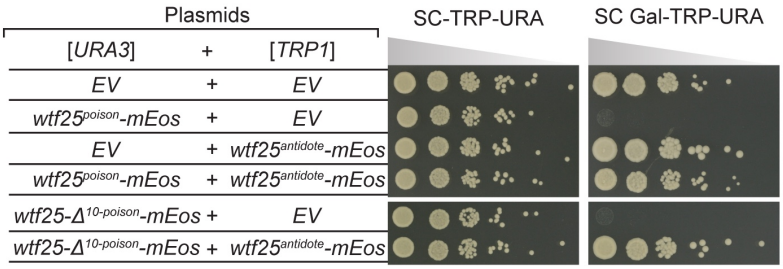

S6 Figure

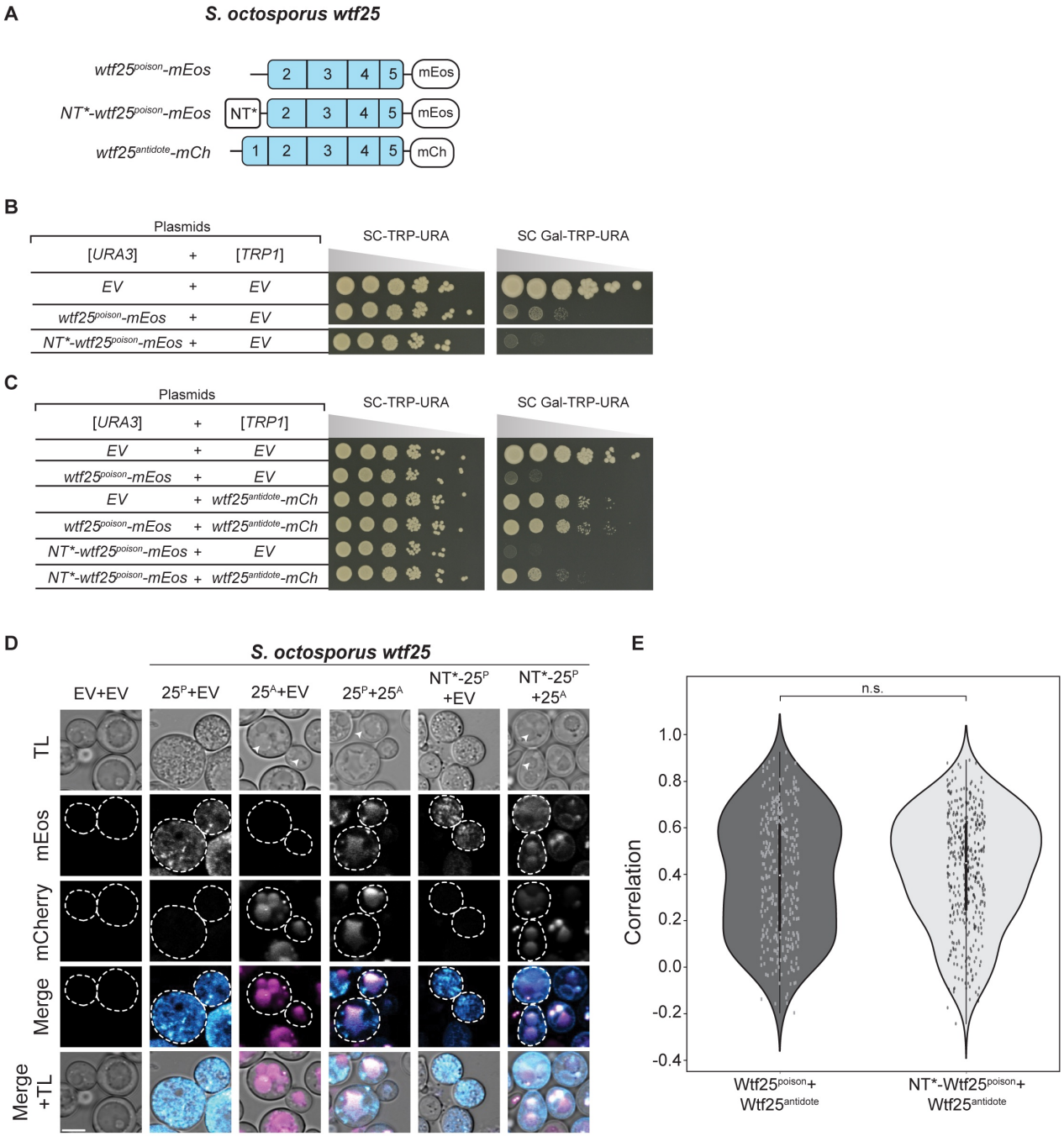
A
S. octosporus wtf25
wtf25poison-mEos
NT*-wtf25poison-mEos
wtf25antidote-mCh
NT*
1
2
3
4
5
mEos
mCh
B
Plasmids
[URA3] + [TRP1]
EV + EV
wtf25poison-mEos + EV
NT*-wtf25poison-mEos + EV
SC-TRP-URA
SC Gal-TRP-URA
C
Plasmids
[URA3] + [TRP1]
EV + EV
wtf25poison-mEos + EV
EV + wtf25antidote-mCh
wtf25poison-mEos + wtf25antidote-mCh
NT*-wtf25poison-mEos + EV
NT*-wtf25poison-mEos + wtf25antidote-mCh
SC-TRP-URA
SC Gal-TRP-URA
D
S. octosporus wtf25
EV+EV
25P+EV
25A+EV
25P+25A
NT*-25P +EV
NT*-25P +25A
TL
mEos
mCherry
Merge
Merge +TL
E
n.s.
Correlation
1.0
0.8
0.6
0.4
0.2
0.0
-0.2
-0.4
Wtf25poison+ Wtf25antidote
NT*-Wtf25poison+ Wtf25antidote

S7 Figure

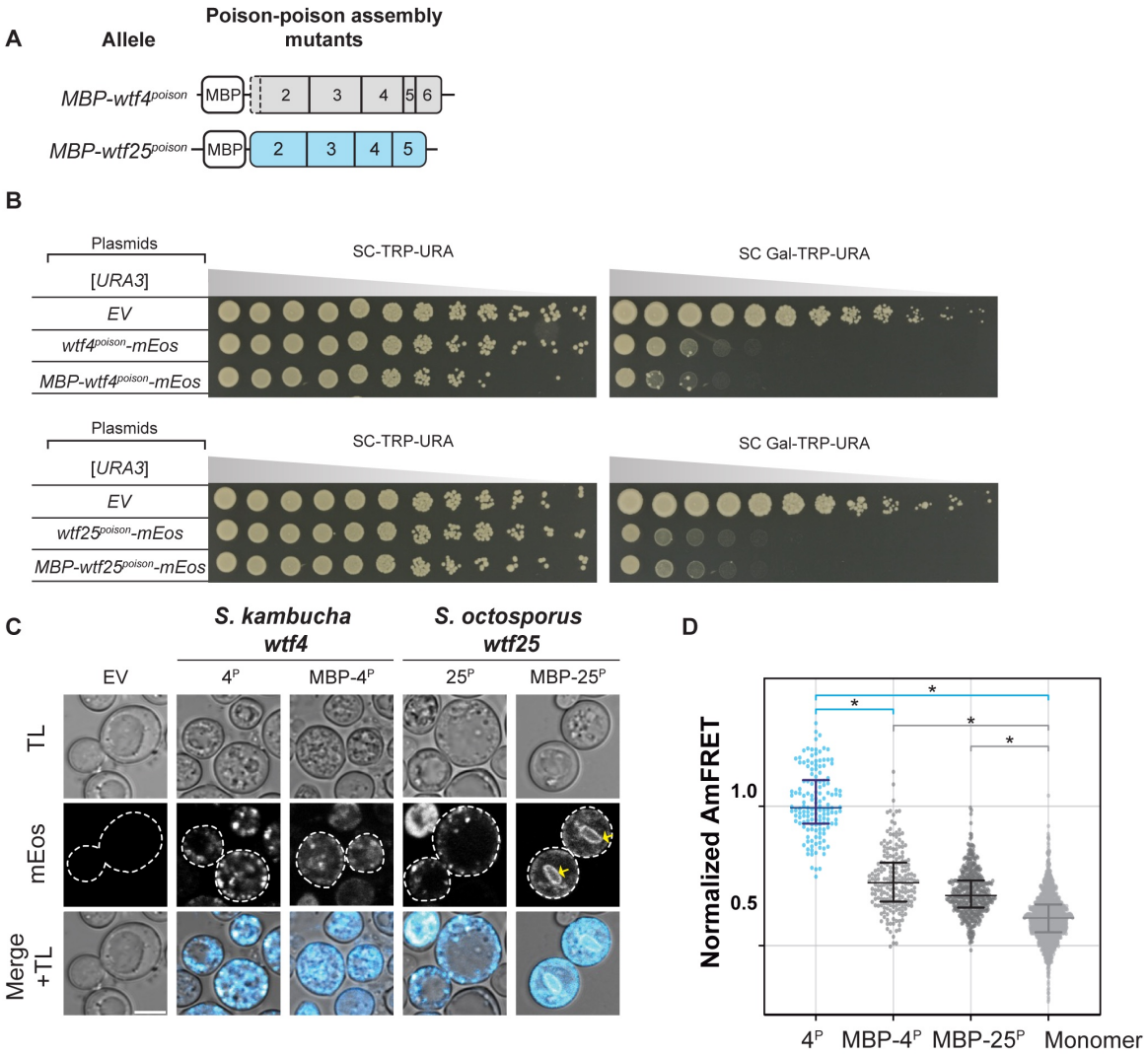
A
Allele
Poison-poison assembly mutants
MBP-wtf4poison
MBP
2
3
4
5
6
MBP-wtf25poison
MBP
2
3
4
5
B
Plasmids
[URA3]
EV
wtf4poison-mEos
MBP-wtf4poison-mEos
SC-TRP-URA
SC Gal-TRP-URA
Plasmids
[URA3]
EV
wtf25poison-mEos
MBP-wtf25poison-mEos
SC-TRP-URA
SC Gal-TRP-URA
C
S. kambucha wtf4
S. octosporus wtf25
EV
4P
MBP-4P
25P
MBP-25P
TL
mEos
Merge +TL
D
Normalized AmFRET
1.0
0.5
*
*
*
*
4P
MBP-4P
MBP-25P
Monomer

S8 Figure

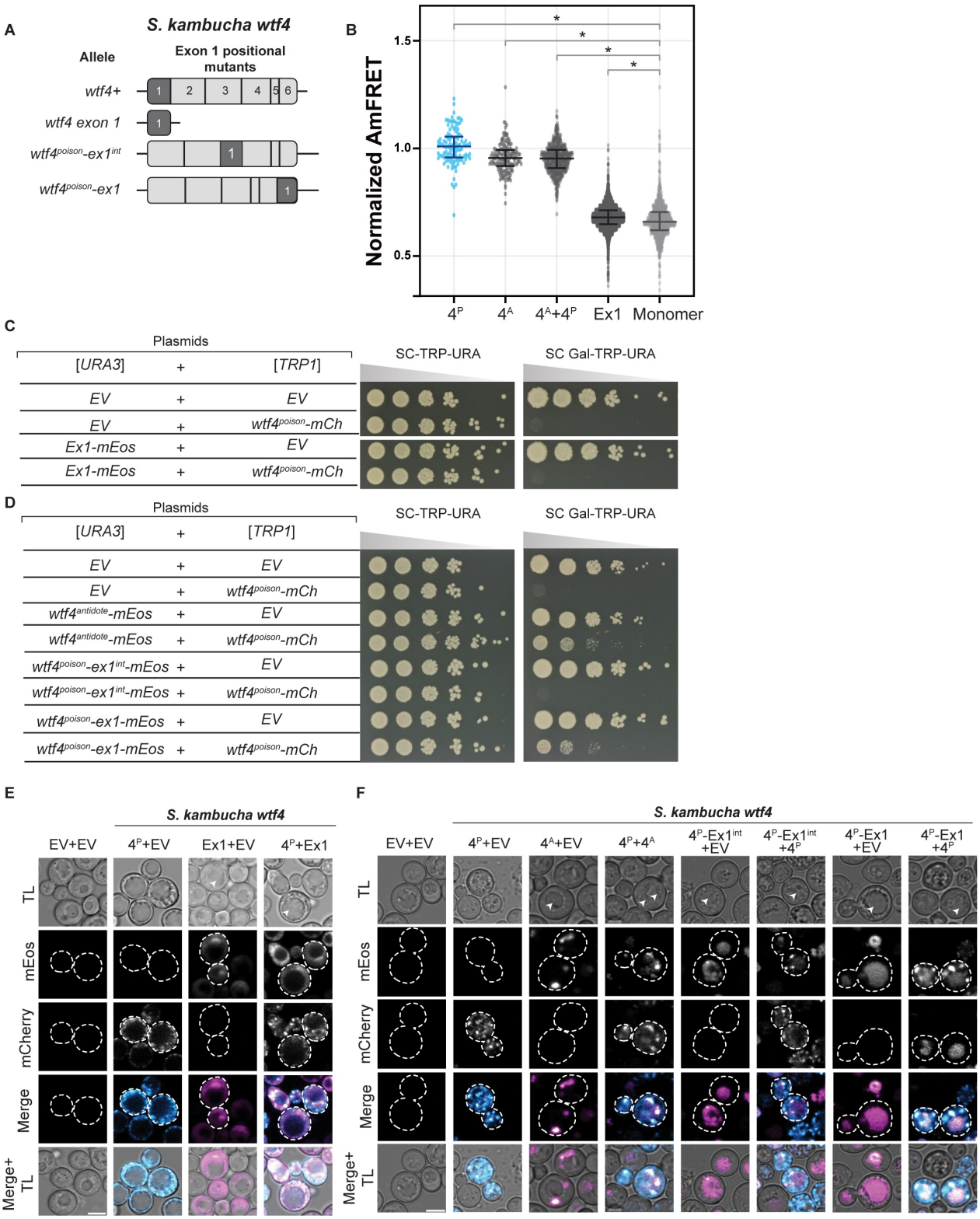
A
S. kambucha wtf4
Allele
Exon 1 positional mutants
wtf4+
wtf4 exon 1
wtf4poison-ex1int
wtf4poison-ex1
B
Normalized AmFRET
1.5
1.0
0.5
4P
4A
4A+4P
Ex1
Monomer
C
Plasmids
[URA3] + [TRP1]
EV + EV
EV + wtf4poison-mCh
Ex1-mEos + EV
Ex1-mEos + wtf4poison-mCh
SC-TRP-URA
SC Gal-TRP-URA
D
Plasmids
[URA3] + [TRP1]
EV + EV
EV + wtf4poison-mCh
wtf4antidote-mEos + EV
wtf4antidote-mEos + wtf4poison-mCh
wtf4poison-ex1int-mEos + EV
wtf4poison-ex1int-mEos + wtf4poison-mCh
wtf4poison-ex1-mEos + EV
wtf4poison-ex1-mEos + wtf4poison-mCh
SC-TRP-URA
SC Gal-TRP-URA
E
S. kambucha wtf4
EV+EV
4P+EV
Ex1+EV
4P+Ex1
TL
mEos
mCherry
Merge
Merge+ TL
F
S. kambucha wtf4
EV+EV
4P+EV
4A+EV
4P+4A
4P-Ex1int +EV
4P-Ex1int +4P
4P-Ex1 +EV
4P-Ex1 +4P
TL
mEos
mCherry
Merge
Merge+ TL

S9 Figure

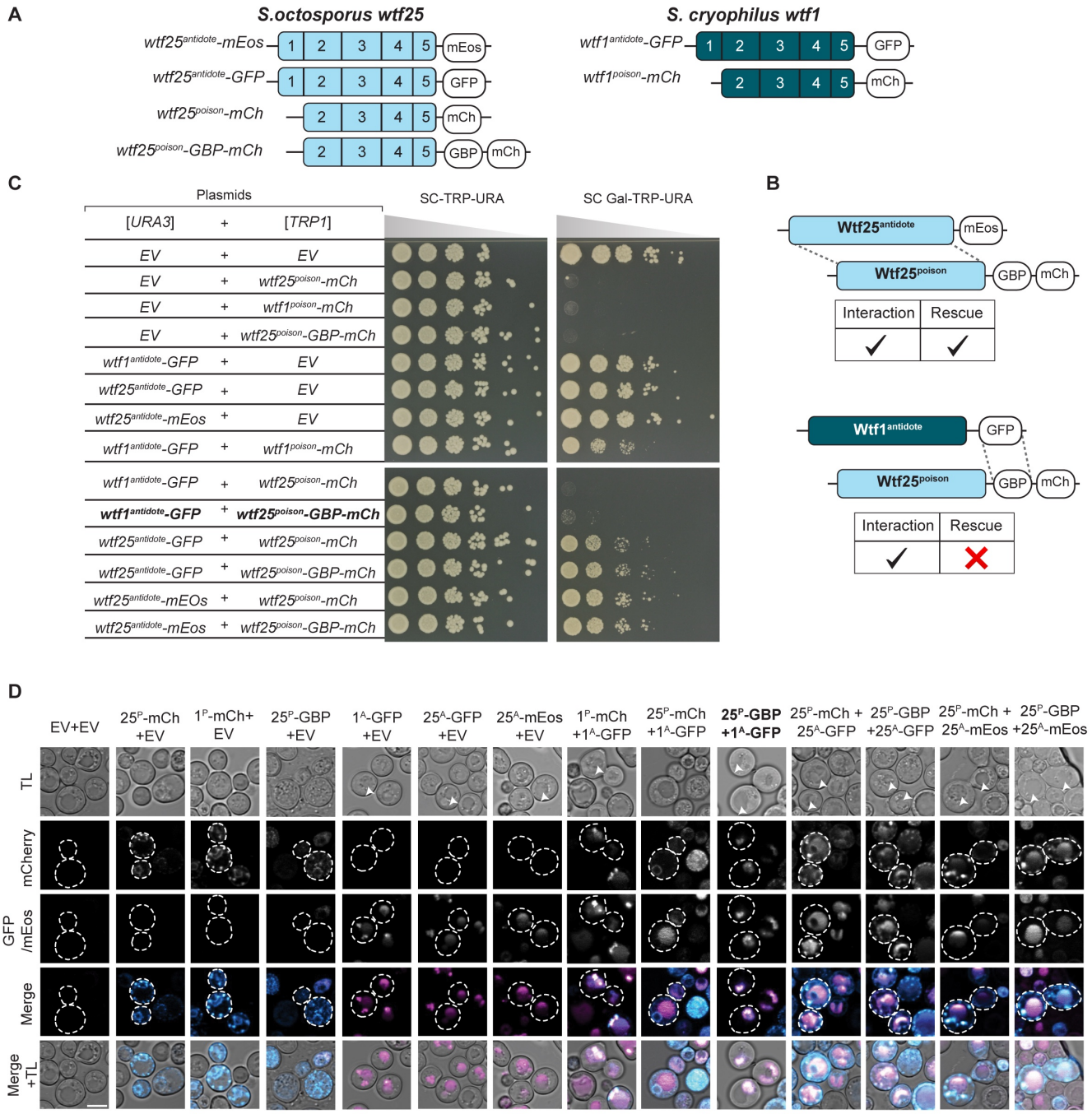
A
S.octosporus wtf25
wtf25antidote-mEos
wtf25antidote-GFP
wtf25poison-mCh
wtf25poison-GBP-mCh
S. cryophilus wtf1
wtf1antidote-GFP
wtf1poison-mCh
C
Plasmids
[URA3] + [TRP1]
SC-TRP-URA
SC Gal-TRP-URA
EV + EV
EV + wtf25poison-mCh
EV + wtf1poison-mCh
EV + wtf25poison-GBP-mCh
wtf1antidote-GFP + EV
wtf25antidote-GFP + EV
wtf25antidote-mEos + EV
wtf1antidote-GFP + wtf1poison-mCh
wtf1antidote-GFP + wtf25poison-mCh
wtf1antidote-GFP + wtf25poison-GBP-mCh
wtf25antidote-GFP + wtf25poison-mCh
wtf25antidote-GFP + wtf25poison-GBP-mCh
wtf25antidote-mEOs + wtf25poison-mCh
wtf25antidote-mEos + wtf25poison-GBP-mCh
B
Wtf25antidote
Wtf25poison
Interaction
Rescue
Wtf1antidote
D
EV+EV
25P-mCh +EV
1P-mCh+ EV
25P-GBP +EV
1A-GFP +EV
25A-GFP +EV
25A-mEos +EV
1P-mCh +1A-GFP
25P-mCh +1A-GFP
25P-GBP +1A-GFP
25P-mCh + 25A-GFP
25P-GBP +25A-GFP
25P-mCh + 25A-mEos
25P-GBP +25A-mEos
TL
mCherry
GFP /mEos
Merge
Merge +TL

S10 Figure

A

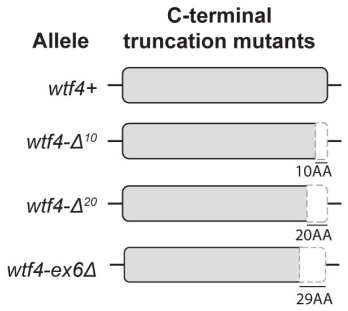

B

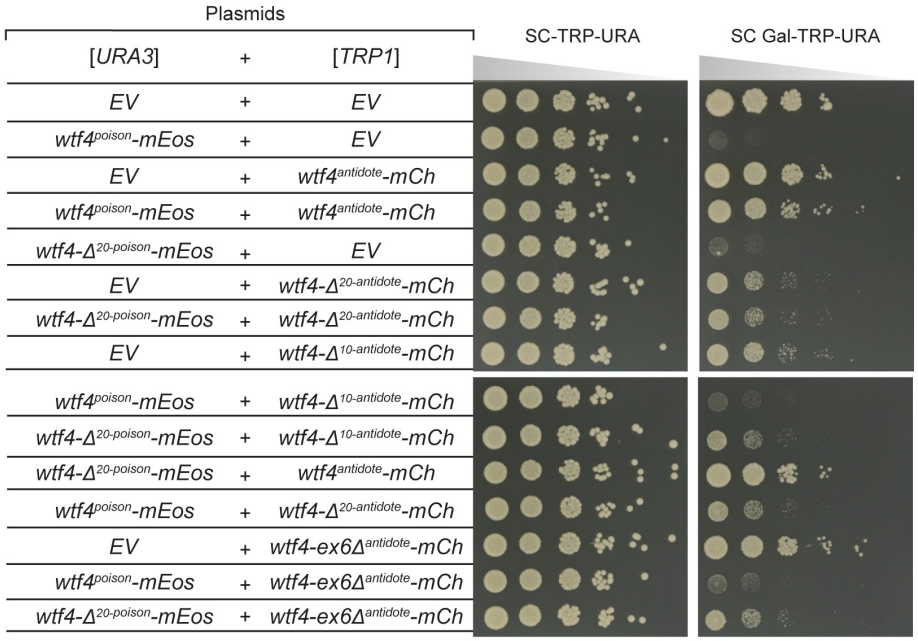

C

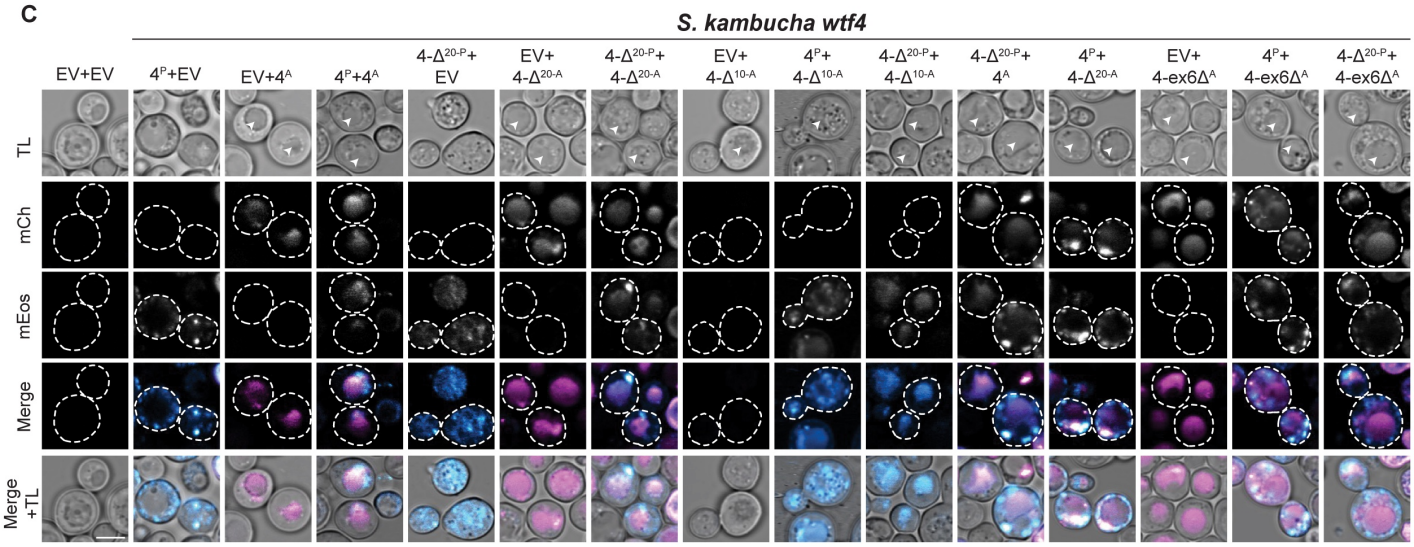

S11 Figure

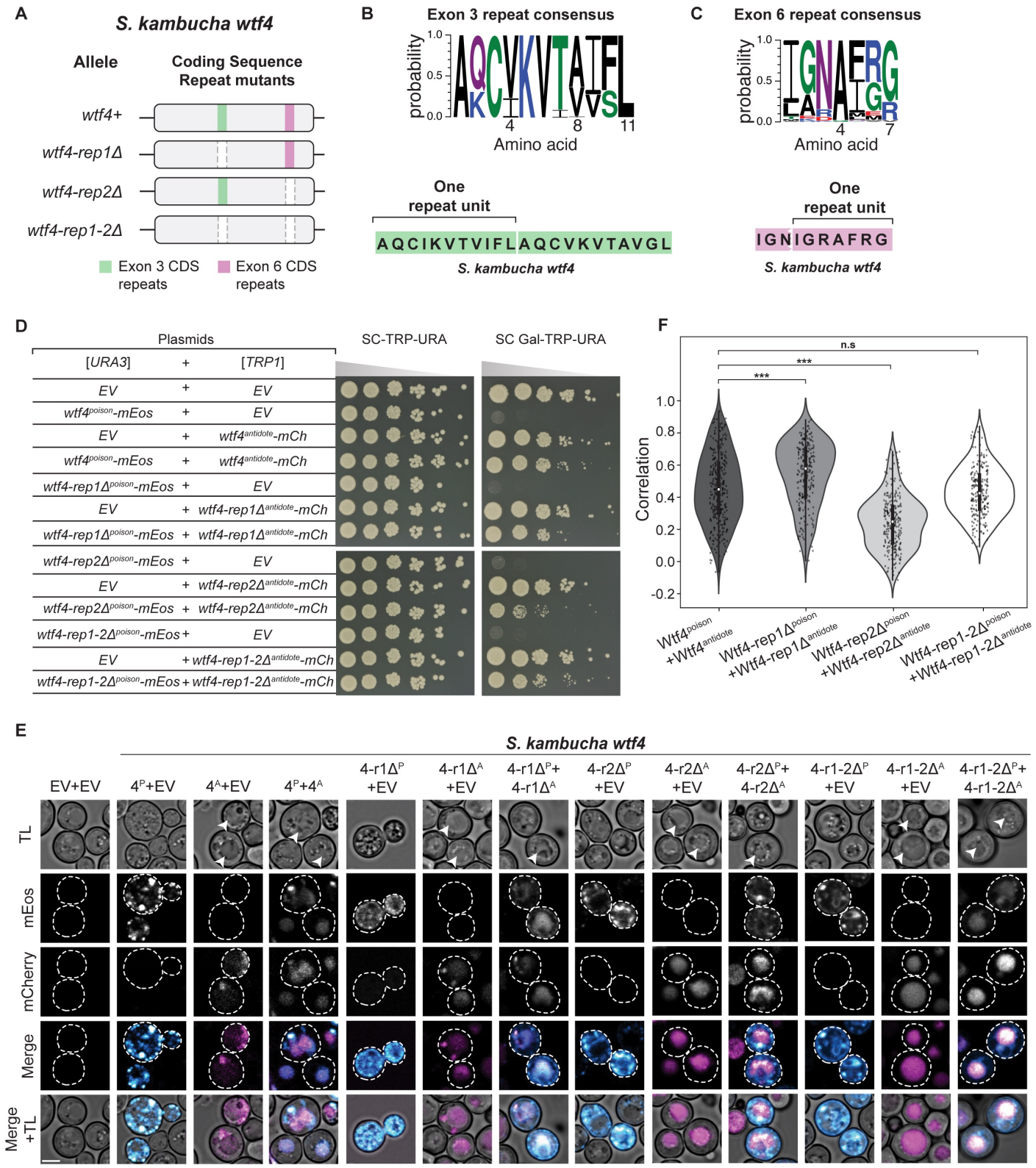
A
S. kambucha wtf4
Allele
Coding Sequence Repeat mutants
wtf4+
wtf4-rep1Δ
wtf4-rep2Δ
wtf4-rep1-2Δ
Exon 3 CDS repeats
Exon 6 CDS repeats
B
Exon 3 repeat consensus
probability
Amino acid
One repeat unit
AQCIKVTVIFLAQCVKVTAVGL
S. kambucha wtf4
C
Exon 6 repeat consensus
probability
Amino acid
One repeat unit
IGNIGRAFRG
S. kambucha wtf4
D
Plasmids
[URA3] + [TRP1]
SC-TRP-URA
SC Gal-TRP-URA
EV + EV
wtf4poison-mEos + EV
EV + wtf4antidote-mCh
wtf4poison-mEos + wtf4antidote-mCh
wtf4-rep1Δpoison-mEos + EV
EV + wtf4-rep1Δantidote-mCh
wtf4-rep1Δpoison-mEos + wtf4-rep1Δantidote-mCh
wtf4-rep2Δpoison-mEos + EV
EV + wtf4-rep2Δantidote-mCh
wtf4-rep2Δpoison-mEos + wtf4-rep2Δantidote-mCh
wtf4-rep1-2Δpoison-mEos + EV
EV + wtf4-rep1-2Δantidote-mCh
wtf4-rep1-2Δpoison-mEos + wtf4-rep1-2Δantidote-mCh
F
n.s
***
***
Correlation
Wtf4poison +Wtf4antidote
Wtf4-rep1Δpoison +Wtf4-rep1Δantidote
Wtf4-rep2Δpoison +Wtf4-rep2Δantidote
Wtf4-rep1-2Δpoison +Wtf4-rep1-2Δantidote
E
S. kambucha wtf4
EV+EV
4P+EV
4A+EV
4P+4A
4-r1ΔP +EV
4-r1ΔA +EV
4-r1ΔP+ 4-r1ΔA
4-r2ΔP +EV
4-r2ΔA +EV
4-r2ΔP+ 4-r2ΔA
4-r1-2ΔP +EV
4-r1-2ΔA +EV
4-r1-2ΔP+ 4-r1-2ΔA
TL
mEos
mCherry
Merge
Merge +TL

S12 Figure

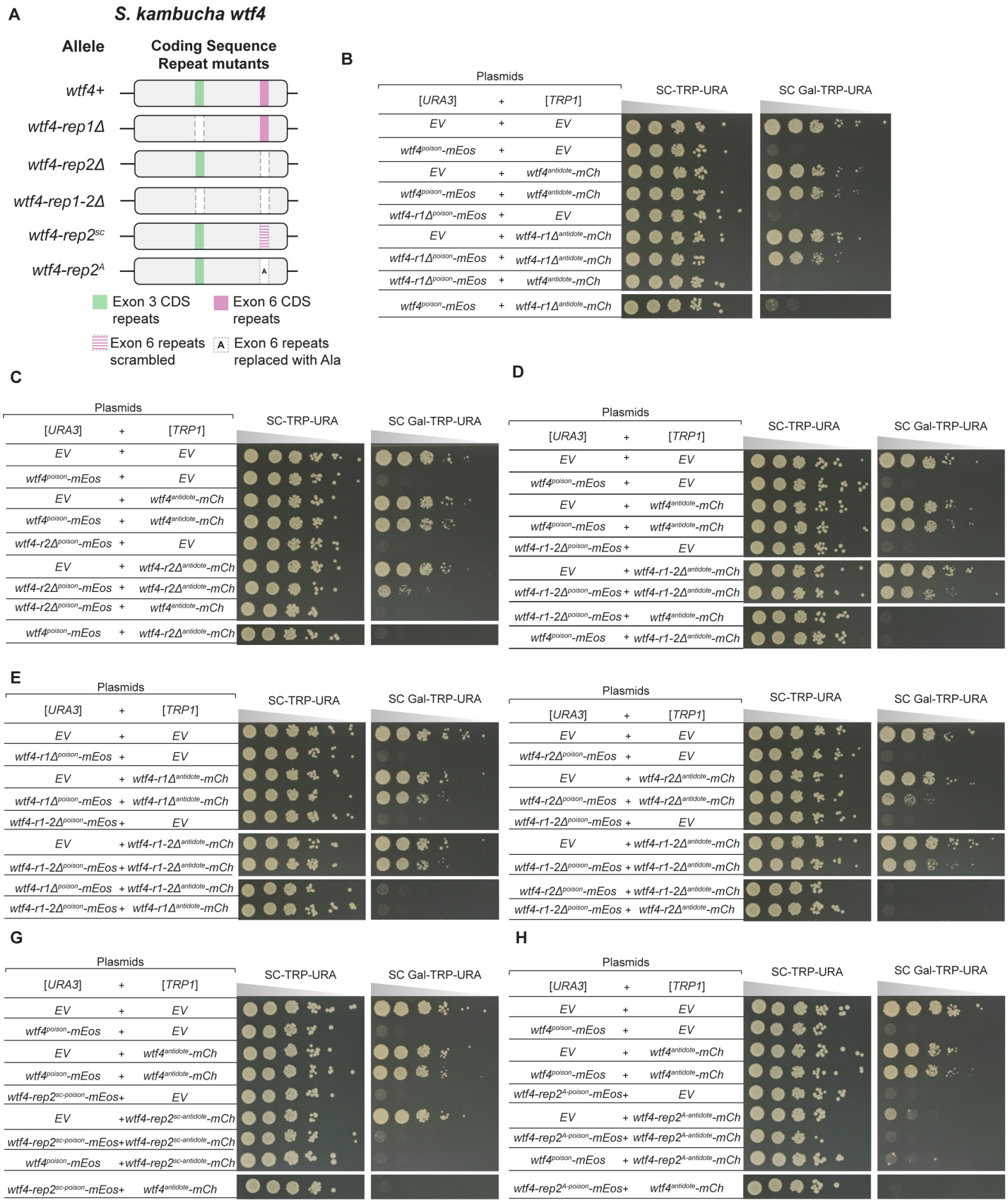
A
S. kambucha wtf4
Allele
Coding Sequence Repeat mutants
wtf4+
wtf4-rep1Δ
wtf4-rep2Δ
wtf4-rep1-2Δ
wtf4-rep2sc
wtf4-rep2A
Exon 3 CDS repeats
Exon 6 CDS repeats
Exon 6 repeats scrambled
Exon 6 repeats replaced with Ala
B
Plasmids
[URA3] + [TRP1]
SC-TRP-URA
SC Gal-TRP-URA
EV + EV
wtf4poison-mEos + EV
EV + wtf4antidote-mCh
wtf4poison-mEos + wtf4antidote-mCh
wtf4-r1Δpoison-mEos + EV
EV + wtf4-r1Δantidote-mCh
wtf4-r1Δpoison-mEos + wtf4-r1Δantidote-mCh
wtf4-r1Δpoison-mEos + wtf4antidote-mCh
wtf4poison-mEos + wtf4-r1Δantidote-mCh
C
Plasmids
[URA3] + [TRP1]
SC-TRP-URA
SC Gal-TRP-URA
EV + EV
wtf4poison-mEos + EV
EV + wtf4antidote-mCh
wtf4poison-mEos + wtf4antidote-mCh
wtf4-r2Δpoison-mEos + EV
EV + wtf4-r2Δantidote-mCh
wtf4-r2Δpoison-mEos + wtf4-r2Δantidote-mCh
wtf4-r2Δpoison-mEos + wtf4antidote-mCh
wtf4poison-mEos + wtf4-r2Δantidote-mCh
D
Plasmids
[URA3] + [TRP1]
SC-TRP-URA
SC Gal-TRP-URA
EV + EV
wtf4poison-mEos + EV
EV + wtf4antidote-mCh
wtf4poison-mEos + wtf4antidote-mCh
wtf4-r1-2Δpoison-mEos + EV
EV + wtf4-r1-2Δantidote-mCh
wtf4-r1-2Δpoison-mEos + wtf4-r1-2Δantidote-mCh
wtf4-r1-2Δpoison-mEos + wtf4antidote-mCh
wtf4poison-mEos + wtf4-r1-2Δantidote-mCh
E
Plasmids
[URA3] + [TRP1]
SC-TRP-URA
SC Gal-TRP-URA
EV + EV
wtf4-r1Δpoison-mEos + EV
EV + wtf4-r1Δantidote-mCh
wtf4-r1Δpoison-mEos + wtf4-r1Δantidote-mCh
wtf4-r1-2Δpoison-mEos + EV
EV + wtf4-r1-2Δantidote-mCh
wtf4-r1-2Δpoison-mEos + wtf4-r1-2Δantidote-mCh
wtf4-r1Δpoison-mEos + wtf4-r1-2Δantidote-mCh
wtf4-r1-2Δpoison-mEos + wtf4-r1Δantidote-mCh
Plasmids
[URA3] + [TRP1]
SC-TRP-URA
SC Gal-TRP-URA
EV + EV
wtf4-r2Δpoison-mEos + EV
EV + wtf4-r2Δantidote-mCh
wtf4-r2Δpoison-mEos + wtf4-r2Δantidote-mCh
wtf4-r1-2Δpoison-mEos + EV
EV + wtf4-r1-2Δantidote-mCh
wtf4-r1-2Δpoison-mEos + wtf4-r1-2Δantidote-mCh
wtf4-r2Δpoison-mEos + wtf4-r1-2Δantidote-mCh
wtf4-r1-2Δpoison-mEos + wtf4-r2Δantidote-mCh
G
Plasmids
[URA3] + [TRP1]
SC-TRP-URA
SC Gal-TRP-URA
EV + EV
wtf4poison-mEos + EV
EV + wtf4antidote-mCh
wtf4poison-mEos + wtf4antidote-mCh
wtf4-rep2sc-poison-mEos + EV
EV + wtf4-rep2sc-antidote-mCh
wtf4-rep2sc-poison-mEos + wtf4-rep2sc-antidote-mCh
wtf4poison-mEos + wtf4-rep2sc-antidote-mCh
wtf4-rep2sc-poison-mEos + wtf4antidote-mCh
H
Plasmids
[URA3] + [TRP1]
SC-TRP-URA
SC Gal-TRP-URA
EV + EV
wtf4poison-mEos + EV
EV + wtf4antidote-mCh
wtf4poison-mEos + wtf4antidote-mCh
wtf4-rep2A-poison-mEos + EV
EV + wtf4-rep2A-antidote-mCh
wtf4-rep2A-poison-mEos + wtf4-rep2A-antidote-mCh
wtf4poison-mEos + wtf4-rep2A-antidote-mCh
wtf4-rep2A-poison-mEos + wtf4antidote-mCh

S13 Figure

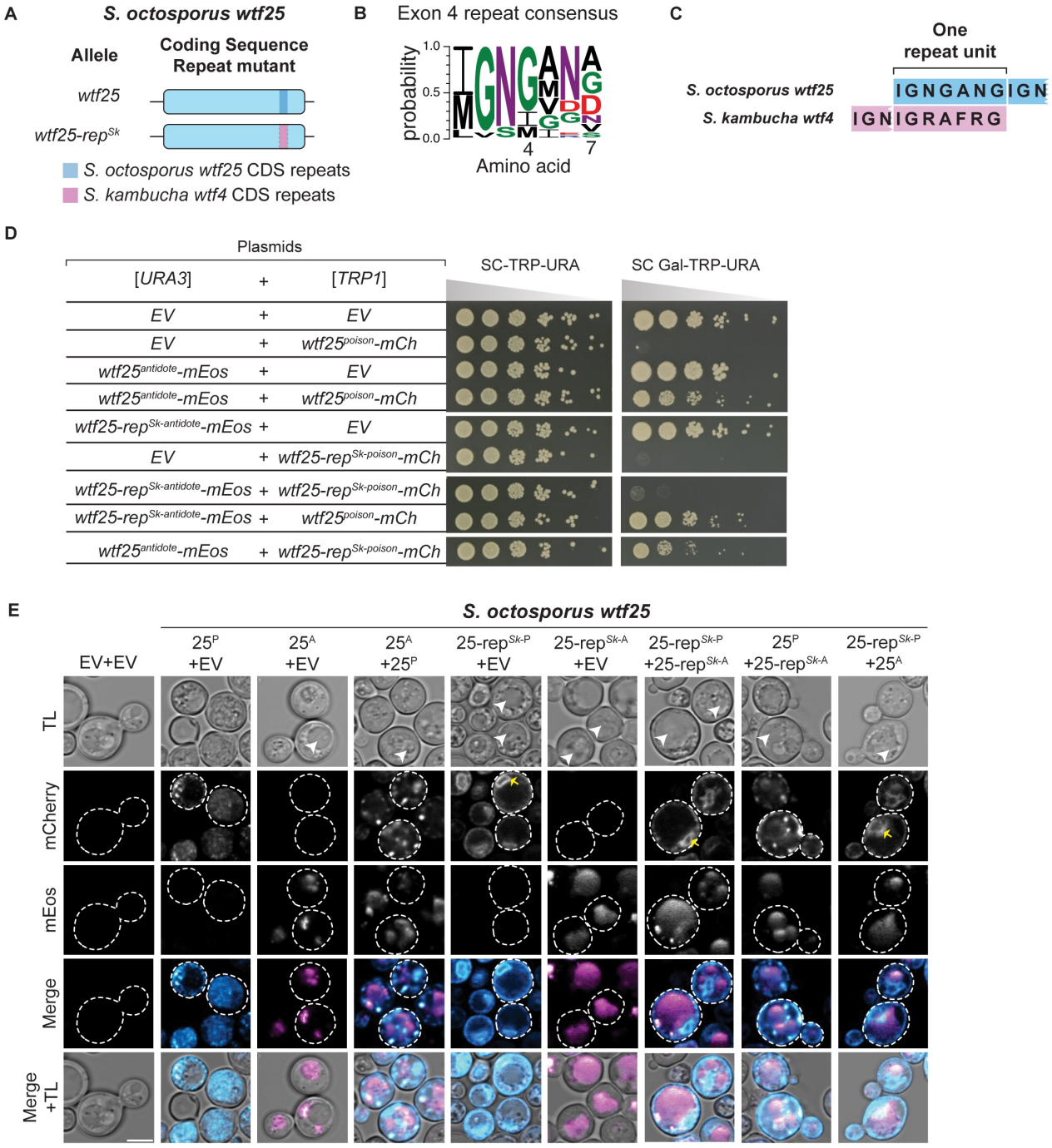
A
S. octosporus wtf25
Allele
Coding Sequence
Repeat mutant
wtf25
wtf25-repSk
S. octosporus wtf25 CDS repeats
S. kambucha wtf4 CDS repeats
B
Exon 4 repeat consensus
probability
1.0
0.5
0.0
4
7
Amino acid
C
One
repeat unit
S. octosporus wtf25
IGNGANGIGN
S. kambucha wtf4
IGNIGRAFRG
D
Plasmids
[URA3] + [TRP1]
SC-TRP-URA
SC Gal-TRP-URA
EV + EV
EV + wtf25poison-mCh
wtf25antidote-mEos + EV
wtf25antidote-mEos + wtf25poison-mCh
wtf25-repSk-antidote-mEos + EV
EV + wtf25-repSk-poison-mCh
wtf25-repSk-antidote-mEos + wtf25-repSk-poison-mCh
wtf25-repSk-antidote-mEos + wtf25poison-mCh
wtf25antidote-mEos + wtf25-repSk-poison-mCh
E
S. octosporus wtf25
EV+EV
25P +EV
25A +EV
25A +25P
25-repSk-P +EV
25-repSk-A +EV
25-repSk-P +25-repSk-A
25P +25-repSk-A
25-repSk-P +25A
TL
mCherry
mEos
Merge
Merge +TL

S14 Figure

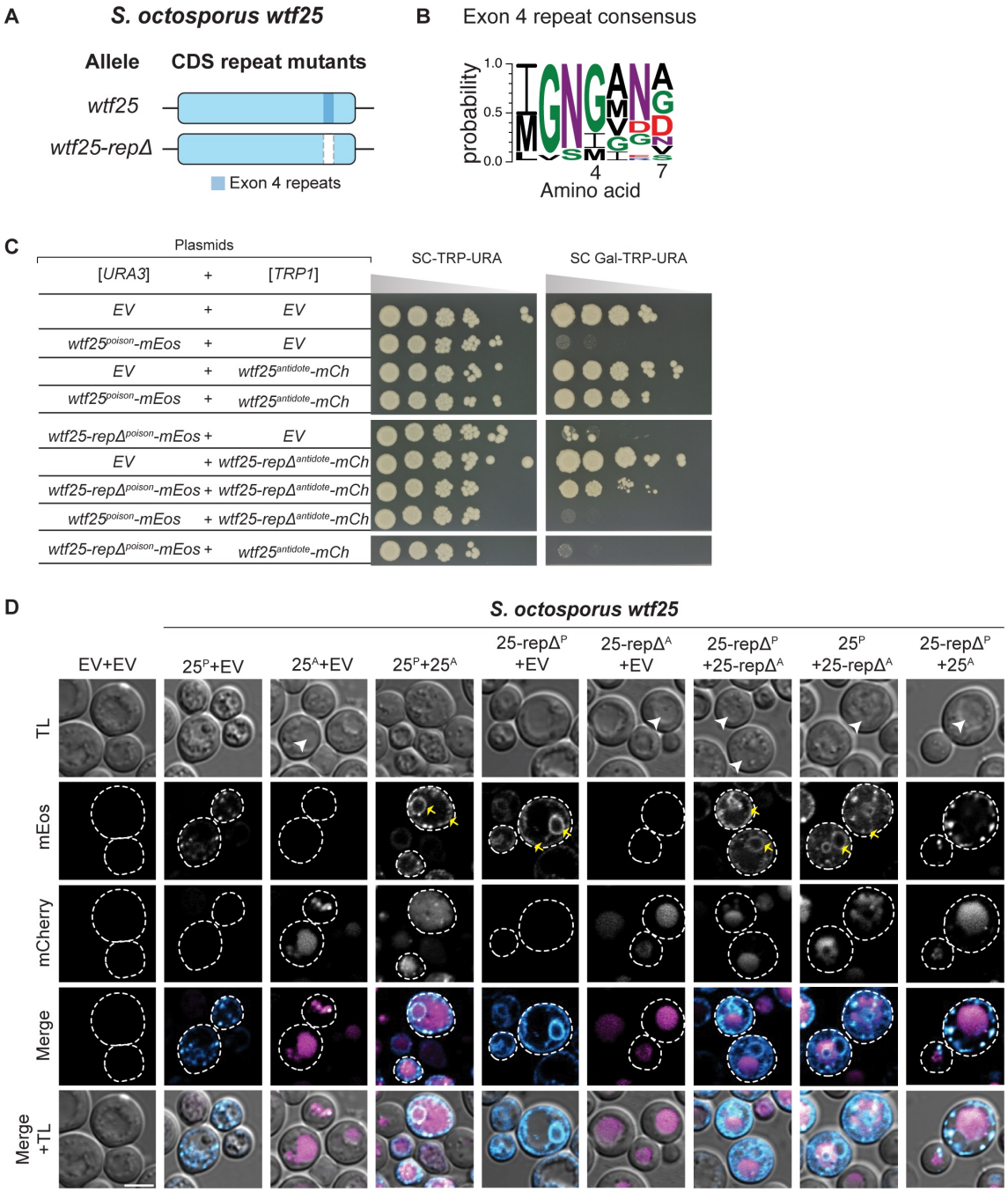
A
S. octosporus wtf25
Allele
CDS repeat mutants
wtf25
wtf25-repΔ
Exon 4 repeats
B
Exon 4 repeat consensus
probability
1.0
0.5
0.0
4
7
Amino acid
C
Plasmids
[URA3] + [TRP1]
SC-TRP-URA
SC Gal-TRP-URA
EV + EV
wtf25poison-mEos + EV
EV + wtf25antidote-mCh
wtf25poison-mEos + wtf25antidote-mCh
wtf25-repΔpoison-mEos + EV
EV + wtf25-repΔantidote-mCh
wtf25-repΔpoison-mEos + wtf25-repΔantidote-mCh
wtf25poison-mEos + wtf25-repΔantidote-mCh
wtf25-repΔpoison-mEos + wtf25antidote-mCh
D
S. octosporus wtf25
EV+EV
25P+EV
25A+EV
25P+25A
25-repΔP +EV
25-repΔA +EV
25-repΔP +25-repΔA
25P +25-repΔA
25-repΔP +25A
TL
mEos
mCherry
Merge
Merge +TL